Plasma assisted thin film formation

Shard, Alexander Gordon

University of Durham.

A thesis entitled

Plasma Assisted Thin Film Formation

Submitted by

Alexander Gordon Shard
B.Sc.(Hons.) (Dunelm.)

A candidate for the degree of Doctor of Philosophy

University College September 1992

Acknowledgements

I would like to thank my supervisors, Hugh Munro (Oct '88 to Dec '88), Nick Canning and Robin Harris (Jan '89 to Sep '89) and last, but not least, Jas Pal Badyal and Robin Harris (Oct '89 to Sep '91) for their support and encouragement throughout my studies in Durham. I would also like to thank Wilkinson Sword for the provision of a research grant. Much appreciation is also due to my colleagues and friends within the surface lab for their suggestions, advice and ideas. These are (in no particular order), Richard Ward, Sue Walker, Gillian Bell, Phil Dyer and Rachel - I'm not sure of her surname since she was wed, and to Trev Glaseby, who wasn't at Durham at all, but proof-read my thesis. Many thanks also to George Rowe for the construction and maintenance of equipment in and around the lab, the glassblowers for at least trying to construct some of my more complex reactors and to all the wonderful ladies who made the much needed coffee in the afternoon. I would like to thank Phil Coates for the supply of material used in chapters 5 and 6. Mixed thanks also to Biocompatibles, the company which saved me from penury whilst I wrote up.

Memorandum

The work described in this thesis has not been previously been published, except in the following journals:

"The variation in chemical character of plasma polymerised perfluorohexane", A. G. Shard, H. S. Munro, J. P. S. Badyal, *Polymer Communications*, **32**, 152, (1991)

"Plasma versus ultraviolet enhanced oxidation of polyethylene", A. G. Shard, J. P. S. Badyal, *Polymer Communications*, **32**, 217, (1991)

"Plasma oxidation versus photooxidation of polystyrene", A. G. Shard, J. P. S. Badyal, *J. Phys. Chem.*, **95**, 9436, (1991)

"Surface oxidation of polyethylene, polystyrene, and PEEK: The synthon approach", A. G. Shard, J. P. S. Badyal, *Macromol.*, **25**, 2053, (1992)

Abstract

Thin films of fluorocarbon-based polymers can be deposited by plasma assisted polymerisation of various perfluorocarbons. The chemical natures of plasma polymers of hexafluoropropene and perfluorohexane were examined as a function of power, flow rate and position in reactor. Polymerised hexafluoropropene displayed increased fluorine contents at high powers; this is at odds with perfluorohexane which demonstrated lower fluorine contents. Differing reaction mechanisms between saturated and unsaturated perfluorocarbons were proposed to explain this. Both perfluorocarbons were found to give increased CF_2 contents out of the plasma glow region. This was demonstrated to be a function of distance from the monomer inlet, and was ascribed to the production of long lived polymer forming species in the gas phase.

Plasma oxidation of low density polyethylene, polystyrene and poly (ether ether ketone) with oxygen and carbon dioxide was modelled by corresponding photooxidation reactions. Correlations between the structure of the polymer, the treatment used, and the final products were drawn. Aliphatic components tended to give carbon-oxygen single bonds, phenyl rings were oxidised to carbonyl and acid groups, and carbonyl groups to acids.

Metal-containing polymeric thin films were produced from plasmas of zinc acetylacetonate and aluminium tri-*sec* -butoxide. The products from each monomer were different, with the zinc compound resulting in a high proportion of zinc carboxylate and the aluminium compound giving the oxide or hydroxide. Incorporation of these compounds into a perfluorohexane plasma resulted in the formation of metal fluoride containing thin films.

Contents

Chapter 1

An Introduction to Glow Discharges

1.1 Scope of Thesis

The work described in this thesis covers the use of plasmas for the production of thin films. An introduction to the field of cold plasma chemistry and thin film analysis is given in this chapter. Chapters two and three are concerned with film deposition from perfluorocarbon plasmas, and the effect of differing monomer functionalities (double bonds, cyclic structures) and reaction conditions are investigated.

Chapter four compares and contrasts the plasma oxidation of polymers with corresponding photooxidation reactions. In particular, the role of vacuum ultraviolet radiation (below 200 nm) on the oxidation of three structurally different polymers, using a variety of gases, is studied.

In chapter five the deposition characteristics of some metallic compounds receives attention. Little work has previously been carried out using inductively coupled reactors, and it is shown here that polymeric films with a substantial metal content can be formed. The last chapter describes the plasma co-deposition of a perfluorocarbon with metallic compounds, the resulting films are shown to contain a high proportion of metal fluoride.

1.2 Plasmas

1.2.1 Introduction

Plasmas are often referred to as the "fourth state of matter". They occur in nature and the laboratory in varying forms which can be

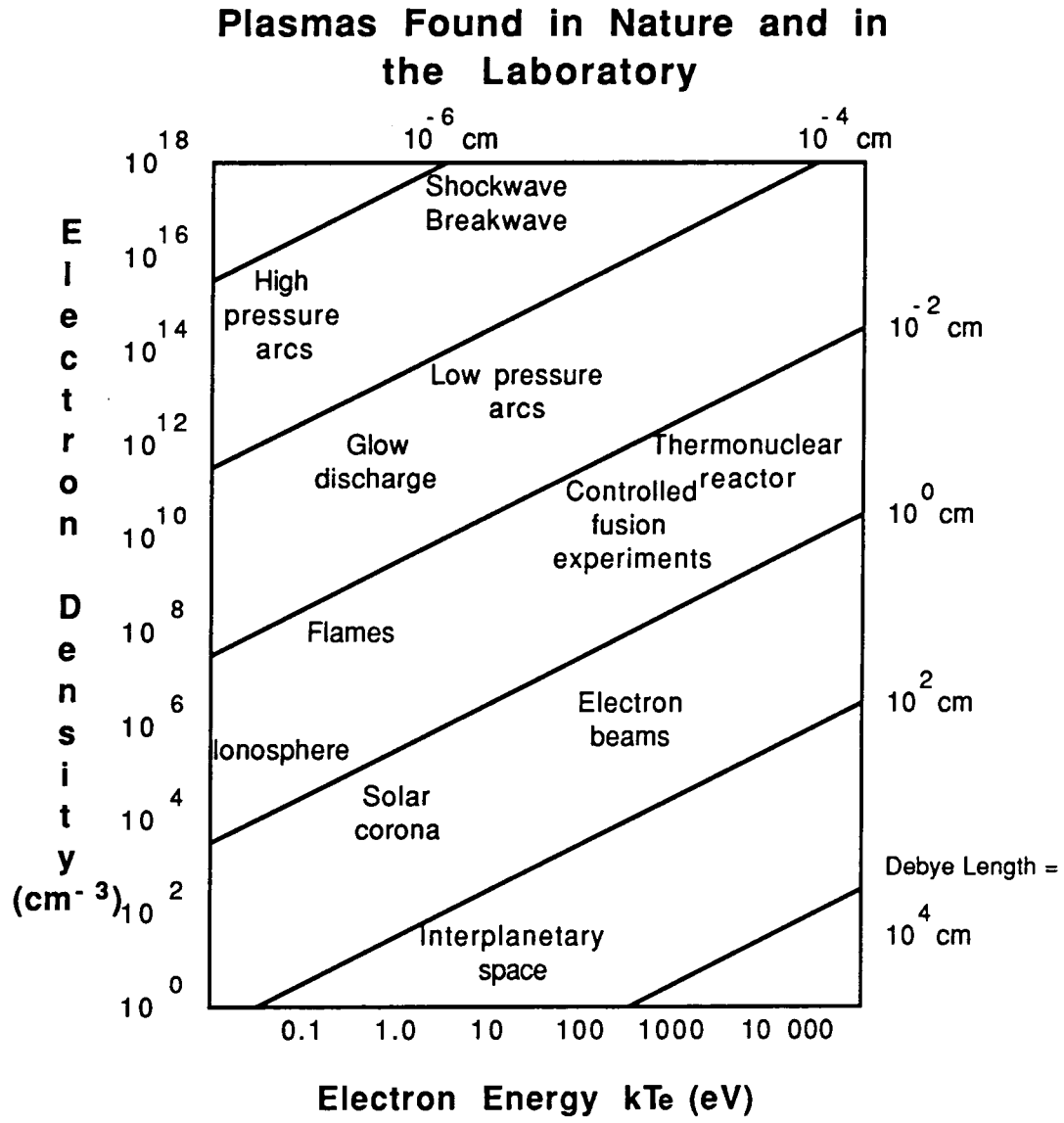

Figure 1.1 Characterisation of plasmas by electron temperature and electron density. Debye length = λ_D (Ref. 1)

classified according to the electron density of the plasma, and the average electron energy[1] (see figure 1.1). The most notable naturally occuring plasmas are stars, in which the conditions of temperature and pressure are extreme enough for nuclear fusion to occur. Other natural occurances include interplanetary space, the aurora borealis, and lightning. The definition of a plasma is given as an assembly of ions,

electrons, neutral atoms and molecules in which the motion of the particles is dominated by electromagnetic interaction[2]. The ions, atoms and molecules may be in either their ground or an excited state. As a whole, the plasma is electrically neutral, and further characterized by the presence of a plasma sheath at all of it's boundaries.

Plasmas may be split into two general types, equilibrium and non-equilibrium plasmas. The former are known as "hot" plasmas; these have roughly equal electron and molecular temperatures. The "cold", non-equilibrium plasmas have gas temperatures much lower than the electron temperature; typically two orders of magnitude lower[3]. For example, in a glow discharge, the electron temperature is roughly 30,000 K (2 eV) whilst the gas temperature is often around 300 K (0.02 eV).

Hot plasmas have use in metallurgy, where metallic ores can be reduced to the base metal[4], and for analysing material by ICP OES (inductively coupled plasma optical emission spectrophotometry) or ICPMS (inductively coupled plasma mass spectroscopy)[5]. These techniques only give elemental analyses, as most materials are reduced to their constituent atoms in a hot plasma. This type of plasma is also used in attempts to produce controlled nuclear fusion.

Cold plasmas can be formed in the laboratory by means of a gas discharge, and have been known for well over a hundred years. Early workers investigating gas discharges had no access to a continuous high voltage source of electricity, until the invention of the induction coil in 1851 by Ruhmkorff[6]. With this discovery, and the technique developed by Geissler which made the fusing of platinum electrodes into glass possible, electrical discharges under reduced pressures of gas could be observed. The typical appearance of a gas discharge is shown in figure 1.2. In the latter half of the nineteenth century, investigations

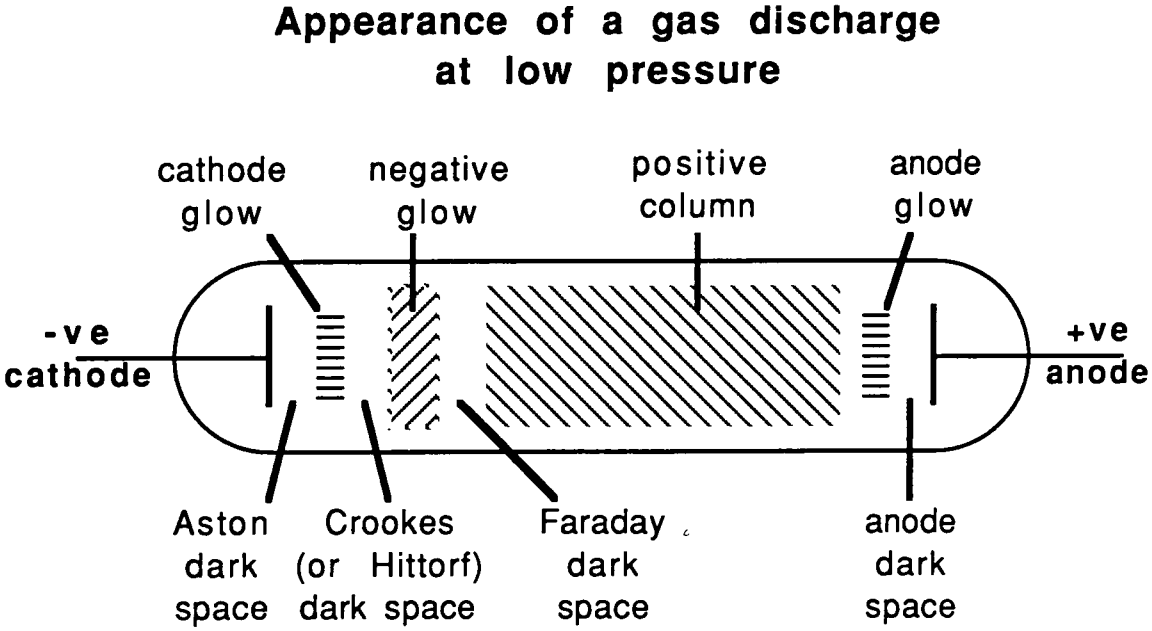

Figure 1.2 Typical gas discharge

into gas discharges, and the "rays" emitted from the cathode were carried out. In 1897 Thompson demonstrated that these rays were negatively charged particles approximately a thousand times lighter than hydrogen. Subsequently, these particles were given the name "electrons" by Lorentz. Soon after the turn of the century[7] it was established that conductivity within the gas discharges resulted from ions formed by collision of electrons with gas molecules.

The word "plasma" was coined by Langmuir to describe the state of ionised gases formed in an electrical discharge[8]. Cold plasmas are also often called glow discharges, as excited species within them produce emission of radiation in the visible region.

1.2.2 Fundamental Aspects of Plasmas

To exhibit electrical neutrality, the dimensions of the discharged gas in a plasma must be greater than the Debye length, λ_D, which

defines the distance over which a charge imbalance may exist[1]. λ_D is given by equation 1.1, where E_0 is the permittivity of free space, k is the Boltzmann constant, T_e is the electron temperature, n is the electron density, and e is the charge on the electron.

$$\lambda_D = \left[\frac{E_o k T_e}{n e^2}\right] \qquad 1.1$$

A plasma is ignited by the occurance of an ionisation event. This can be caused either naturally from background radiation, such as cosmic rays; or artificially through such means as a spark generator. If the applied electric field is large enough, dielectric breakdown of the gas will ignite the plasma. The free electrons formed during ionisation are then accelerated by the applied electric field, and collide with other gas molecules. Inelastic collisions with these molecules produce vibrational, rotational, and electronic excitations along with further ionisations. These additional ionisations release more electrons, which sustain the plasma. However, if the electron mean free path within the gas is too low for electrons to be accelarated (by the applied electric field) to the energy required for ionisation of gas molecules, then the plasma will not be sustained. This will occur if the pressure of the gas is too high. When the gas pressure is too low, the mean free path of the electron is large compared to the size of the reactor, and gas collisions become unimportant[1]. The typical pressure range for cold plasma experimentation is limited by these constraints, and the working range is between 0.05 and 10 torr.

The basic reactions within a plasma can be divided into ionisation or activation processes, and recombination or deactivation processes[3,9]. Some examples of these reactions are shown in table 1.1[10].

I	Ionisation	$e + O_2 - O_2^+ + 2e$ $e + O - O^+ + 2e$
II	Dissociative ionisation	$e + O_2 - O^+ + O + 2e$
III	Dissociative attachment	$e + O_2 - O^- + O$
IV	Metastable formation	$e + H_2(^1\Sigma_g^+) - e + H_2(^3\Sigma_g^+)$ $e + O_2 - O_2(^1\Delta_g)$
V	Charge transfer	$O^- + H_2O - OH^- + OH^*$ $O^+ + N_2 - O^* + N_2^+$
VI	Penning ionisation	$He\ (1s\ 2s\ ^1S) + Ar - He + Ar^+(^2P_{3/2}) + e$
VII	Photo ionisation	$O_2 + h\nu - O_2^+ + e$
VIII	Photo detachment	$NOO^- + h\nu - NO + O^* + e$
IX	Radiative recombination	$H^+ + e - H^* + h\nu$
X	Dissociative recombination	$He_2^+ + e - 2\,He$

Table 1.1 Examples of fundamental reactions within plasmas

The number of specific reactions however, even in a simple plasma, is very large; for example an oxygen plasma has over thirty individual basic reactions[1] which may be occuring within it. The activation/ionisation processes can be initiated by electron impact, as mentioned previously, or by collision with ions, atoms or molecules. These species seldom attain the kinetic energy required for an ionisation event to occur through impact, but processes such as charge transfer, Penning ionisation, and associative ionisation may occur. Photon impact will also produce excitation or ionisation within a glow discharge.

Recombination and deactivation reactions are the processes whereby the various activated and ionised species lose their energy or charge. One of the simplest is by diffusion to the side of the reaction vessel where upon impact, charge may be neutralised and energy exchanged. Another simple process is radiative recombination of ions and electrons. However, this is not thought to be as common as dissociative recombination or ternary collisions resulting in electron - ion recombination.

The average velocity of an electron between collisions is given in equation 1.2[9], where M is the mass of the heavier particle, e is the electron charge, E is the electric field, λ is the electron mean free path, and m is the mass of the electron.

$$\bar{c} = \left[\frac{Me^2E\lambda}{m^3}\right]^{1/4} \qquad \text{Eq. 1.2}$$

The distribution of electron energies in a plasma is close to a Maxwellian distribution[3]. Which may be expressed as;

$$f_m(\varepsilon) = 2.07 \langle\varepsilon\rangle^{-3/2}\, \varepsilon^{1/2}\, e^{(-1.5\,\varepsilon/\langle\varepsilon\rangle)} \qquad \text{Eq. 1.3}$$

in which ε represents a specific electron energy, and $\langle\varepsilon\rangle$ is the mean electron energy. The electron temperature T_e is defined in equation 1.4.

$$\langle\varepsilon\rangle = 3/2\, k\, T_e \qquad \text{Eq. 1.4}$$

A better approximation to experimental results (by probe measurements[11] and direct electron sampling[12]) is given by the Druyvesteyn distribution function, which, as shown in figure 1.3 has a

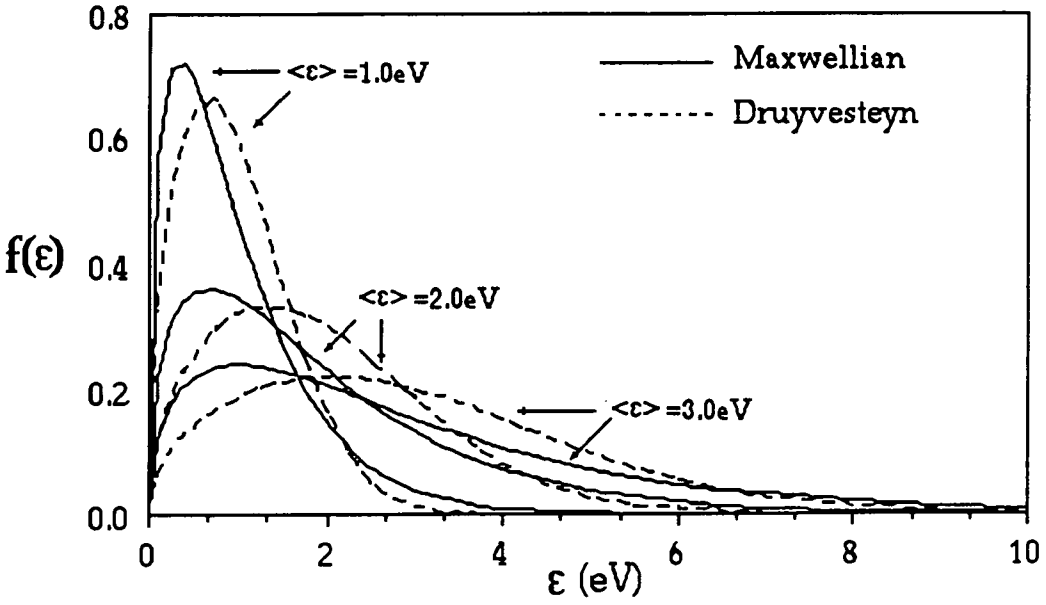

Figure 1.3 Energy distributions of electrons in an inert gas plasma

shorter high energy tail than the Maxwellian function. The Druyvesteyn distribution holds for cases where the electron velocities are much greater than those of ions or molecules, but fails when inelastic processes are occuring. The Druyvesteyn distribution function is shown in equation 1.5.

$$f_m(e) = 1.04<\varepsilon>^{-3/2} e^{1/2} e^{(-0.55\, e^2/<\varepsilon>^2)} \qquad \text{Eq. 1.5}$$

Most of the electrons within a glow discharge have insufficient energy to produce ionisation, molecules commonly having a first ionisation energy in the region of 10 eV. Thus the ion concentration tends to be small, with neutral species predominating. The most common events within the glow discharge then may be connected more with excitation of molecules, rather than their ionisation. Organic bond energies are of the order of a few electron volts (see table 1.2), the energies required to

C—H	4.3	C=O	8.0
C—N	2.9	C—C	3.4
C—Cl	3.4	C=C	6.1
C—F	4.4	C≡C	8.4

Table 1.2 Typical bond energies for organic compounds (energies in electron volts.)

disrupt such bonds more easily attainable by species in the plasma than those needed for ionisation. In a glow discharge of an organic vapour, reactions which may take place include elimination[13], isomerisation[14], dimerisation[15] and oligomerisation[16], as well as polymer formation on surfaces in contact with the plasma.

Chemical changes within a plasma can also arise from absorption by molecules of electromagnetic radiation causing rotational, vibrational and electronic excitation. The propagation of radiation in a plasma occurs as a result of radiative recombination (see table 1.1), or radiative decay of an excited state (produced, for example, by electron collision). In most laboratory plasmas, the probability of an excited species undergoing a radiative deactivation is comparable to it undergoing a collisional deactivation[17]. Radiative energy loss can occur spontaneously, excited species generally emit within ~10^{-8} seconds of being formed. Metastable species have a longer life (~10^{-3} seconds) and are therefore more likely to undergo collisional deactivation, or stimulated emission. Stimulated, or induced emission occurs when a photon of the emission frequency impinges on the excited atom causing the atom to decay. The emitted photon is in phase with the incident photon, and this is the principle behind laser action.

The probability of stimulated emission occuring is proportional to the population of the excited state, and the density of radiation of the appropriate frequency in the vicinity of the atom or molecule[18].

1.2.3 Plasma Techniques

In a glow discharge there are three main subjects of interest; the type of electrical power used, the method of coupling the power source to the plasma and the conditions within the reactor itself. These are shown schematically in table 1.3[19]. The use of a D.C. power source, or an A.C. power source with a frequency of less than 1 MHz. restricts the coupling mechanism used to that of a direct (or resistive) nature[20], see figure 1.2. The electrodes need to be placed within the reactor when this coupling mechanism is used, and contamination of the electrodes by species in the glow discharge may occur. In a plasma polymerisation experiment, for example, although direct coupling gives the highest deposition rates, problems are often caused by polymer deposition on the electrodes. Indirect coupling (either capacitive, or inductive; see figure 1.4) eliminates this problem, but an R.F. or microwave power

Electrical Power	→	Coupling Mechanism	→	Plasma Environment
D.C. A.C. R.F. Microwave	}	Resistive Capacitive Inductive	}	Current Pressure Gas Flow & Temp. Reactant Phases Electric & Magnetic Fields

Table 1.3 Elements involved in a glow discharge experiment

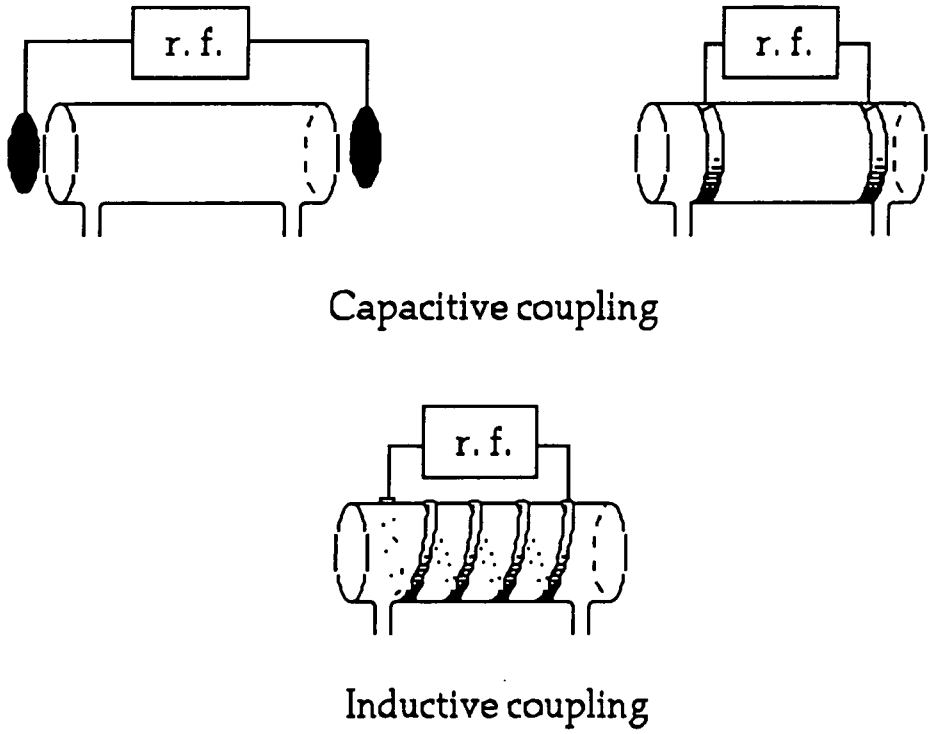

Figure 1.4 Indirect coupling methods for glow discharge

source must be used.

For reasons stated earlier normal operating pressures in a glow discharge are between about 0.05 and 10 torr. Higher pressure plasmas can be sustained by using very high powers. However, powers are normally ranged from between 0.1 watts to a few kilowatts, but for plasma polymerisation the glow discharge power tends to be less than 150 watts. Sustainable plasmas are not often achievable below 1 watt, but low average powers are possible using pulsed RF power. Gas temperature may be affected by high power, or if the power is concentrated into a small volume. In such cases a cooling system may become necessary.

Electrical and magnetic fields may be applied to a glow discharge, the charged species formed in the plasma being affected by such fields.

Studies using these techniques are often involved in investigating the role of ions within plasmas[21].

1.2.4 Uses of Cold Plasmas

Cold plasmas have found use in several areas, including synthetic organic and organometallic chemistry[20] where the high energies available from the discharge enable the exploitation of reaction pathways not normally accessible. The product of this type of reaction can often be a complex mixture of compounds, and yields of the desired reaction product may be low. To avoid excessive rearrangement of organic precursors within the plasma, high electron energies are best avoided.

Another, far more widespread, use of plasmas is in the field of surface modification. Plasmas can be used to create reactive sites on the surface of a polymeric material, and these sites can initiate a conventional free radical polymerisation at the surface. This is known as surface grafting[22] and can be used to improve, for example, the flame retardancy[23] or the wettability[24] of fabrics, depending on the properties of the grafted polymer. Cross-linking of polymer surfaces can be achieved by using direct and radiative energy transfer from inert gas plasmas. Adhesive bonding to the polymer[25] can be improved by this method.

Chemical modification of a surface may be accomplished directly by using reactive gas plasmas. Glow discharges of oxygen and water have been used to increase the wettability of a surface[26,27], whereas tetrafluoromethane plasmas are used to increase the hydrophobicity of surfaces[28]. Ammonia or nitrogen gas have been used to incorporate nitrogen atoms into a surface[29].

Plasmas are frequently used in the electronics and semiconductor industry for etching[30]. Usually oxygen or halocarbon discharges are used to remove resists and etch silicon wafers. The advantage over chemical etching being that no undercutting of the resist occurs[31]. Etching of Indium-Tin-Oxide semiconductors has been carried out using glow discharges of hydrocarbon gases, in this case it is thought that methyl radicals produced from high energy processes are the main etching species[32,33].

Deposition of organic, inorganic and metallic thin films from plasmas has been studied for a number of years[34,35,36]. The general term for the production of organic films in a plasma, is plasma polymerisation, whereas plasma enhanced chemical vapour deposition (PECVD) is often used to describe the process of forming films from organometallic precursors. Plasma polymers form on all surfaces in contact with the plasma, and are generally different in nature to conventional polymers. The deposition of inorganic compounds from plasmas, such as silicon nitride[37] and silicon oxide[38] have particular application in the electronics industry. Attempts have been made to fabricate high temperature superconducting thin films using plasma techniques[39].

Plasmas may also be used to initiate conventional polymerisations in both solid and liquid monomers; excitation being caused by either direct contact with a plasma, or by excited species generated from a plasma[40]. These processes are known as plasma induced polymerisation.

1.2.5 Plasma Diagnostics

As mentioned previously, the electron energy distribution of a discharge may be obtained using probe techniques[11] but this is an intrusive method, and the presence of the probe within the plasma will perturb it. There are other techniques which can give information concerning species within a plasma.

Optical Emission Spectrophotometry (OES) is a non-intrusive technique, which relies upon characterisation of emitted radiation from a plasma[41]. Emission lines within the infra-red, visible and ultra-violet regions can often be attributed to the presence of individual species[42]. The radiation observed is due only to excited states of certain species relaxing by photon emission, and so the complete chemical composition of the plasma is unobtainable via this method. OES is semi-quantative because the intensity of emission from a species is not directly proportional to its concentration, and there is no simple way of relating emission intensity to concentration. The probabilities of excitation and emission under a given mode of excitation are difficult to determine for any species being studied. Optical emission spectroscopy has been applied to the production of amorphous silicon from mixed silane/argon plasmas, and according to some investigations the deposition rate is proportional to the SiH* emission line[43]. In fluorocarbon plasmas, the CF_2* emission and F* emission are prominent, and the addition of hydrogen to a hexafluoroethane plasma drastically reduces the line due to the fluorine radical[44].

Ground state species, particularly small ions and radicals (for example species such as the CF_2 radical and the SiH radical[45]) can be investigated using laser induced fluorescence (LIF). Laser light is shone through the plasma, causing excitation; characteristic fluorescence lines

are then observed from the excited species under study. For this technique to work the species under study must fluoresce with reasonable quantum efficiency. Large polyatomic molecules tend to lose energy non-radiatively or dissociate, so LIF is not often applicable to them. Laser optogalvanic spectroscopy has been used[46] to supplement LIF; positive ions within the cathode sheath may not have time to fluoresce before striking the cathode, but a difference in the mobility between excited and ground state ions will affect the discharge current. The change in current can be used to help determine the concentration of these ions close to the cathode.

Infra-red absorption has been used to monitor molecules within glow discharges[47]. A wider range of species can be monitored than with OES, but sensitivity is low, necessitating the presence of large concentrations of strongly absorbing species, or a long optical path length.

Mass spectrometry can be used to examine both ions and neutral species within a plasma[48]. A small hole connects the plasma chamber to a mass spectrometer, and all species with sufficient lifetime to reach the spectrometer can be analysed. The technique is intrusive and therefore could affect processes occuring within the plasma, but substantial information can be gained in the way of mass and energy distribution for those species analysed.

A mathematical treatment of a plasma or a particular reaction or property of a plasma is termed plasma modelling. Such models have use for example, in following the kinetics of fundamental reactions in a plasma[49], predicting the densities of particular reactive species[50] and studying deposition rates, deposition processes and film properties[51].

1.3 Plasma Polymerisation

1.3.1 Introduction

The process of polymer formation in a plasma is generally referred to as plasma polymerisation or glow discharge polymerisation. Plasma polymerisation occurs when an organic or organometallic vapour is injected into an inert gas plasma, such as argon, or when a plasma is struck in the pure vapour of such a compound. Usually the polymer forms as a thin film on all surfaces in contact with the plasma. Such deposits have been known of for many years[52], but at first were regarded as unwanted by-products of the discharge experiment[53].

There are very few restrictions upon the choice of monomer for plasma polymerisation, as unlike conventional polymerisation, no particular functional group is necessary for the process to occur. The structure of such polymers often differs from conventional polymers in that the molecular structure of the starting material not commonly retained during the transition from monomer to polymer. A plasma polymer will contain no regular repeat unit and generally consists of a random, highly cross-linked organic network containing a number of trapped free radicals. The cross-linked nature of these polymers makes them very brittle and rigid, and if they become too thick internal stress will cause them to crack and flake. Plasma polymers are often strongly adherent to the surfaces they are deposited upon, and due to cross-linking tend to be insoluble in most common solvents.

The number of radicals present in the plasma polymer depends greatly upon the monomer used for polymerisation. Unsaturated monomers such as benzene and acetylene polymerise mainly through difunctional intermediates, while saturated monomers such as

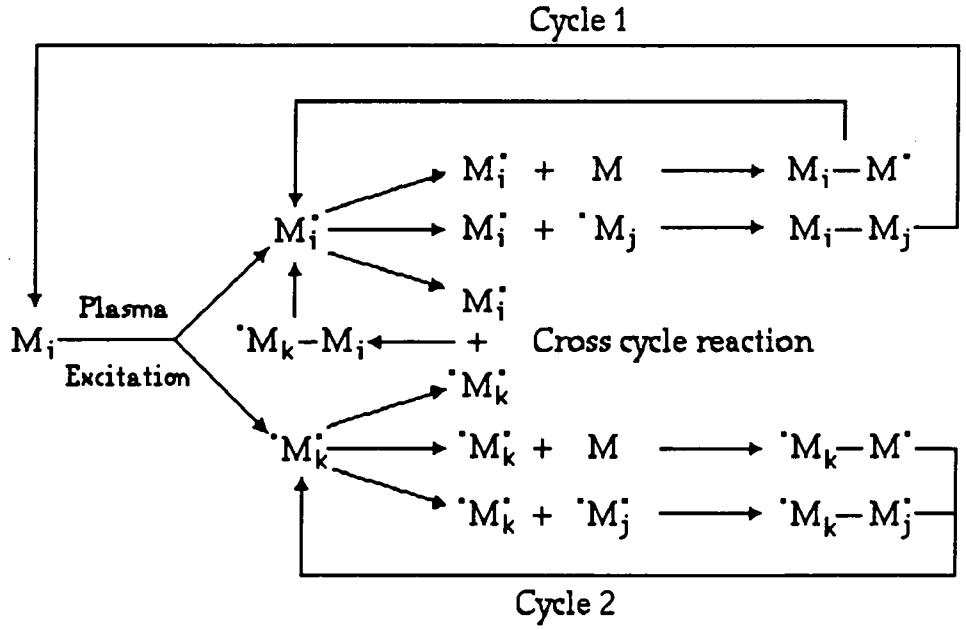

Figure 1.5 Rapid step growth mechanism for plasma polymerisation (ref. 34)

methane tend to polymerise via monofunctional species giving rise to fewer radicals in the polymer. Figure 1.5 shows a proposed mechanism for plasma polymerisation[34]. Cycle 1 shows a monofunctional route to polymer formation, and cycle 2 the difunctional route. The active species may be radicals or ions or both.

Once formed, the deposited material is subject to further change by contact with the plasma. Species within the glow discharge can cause ablation and chemical modification. The final product is a result of an equilibrium between the competing processes[54], as shown in figure 1.6. Ablation is a key feature of fluorocarbon plasmas. In the case of tetrafluoromethane, the ablation rate is higher than the polymerisation rate with the result that no film is formed[55]. This is due to the presence of highly reactive fluorine species which etch the surface. Polymer formation in a tetrafluoromethane plasma can only occur by the addition of hydrogen, or gases which naturally form plasma polymers. These gases react with the etchant species, reducing the

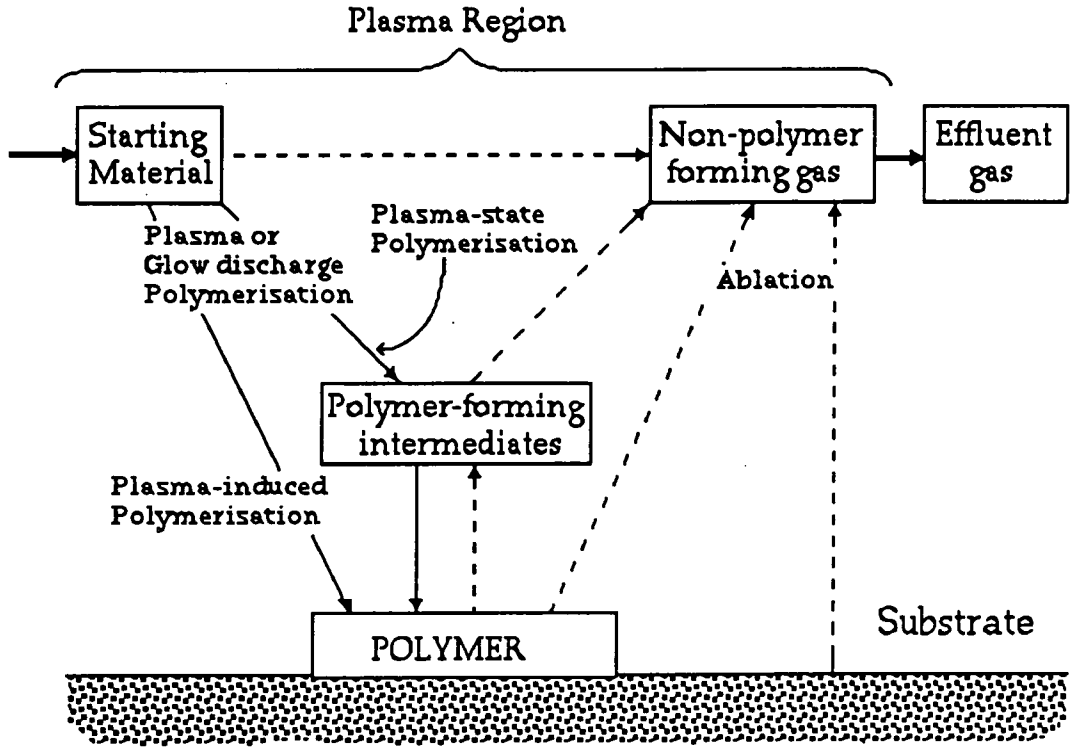

Figure 1.6 Competitive ablation and polymerisation in a plasma, showing the formation of gas phase products (ref. 54)

concentration of them in the gas phase, and hence decreasing the rate of chemical etching at the surface.

The competitive ablation and polymerisation process is extremely dependent upon plasma conditions, especially the power of the discharge and the monomer flow rate. The deposition rate of the polymer for a particular monomer has been shown[56] to vary with the parameter W/F, as demonstrated in figure 1.7, where W is the discharge power in watts, and F is the monomer flow rate in moles per unit time. When the W/F ratio is low there is insufficient power to cause a great deal of polymerisation, with reactive species being

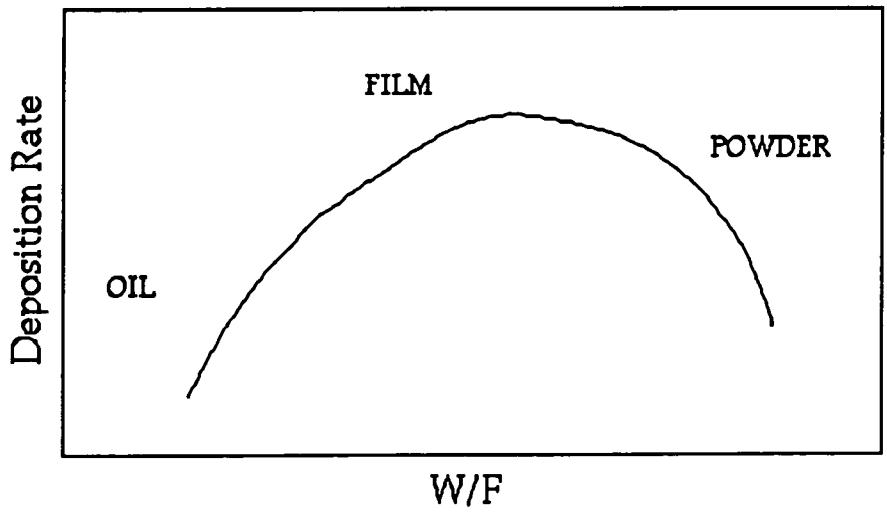

Figure 1.7 The variation of polymer deposition rate with W/F

removed in the comparatively high flow; the resulting deposit is of a low molecular weight and oily. When the parameter is large there is a monomer deficiency and the result is often a powder as the polymerisation occurs rapidly in the gas phase. In many cases the chemical nature of the film can also be related to the W/F parameter. Increasing the average power available to each unit of monomer (increasing W/F) is likely to increase disruption to its molecular structure.

The nature and distribution of the polymer depends to a large extent upon the geometrical shape and size of the plasma reactor[57]. Therefore comparisons between plasma polymers are difficult to make unless the same or identical apparatus is employed. The site of deposition within a reactor will also affect the composition of the deposit[58], and for that reason if comparisons between plasma polymers are to be made then the samples should be taken from the same position in a reactor.

1.3.2 Uses of Plasma Polymers

Plasma polymerisation is a simple, one-step process for depositing thin polymeric films. As such it has potential application in forming resist materials[59] in the electronics industry. Plasma polymers can be made to be inert and electrically insulating giving them use as protective coatings for electronic devices[60], KBr optical windows[61], insulating films[62], and thin film capacitors[63]. The strong adhesion of plasma polymers to substrates allows them to be used to enhance adhesion between materials which do not bond together strongly[64], for example teflon and steel.

Plasma polymers are often used to alter the surface properties of a material. Fluorocarbon monomers are employed to produce hydrophobic and low friction coatings[65], whereas hydrophilic films can be produced from compounds such as N-vinyl pyrrolidone for such uses as enhancing the comfort of contact lenses[66]. Plasma polymers can have properties that enable them to be used as semi-permeable membranes[67] and ion exchange membranes[68]. Organotin plasma polymers have been proposed as gas sensor devices[69] and also there are a number of potential biomedical uses for plasma polymers[70]. These include the provision of biocompatible surfaces for implants into the body, barrier films preventing the diffusion of small molecules to a substrate and controlled drug release systems.

A number of problems are associated with plasma polymers in some applications. The presence of free radicals in the surface of plasma polymers results in an aging affect as these react with atmospheric oxygen. The change in some cases can be quite rapid and the properties of the film adversely affected. Another problem is that the mechanisms of plasma polymerisation and the affect of the various

parameters such as power, flow rate and reactor design are poorly understood. The nature and properties of a plasma polymer cannot always be predicted given these restraints and the preparation of polymers with a specific composition or property is difficult. Processing on a large, industrial scale can be expensive and difficult due to the initial equipment costs.

1.4 Plasma Enhanced Chemical Vapour Deposition

1.4.1 Introduction

Organometallic and organosilicon compounds, like almost all volatile organic molecules, can be converted into thin films by plasmas. Since few organometallics have sufficient volatility and are often highly poisonous or difficult to handle, little work has been done until recently on these materials[71]. Organosilicon compounds and in particular silane have found extensive use as precursors in the semi-conductor industry. Silicon oxide[72], and silicon nitride[73] formed from plasmas provide protective, insulating layers and amorphous silicon[73] (α-Si:H) can be used as a semi-conductor.

The production of novel metal-polymer and metal oxide-polymer composite thin films is an area in which plasma enhanced CVD has an important role to play[74]. Methods of incorporating metals into polymers include the ion implantation of metals into an already formed polymer[75], plasma polymerisation of organic vapour whilst sputtering or etching a metal electrode[76], the evaporation of a metal into a plasma which is capable of polymerisation[77] and plasma enhanced CVD. Initially, work with organotin compounds, particularly

tetramethyltin received the most interest[78], but a wide variety of organometallic compounds have now been studied[79].

Thin films of metals[80], metal oxides[39] and metal nitrides[81] containing little or no carbon can also be formed by plasma enhanced CVD. In many of these experiments the substrate for collection was heated to assist removal of polymeric material and to obtain substantial metal content.

The basic techniques of plasma enhanced CVD are very similar to plasma polymerisation, as are the limitations on the understanding of the reactions occuring within the plasma. Due to the low volatility of some of these compounds it is often necessary to heat the reservoir containing the monomer to obtain a reasonable vapour pressure.

1.4.2 Plasma enhanced CVD precursors

Ideally a monomer for plasma work should have a vapour pressure of at least a few pascals at room temperature, or should be stable to heating until such a pressure is reached. A few metallic elements form volatile halides and hydrides, and some, such as nickel and chromium, have volatile carbonyl complexes. In the case of metal carbonyls the deposit formed is often an oxide because of the high concentration of oxygen in the parent molecule[79].

The methyl and ethyl compounds of tin, germanium, indium, zinc and aluminium all have high volatility and have good thermal stability. Aluminium alkyls are extremely sensitive toward oxygen and moisture, and must be handled with extreme care. Aluminium nitride has been formed using trimethyl aluminium[81], and a great deal of work has been carried out on tetramethyltin[78].

Metal Chelates

Ferrocene Vinylferrocene

Figure 1.8 Some precursors used in plasma enhanced CVD

Metal π-complexes often have sufficient volatility for use in plasma enhanced CVD. Ferrocene and ferrocene derivatives, see figure 1.8, have been studied[82] as monomers. It was found that the iron contained in the plasma deposit mostly retained its ferrocene-like environment.

Some metal chelates, especially acetylacetonate derivatives such as those shown in figure 1.8, have reasonable volatilities and can be used as precursors for plasma work, although heating is often required. Metal films may be prepared with these precursors[80,83], but the close proximity of metal and oxygen atoms tends to favour oxide formation. The production of thin films of superconducting Y-Ba-Cu-O films from the respective β-diketonates of the metals has been carried out using conventional CVD methods[84] and is possible using lower temperature plasma techniques[39]. Iron and cobalt acetylacetonate precursors have also been used to produce thin magnetic film capable of recording data for use in such devices as video tapes and magnetic discs[85].

1.5 Plasma Oxidation of Polymers

The controlled surface oxidation of polymers is of considerable importance, particularly with a view to improving the adhesion properties and wettability/printability[86]. Many techniques are available to acheive this (see chapter 4), but plasma oxidation offers a convenient, one step route and does not involve high temperatures or hazardous chemicals. The process is applicable to any polymer, and has even been succesfully applied to polytetrafluoroethylene[27], a material which is often regarded as inert.

Usually oxygen is used as the modifying gas, and in a glow discharge produces numerous reactive species including ions, atoms, ozone and singlet oxygen[1]. It has been shown that in oxygen glow discharges the negative ion density (i.e. O^- and O_2^-) is often greater than the electron density[87]. Ozone, however, is fairly scarce at the pressures used to oxidatively modify polymers, this is due to the infrequency of collisions at low pressures; ozone producing intermediates are highly energetic, and collisional deactivation is required within the vibrational lifetime of the molecule[88]. Gases apart from oxygen may be used to oxidise polymers, such as water[27], nitrous oxide[89] and carbon dioxide (chapter 4). Gases such as argon[90] and ammonia[91] can induce surface oxidation by producing trapped free radicals which subsequently react with atmospheric oxygen.

The surface examination of plasma oxidised polymers can be very effectively carried out using XPS[92]. Polymers are found to produce a wide range of oxidised functionalities including alcohol, carbonyl and carboxylic acid groups. The time used for treatment and plasma power can be very important in determining the exact distribution of functionalities; although after a certain time a "steady state" chemistry

forms as the exposure of fresh polymer and removal of oxidised species (such as water and carbon dioxide) reach equilibrium. It has been found that the surfaces created by this process revert toward the chemistry of the unoxidised polymer over a period of days. This has been attributed to the reorientation of hydrophilic groups[93], or diffusion of highly oxidised low molecular weight segments into the bulk[94]. Some interesting features in this process include the reappearance of hydrophilicity for a short time[95]. This phenomenon is reproducible and the time at which it occurs in a given system is constant[94].

Further chemistry can be done on functionalities produced at polymer surfaces, and of particular interest is the initiation of graft reactions. Hydroperoxides are often produced as a result of polymer oxidation in the presence of molecular oxygen[96]. These may be thermally cleaved to produce initiating species for conventional polymerisation[97]. Alcohol groups may also be used to initiate a grafting reaction in the presence of ceric ions which produce a one electron oxidation of the hydroxyl functionality[98], and this reaction has been succesfully applied to plasma oxidised polymers[99].

1.6 Analytical Techniques

1.6.1 Introduction

Several techniques have been used to examine plasma deposited films, and these can be broadly classified into two groups, bulk analytical techniques and surface analytical techniques. The most important and recent techniques are listed in table 1.4. Many bulk analytical techniques are difficult to apply to plasma polymers since the

Bulk Characterisation

1	Elemental Analysis
2	Electron Spin Resonance (ESR)
3	Solid State NMR
4	Infra-Red Spectroscopy
5	Differential Scanning Calorimetry
6	Pyrolysis Gas Chromatography
7	Neutron Reflectivity Measurements

Surface Characterisation

1	Contact Angle Measurement
2	Electron Microscopy
3	Scanning Tunneling Microscopy (STM) and Atomic Force Microscopy (AFM)
4	Reflectance Infra-Red
5	X-Ray Photoelectron Spectroscopy (XPS)
6	Secondary Ion Mass Spectroscopy (SIMS)

Table 1.4 Analytical techniques used to study plasma polymers

mass of deposited material is usually a great deal smaller than that of the substrate. Prolonged experiments will produce larger quantities of polymer, which can be collected from the walls of the reactor and analysed. Transmission infra-red experiments may be carried out more easily by depositing the plasma polymer onto a potassium bromide window.

Plasmas are often used to alter the surface properties of materials, and so surface characterisation techniques are usually more

applicable to plasma polymers. It is often very easy to apply surface techniques to such films, however the properties of the surface may not be representative of the bulk properties. It is often assumed that the initial surface characteristics of plasma polymers are generally considered to be representative of the bulk. If this assumption is made it is important to examine the product as quickly as possible before significant surface changes can occur. Exposure to air before analysis may cause some degree of surface oxidation as free radicals trapped in the polymer surface react with atmospheric oxygen. This will lead to an higher oxygen content at the surface than in the bulk.

1.6.2 Bulk Analysis

Plasma polymers examined by elemental analysis often show an increase in carbon content compared to the content of carbon in the monomer[100,101]. The elimination of other elements as volatile products during the plasma process is particularly marked with the halogens. The high carbon content, compared to the hydrogen content, is evidence of the cross-linked nature of these films. Oxygen is usually observed, resulting either from contamination or from reaction of the deposit with atmospheric oxygen.

Electron spin resonance (ESR) can detect the presence of unpaired spins in a material, and thus can be used to monitor the concentration of trapped free radicals in a plasma polymer[102]. It has been found that the trapped radicals have low mobilities probably due to cross-linking in the polymer, and that the highest concentrations of radicals result in films formed from highly unsaturated monomers. The fact that films with high free radical concentrations oxidise the

most quickly implies that the presence of free radicals is a large contributory factor to atmospheric oxidation.

The generally insoluble nature of plasma polymers makes them unsuitable to be studied by solution state NMR analysis. High resolution solid state NMR spectroscopy can be carried out on them[103] if enough material is made. The large number of non-identical but similar chemical environments in these materials give rise to broad peaks. Ethane, ethene and acetylene plasma polymers have been studied by ^{13}C NMR, showing the presence of $=CH_2$, CH, CH_2, CH_3 and quaternary carbon groups[103]. A large number of carbon atoms where not directly bonded to hydrogen, again suggesting a high degree of branching and cross-linking. Isotopically labelled materials can be used to identify the chemical environments a particular atom in the monomer finds itself in following plasma treatment. ^{13}C labelled toluene[104] has been plasma polymerised and NMR analysis has shown that some methyl carbon atoms become unsaturated and some ring atoms become saturated. This partial saturation of the ring atoms led to a proposed structure of plasma polymerised toluene, shown in figure 1.9.

The thermal decomposition of plasma polymers has been studied using differential scanning calorimetry[105]. There is no phase transition point where decomposition starts to occur, but a very gradual decomposition as the temperature is increased. The good thermal stability of plasma polymers is demonstrated by this experiment, and has been taken as evidence of cross-linking within the polymer. The complete absence of crystallinity has been demonstrated by X-ray diffraction techniques[106].

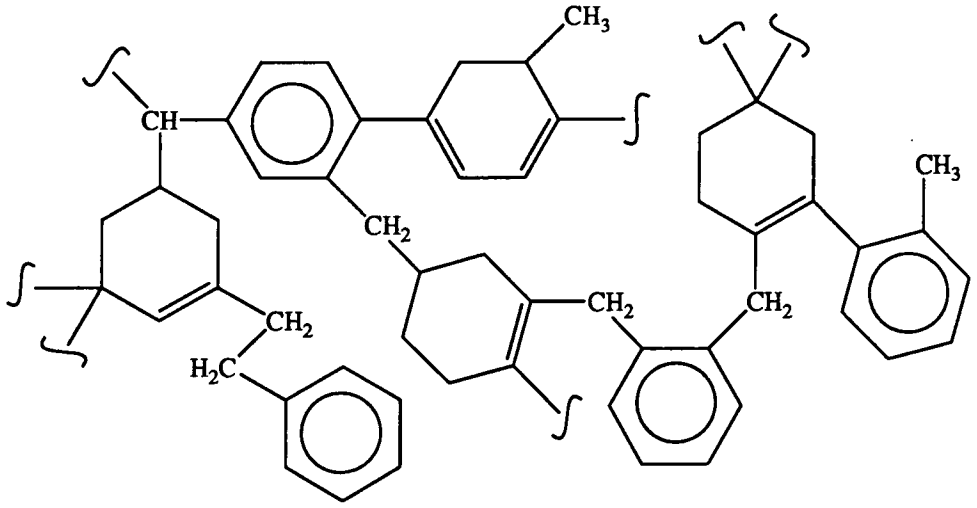

Figure 1.9 A proposed structure for plasma polymerised toluene

The structure of a number of hydrocarbon plasma polymers have been investigated using pyrolysis gas chromatography[107]. They were all found to be highly branched and cross-linked, partially unsaturated and containing short alkyl chains and aromatic rings. In powders formed at very high powers the amount of branching and cross-linking was found to be greater than those formed at lower powers. Toluene plasma polymers were found to have similar structures[108] using pyrolysis GC mass spectroscopy. In conjunction with isotopic labelling experiments this technique also gave evidence for the scrambling of the methyl and aromatic ring carbon atoms of toluene molecules subjected to a plasma environment, leading to the proposal of a tropylium cation intermediate. GC mass spectroscopy is highly useful in that each peak in the gas chromatogram can be firmly identified while the gas chromatography is taking place.

Neutron reflectivity measurements have recently been applied to plasma polymerised hydrocarbon films[109]. This technique involves reflecting a neutron "ray" through a thin film, see figure 1.10. The reflected intensity is dependent upon the constructive or destructive interference of neutrons reflected from each interface. Analysis of the

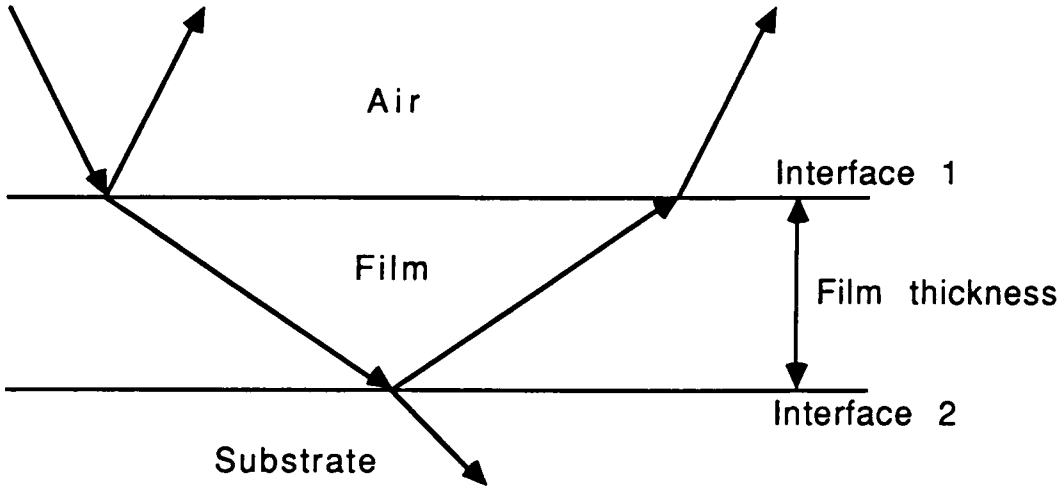

Figure 1.10 Passage of a neutron "ray" through a thin film

interference fringes gives accurate film thickness, film composition and an idea of the width of each interface. This experiment gave information on the carbon to hydrogen ratio of the films examined, information difficult to obtain using other techniques.

1.6.3 Infra-Red Spectroscopy

Both bulk and surface analysis can be carried out using infra-red spectroscopy, depending upon whether transmission or reflectance techniques are used. Reflectance infra-red is used to analyse surfaces but the depth to which it penetrates the sample is of the order of one wavelength (about 10 000 Å), which is much greater than techniques such as XPS and SIMS. Infra-red spectroscopy was commonly applied to plasma polymers, particularly in the 1960's and early 1970's when other forms of surface analysis were unavailable.

Infra-red spectra of plasma polymers often bear some relationship to the spectrum of the monomer or a conventional polymer of the monomer. Peaks in the spectra of the monomer tend to

become broader and less well defined upon plasma polymerisation. This indicates the formation of a large variety of slightly different chemical environments for each functional group within the product. Figure 1.11 shows the infra-red spectra of plasma polymerised N-vinyl pyrrolidinone prepared at high and low powers and compared with the spectrum of the monomer[110]. The broadening of the peaks can be seen clearly in the spectra of the solid films, especially in the case of the high power polymer. The presence of functional groups in the plasma polymer not present in the monomer can be detected by infra-red analysis. For example, in the 50W plasma polymer of NVP a peak at about 2200 cm^{-1} appears which the spectrum of the monomer does not have. This peak probably corresponds to C≡N, C≡C or N=C=O groups formed during the plasma polymerisation process, see figure 1.11.

The disappearance of certain peaks upon polymerisation may give an indication of the mechanism of polymerisation. In the case of NVP, the C=C peak at 1620 cm^{-1} is lost during the deposition process

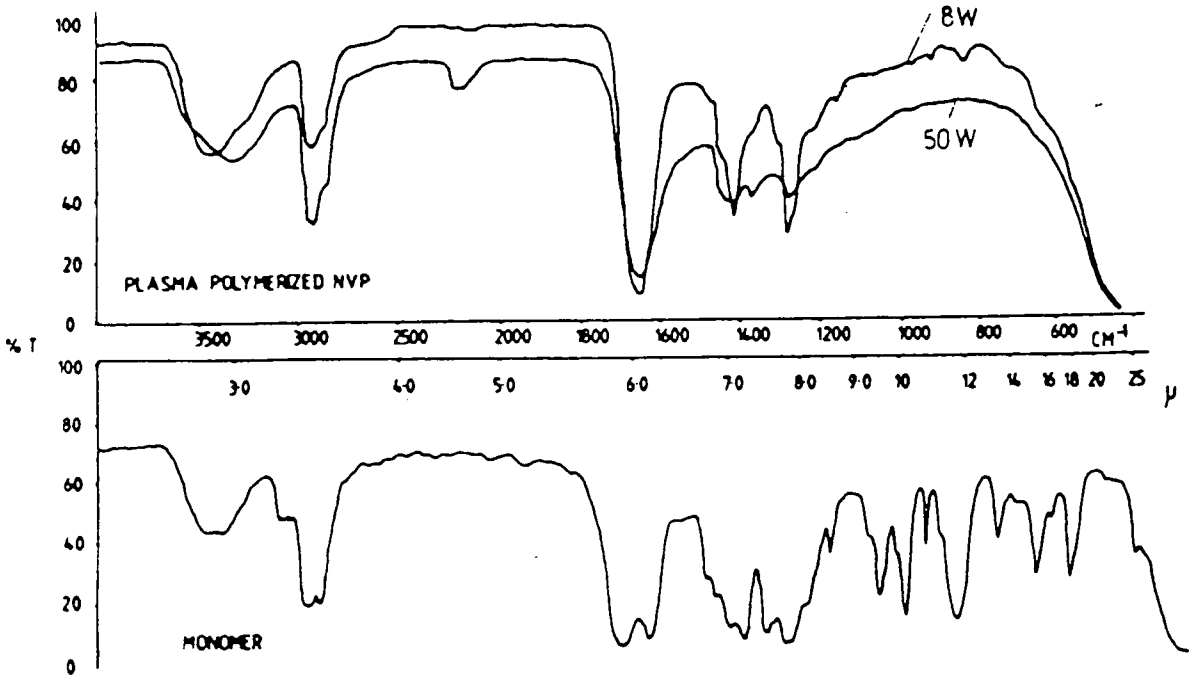

Figure 1.11 Infra-red spectra of plasma polymerised N-vinyl pyrrolidinone (NVP) and monomer

indicating that polymer formation occurs to a large extent through the opening of the carbon double bond in the manner of conventional addition polymerisation.

Infra-red analysis has been used to examine many aspects of plasma polymers, including the oxidation of a film upon aging, by following the growth of peaks associated with C=O and O-H groups[111]. The formation of fluorine containing cations at the boundary between a fluorocarbon plasma polymer and its substrate has also been studied by infra-red analysis[112].

1.6.4 Surface Analysis

The contact angle between a surface and a drop of liquid (usually distilled water) gives an indication of the surface energy of the material. With a number of liquids of known surface energy a fairly accurate value for the surface energy of a solid material can be calculated. Polar surfaces such as polymers with an high level of oxygen functionalities have large surface energies, and have small contact angles with water. Low energy surfaces, such as fluorocarbon polymers have a large contact angle with water. Plasma polymers can be deposited on a surface to give contact angles from zero[110] to almost 180°[113]. Very high and very low contact angles usually result from surface roughness, and therefore it is important to have a smooth surface if accurate contact angle measurements are to be made. Contact angle measurements are a quick and cheap method of obtaining information about a surface, but it cannot provide data on the chemical composition of the surface.

Electron microscopy has been used to examine the surface morphology of plasma polymers[114]. These studies show plasma

polymers to be mainly smooth and pinhole free, although those formed at high power and low flow rates tend to be rougher. The study of deposition characteristics of silicon containing films from plasmas is very important for the semi-conductor industry. Electron microscopy is often employed to study the thickness and evenness of the growth of such films[115].

Although scanning tunnelling microscopy (STM) and atomic force microscopy (AFM) have not been applied to plasma polymers they have recently been used on conventional polymers such as polyethylene[116]. The heights of structures at the surface of polyethylene were measured more accurately than they had previously been measured using electron microscopy, the same increased accuracy could be applied to plasma formed deposits. The disadvantage of these techniques is that a thin conducting layer sometimes has to be applied to the surface which may alter some of the features of the surface. Unlike most surface analytical techniques however, high vacuum equipment is not needed to operate STM or AFM making them relatively easy to use.

Secondary ion mass spectroscopy (SIMS) has not yet been applied to plasma polymers to a great extent, although its use on conventional polymers is well established[117]. The technique involves bombardment of the surface by a beam of high energy ions. The ablated fragments from the surface are analysed by mass spectroscopy. The two modes of use of SIMS are termed static SIMS, where a low ion current is rastered across the surface of the sample, and dynamic SIMS in which an high ion current is focused in a particular area and substantial material is ablated. The first mode avoids sampling material already damaged by the ion beam and is useful for chemical analyses of fragments. The latter mode (dynamic SIMS) is used as a depth profile technique, giving

information mainly on elemental composition. The comparison of static SIMS spectra of plasma polymers with conventional polymers and mass spectra of organic compounds can give considerable chemical information when coupled with other data, such as XPS.

1.6.5 X-ray Photoelectron Spectroscopy

X-Ray photoelectron spectroscopy (XPS), also known as ESCA (electron spectroscopy for chemical analysis), was first applied to plasma polymers in the 1970's[118], and has since become the standard technique for analysing plasma polymers. Samples are irradiated by a monochromatic X-ray source, and the energy of photoelectrons emitted from the surface of the sample are analysed. The binding energies of the electrons can be calculated from equation 1.6 where BE is the binding energy of the electron, hν is the energy of incident X-rays and KE is the measured energy of the escaped electron.

$$BE = h\nu - KE \qquad \text{Eq. 1.6}$$

XPS studies are most often used for examining the photoelectrons evolved from the core levels of particular elements. Each atomic core level of each element has a particular binding energy, and a knowledge of the sensitivity factor for each level can give a semi-quantative elemental analysis of a surface (accurate to about ± 5%). The only element which cannot be detected in a surface by XPS is hydrogen since it does not possess any core level electrons.

The removal of a core electron from an atom leaves a vacancy which is filled by an electron from an higher energy shell falling to occupy it. The energy of this transition is lost by one of two processes,

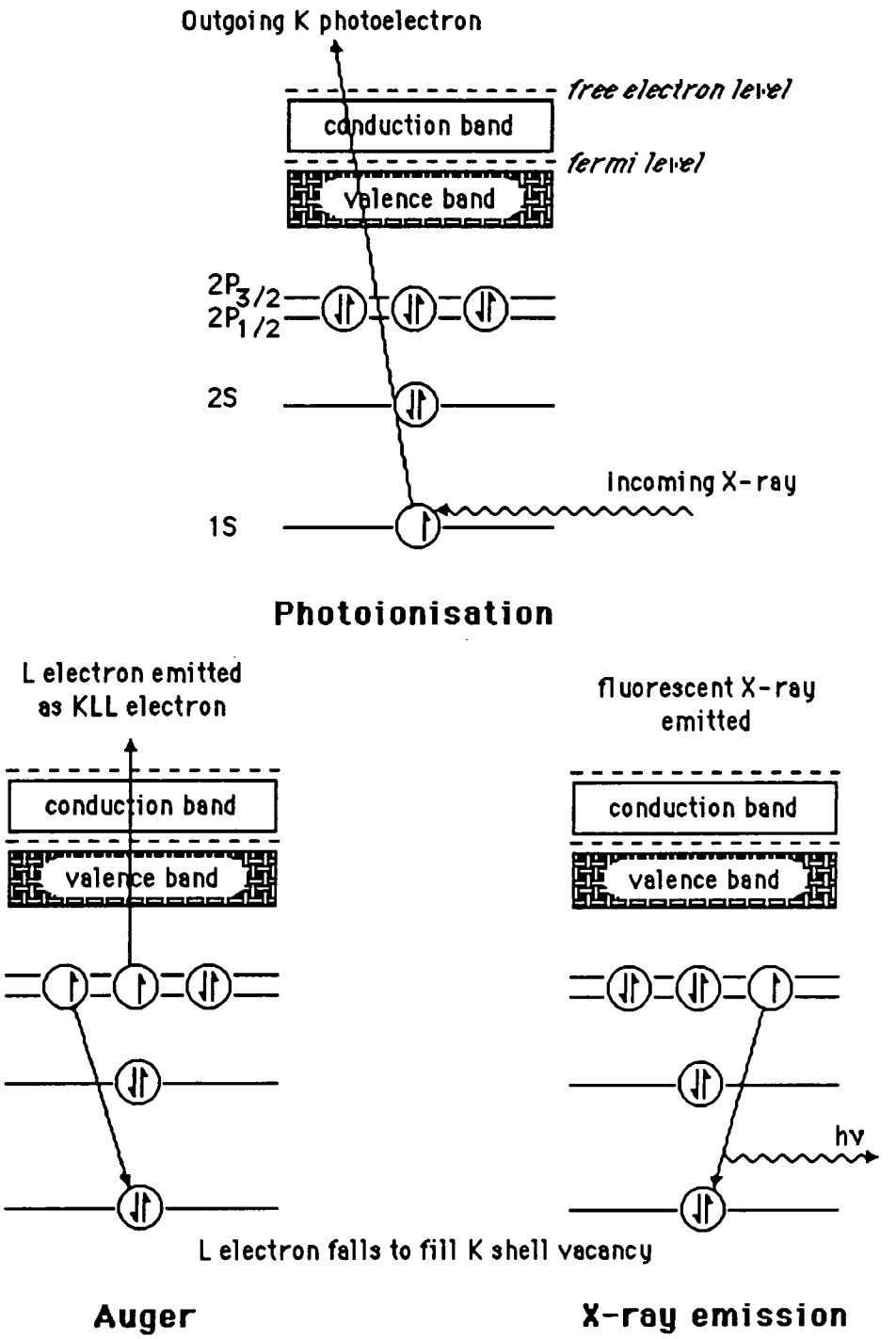

Figure 1.12 Photoionisation, Auger and X-ray fluorescence

Auger emission of an electron or X-ray fluorescence[119] (see figure 1.12). The energy of ejected Auger electrons is related to the energies of both valence and core orbitals, and not the energy of the exciting radiation. Auger peaks can be distinguished from photoelectrons by changing the

energy of the X-ray source. The excitation energy for photoionisation has no effect on the kinetic energy of the Auger electrons, but has on the photoelectrons, as equation 1.6 demonstrates. Analysis of Auger electrons is the key to Auger electron spectroscopy, which is used primarily for the analysis of metal and semiconductor surfaces and has been applied to PECVD formed material[82]. The large flux of electrons which is used for ionisation during Auger Electron Spectroscopy causes radiation damage to polymer surfaces, and so is not often used to study such materials[120].

The photoionisation event may also be accompanied by an excitation or emission of a valence electron. These processes are respectively termed shake-up and shake-off transitions, and are illustrated in figure 1.13. The shake up and shake-off processes give rise to satellite peaks appearing on the low kinetic energy side of the direct photoionisation peak. In organic compounds the presence of shake up satellites is indicative of aromatic species or other short range

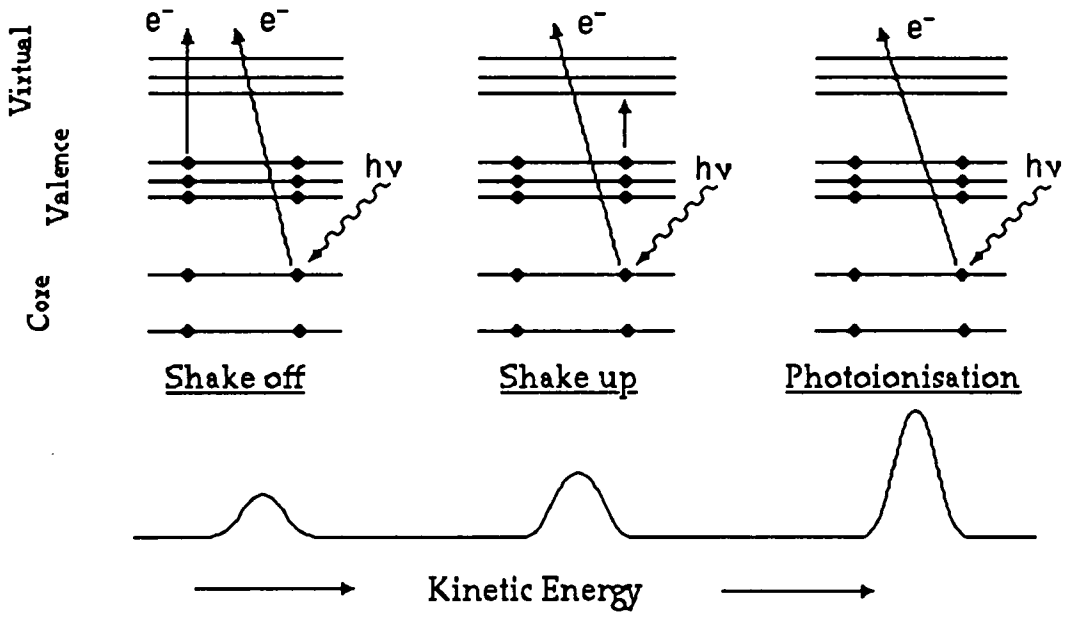

Figure 1.13 Photoionisation, shake-up and shake-off processes

unsaturations[121]. This peak generally arises from a π-π^* transition occuring simultaneously with the photoionisation event, and can be used as a probe for unsaturation in plasma polymers.

The electronic charge on an atom will have an influence upon the kinetic energy of the photoelectron leaving the atom. Electron withdrawing or donating groups bonded, or in close proximity to the atom will accordingly raise or lower the apparent binding energy of the electron leaving that atom. This change in binding energy is known as chemical shift, and is particularly useful for analysis of the C_{1S} core level in the presence if highly electron withdrawing elements, such as oxygen and fluorine. A good illustration of chemical shift is the C_{1S} spectrum of ethyl trifluoroacetate[122], shown in figure 1.14.

XPS samples to a depth of approximately 50 Å, the exact depth depending upon the mean free path of the electron in the solid. This sampling depth can be varied to allow a degree of depth profiling. One

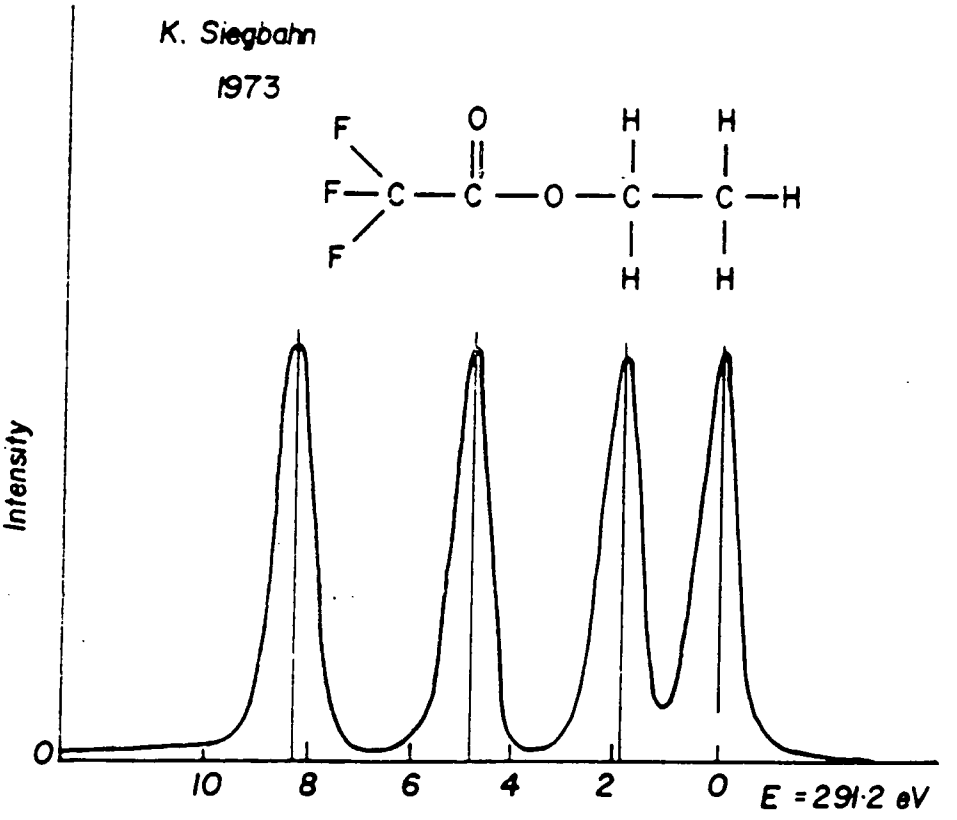

Figure 1.14 C_{1S} spectrum of ethyl trifluoroacetate

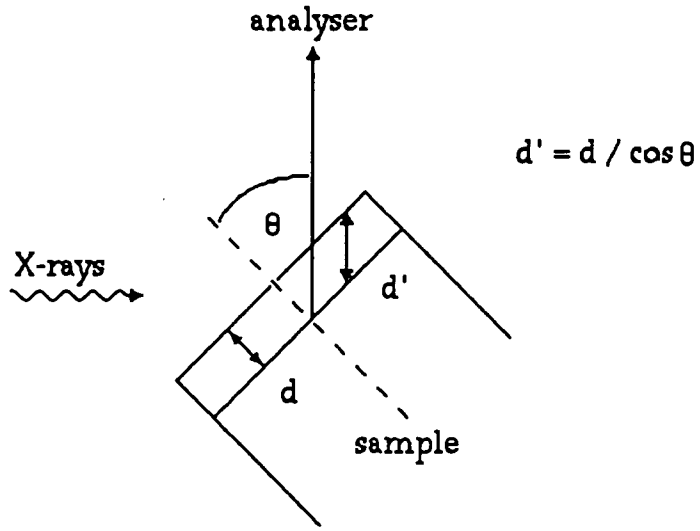

Figure 1.15 Effect of take off angle on sampling depth

wa of achieve in this is by altering the take off angle of electrons[123], see figure 1.15. At an high value of θ an electron from a certain depth (d) has to travel through more of the sample to reach the analyser (actual distance d') than at a low angle. Examination of two different core levels of the same element (for example O_{1S} and O_{2S}) can also give depth profiling, the electron mean free path for electrons from each level is different as they have differing kinetic energies.

The principle method of analysis used in these studies is XPS, which is generally a very powerful tool for examining glow discharge polymers. Core level spectra from XPS give little information, however, about hydrocarbon polymers, and, as for all forms of surface analysis, the sample must be clean because even a very thin layer of contamination will obscure the signal from the sample.

References

1 A.T. Bell in "Techniques an Applications of Plasma Chemistry", Chap.1, Eds. J. R. Hollahan, A. T. Bell, Wiley, New York,(1974)

2 CRC Handbook of Chemistry and Physics, Ed. R. C. Weast, (1982)

3 W. L. Fite in "Chemical Reactions in Electrical Discharges" Ed. R. F. Gould, ACS, Advances in Chemistry Series, Washington DC, (1969)

4 K.Upudha, *Trans. Ind. Ins. Met.*, **38**, 472, (1985)

5 A. C. Gray, *Spectrochim. Acta*, **40B**, 1525, (1985)

6 S. C. Brown in "Gaseous Electronics", Vol. 1, Eds. M. N.Hirsh, H. J.Oskan,Academic Press, New York, (1978)

7 J. S. Townsend, *Phil. Mag.*, **8**, 733, (1904)

8 L. Tonks, I. Langmuir, *Phys. Rev.*, **33**, 195, (1929)

9 "Electrical Breakdown of Gases", Eds. Meek and Craggs, Wiley, New York, (1978)

10 H. F. Beer, thesis, Durham University, (1980)

11 P. Brassem and F. J. M. J. Massen, *Spectrochimica Acta*, **29B**, 203, (1974)

12 D. T. Clark and A. Dilks in "Characterisation of metal and polymer surfaces" chapter 2, vol.2, Ed. L. H.Lee, Academic press, New york. (1977)

13 Y. I. Shmykov, S. N. Shorin, A. L. Suris, N. L. Volodon, V. T. Dyatlov, Y. V. Irzinger, A. M. Tukhvatullin, *Khim. Vys. Energ.*, **11**, 371, (1977)

14 H. Suhr, U. Schucker, *Synthesis*, **431**, (1970)

15 C. Boelhouwer, H. I. Waterman, *Research(London)*, **9**, 5511, (1956)

16 I. Platzner, P. Marcus, *Int. J. Mass Spectrom. Ion Phys.*, **41**, 241, (1982)

17 R. E. McIntosh, M. S. Kotfila, *IEEE Trans. Plasma Sci.*, **9**, 63, (1981)

18 A. M. Howatson, "An Introduction to Gas Discharges", 2nd Ed., Pergamon, (1976)

19 D. T. Clark, A. Dilks, D. Shuttleworth, in chap.9 of "Polymer Surfaces", Eds. D. T. Clark, W. J. Feast, Wiley, New York, (1978)

20 H. Suhr in Ref. 2, Chap. 3

21 R. D'Agostino, F. Cramarossa, F. Illuzi, *J. Appl. Phys.*, **61**, 2754, (1987)

22 a C. I. Simonescu, F. Denes, *Cellulose Chem. Technol.*, **14**, 285, (1980)

b A. E. Pavlath, K. E. Lee, *J. Macromol. Sci. Chem.*, **A10**, 579, (1976)

23 D. M. Soignet, R. J. Berni, R. R. Banerito, *J. Appl. Polym. Sci.*, **20**, 2483, (1976)

24 M. M. Millard, K. S. Lee, A. E. Pavlath, *Text. Res. J.*, **42**, 307, (1972)

25 M. M. Millard, A. E. Pavlath, *Text. Res. J.*, **42**, 460, (1972)

26 P. M. Tricolo, J. D. Andrade, *J. Biomed. Mater. Res.*, **17**, 129, (1983)

27 D. Youxian, H. J. Griesser, A. W.-H. Man, R. Schmidt, J. Liesegang, *Polymer*, **32**, 6, 1126, (1991)

28 M. Strobel, S. Corn, L. S. Lyon, G. A. Korba, *J. Polym. Sci., Polym. Chem. Ed.*, **23**, 1125, (1985)

29 L. T. Nguyen, N. H. Sung, N. P. Suh, *J. Polym. Sci., Polym. Chem. Ed.*, **18**, 541, (1980)

30 R. W. Kirk, "Applications of Plasma Technology to the Fabrication of Semiconductor Devices" in Ref. 2

31 B. Chapman, "Glow Discharge Processes", Wiley-Interscience, New York, (1980)

32 R. J. Saia, R. F. Kwasnick, C. Y. Wei, *J. Electrochem. Soc.*, **138**, 2, 493, (1991)

33 C. Haag, H. Suhr, *Plasma Chem., Plasma Proc.*, **6**, 197, (1986)

34 H. Yasuda in "Plasma Polymerisation", Academic Press, London, (1985)

35 J. R. Hollahan, R. S. Rossler in "Thin Film Processes", Eds. J. Vossen, W. Kern, Academic press, New York, (1979)

36 C. Oehr, H. Suhr, *Appl. Phys.*, **A45**, 151, (1988)

37 a L. S. Vanasupa, M. D. Deal, J. D. Plummer, *J. Electrochem. Soc.*, **138**, 3, 870, (1991)
b R. Chow, W. A. Lanford, W. Ke-Ming, R. S. Rosler, *J. Appl. Phys.*, **53**, 8, 5630, (1982)

38 T. T. Chau, S. R. Mejia, K. C. Cao, *J. Electrochem. Soc.*, **138**, 1, 325, (1991)

39 H. Suhr, C. Oehr, H. Holtzschuh, F. Schmaderer, G. Wahl, T. Kruck, A. Kinnen, *Physica C*, **153-155**, 784, (1988)

40 Y. Osada, M. Hashidzume, E. Tsuchida, A. T. Bell, *Nature*, **286**, 693, (1980)

41 R. A. Gottscho, T. A. Miller, *Pure. Appl. Chem.*, **56**, 189, (1984)

42 H. S. Munro, C. Till, *J. Polym. Sci., Polym. Chem. Ed.*, **24**, 279, (1986)

43 H. Kawasaki, Y. Matsuda, H. Fujiyama, *IEEE Trans. Plasma Sci.*, **19**, 445, (1991)

44 R. d'Agostino, *Polym. Mater. Sci. Eng.*, ACS, Denver, **56**, 221, (1987)

45 a S. Pang, S. R. J. Brueck in "Laser Diagnostics and Photochemical Processing for Semiconductor Devices" Eds. R. M. Osgood, S. R. J. Brueck, H. R. Schlossberg, North Holland, New York, (1983)
b P. J. Hargis Jr., M. J. Kushner, *Appl. Phys. Lett.*, **40**, 779, (1982)
c D. Mataras, S. Cavadias, D. E. Rapakoulias, *Int. Symp. Plasma Chem.* 9, **3**, 1293, (1989)

46 A. Margulis, J. Jolly, *Revue Phys. Appl.*, **24**, 323, (1989)

47 a H. Sakai, P. Hansen, M. Esplin, R. Johansson, M. Peltola, *J.Strong, Appl. Opt.*, **21**, 228, (1982)
b H. U. Poll, D. Hinze, H. Schlemm, *Appl. Spec.*, **36**, 445, (1982)

48 a M. J. Vasile, G. Smolinsky, *Int. J. Mass Spectrom. Ion Phys.*, **12**, 133, (1973)

b M. J. Vasile, G. Smolinsky, *J. Phys. Chem.*, **81**, 2605, (1977)

49 Z. Petrovic, B. Jelenkovic, S. Vrhovac, S. Radovanov, *Int. Symp. Plasma Chem.* 9, **1**, 217, (1989)

50 S. Ono, A. Suzuki, S. Teii, J. S. Chang, *Int. Symp. Plasma Chem.* 9, **1**, 174, (1989)

51 a A. J. Bariya, C. W. Frank, J. P. Mcvittie, *J. Electrochem. Soc.*, **137**, 8, 2575, (1990)
b M. Maurizio, M. Morbidelli, S. Carra, *Int. Symp. Plasma Chem.* 9, **1**, 145, (1989)

52 J. Goodman, *J. Polym. Sci., Lett. Ed.*, **44**, 144, (1960)

53 a P. DeWilde, *Ber.*, **7**, 352, (1874)
b P. Thernard, *Compt. Rend.*, **78**, 218, (1874)

54 H. Yasuda, T. Hsu, *Surf. Sci.*, **76**, 232, (1978)

55 E. Kay, Invited Paper, *Int. Round Table Plasma Polym. Treat., IUPAC Symp. Plasma Chem.*, (1977)

56 H. Yasuda, T. Hirotsu, *J. Polym. Sci., Polym. Chem. Ed.*, **16**, 743, (1976)

57 Y. S. Yeh, I. N. Shyy, H. Yasuda, *ACS Polym. Mater. Sci.*, **56**, 141, (1987)

58 D. F. O'Kane, D. W. Rice, *J. Macromol. Sci. Chem.*, **A10**, 567, (1976)

59 M. Hori, H. Yamada, T. Yoneda, S. Morita, S. Hattori, *J. Electrochem. Soc.*, **134**, 707, (1985)

60 W. D. Freitag, H. Yasuda, A. K. Sharma, *Org. Coat. Appl. Polym. Sci. Proc.*, **47**, 449, (1982)

61 T. Wydeven, C. C. Johnson, *Polym. Prep. Am. Chem. Soc., Div. Polym. Chem.*, **21**, 62, (1980)

62 M. Kobale, H. Pachonik, Ger. Patent, 2 105 003, (1972)

63 J. C. Dubois, Fr. Patent, 2 379 889, (1978)

64 N. Inagaki, H. Yasuda, *J. Appl. Polym. Sci.*, **26**, 3333, (1981)

65 M. M. Millard, A. E. Pavlath, *J. Macromol. Sci., Chem. Ed.*, **A10**, 579, (1976)

66 M. Kuriaki, M. Hasebe, Y. Miwa, Y. Mizutani, *Kobunshi Ronbunshu*, **42**, 11, 841, (1985)

67 a H. Yasuda, *Appl. Polym. Symp.*, **22**, 241, (1973)
b J. Sakata, M. Hirai, I. Tajima, M. Yamamoto, *ACS Polym. Mater. Sci. Eng.*, **56**, 802, (1987)

68 Z. Ogumi, Y. Uchimoto, K. Yasuda, Z. Takehara, *Chem. Lett.*, **6**, 953, (1990)

69 N. Inagaki, Y. Hashimoto, *ACS Polym. Mater. Sci. Eng.*, **56**, 515, (1987)

70 A. S. Hoffman, *ACS Polym. Mater. Sci. Eng.*, **56**, 699, (1987)

71 H. Suhr, A. Etspuler, E. Feurer, C. Oehr, *Plasma Chem. Plasma Process.*, **8**, 1, (1988)

72 a J. Batey, E. Tierney, J. Stasiak, T. N. Nguyen, *Appl. Surf. Sci.*, **39**, 1, (1989)
b N. N. Selamoglu, J. A. Mucha, D. E. Ibbotson, D. L. Flamm, *J. Vac. Sci. Technol.*, **B7** (6), 1345, (1989)

73 G. Lucovsky, D. V. Tsu, *J. Non-Crystalline Solids*, **97-98**, 265, (1987)

74 H. Biederman, L. Martinu, D. Slavinska, I. Chudacek, *Pure Appl. Chem.*, **60**, 607, (1988)

75 T. Venkatesan, *J. Vac. Sci. Technol.*, **19**, 1379, (1981)

76 E. Kay, A. Dilks, *J. Vac. Sci. Technol.*, **18**, 1, (1981)

77 Y. Asano, *Thin Solid Films*, **105**, 1, (1983)

78 a E. Kny, *Thin Solid Films*, **64**, 395, (1979)
b N. Inagaki, T. Yagi, K. Katsuura, *Eur. Polym. J.*, **18**, 621, (1982)
c N. Inagaki, M. Mitsuuchi, *J. Polym. Sci., Polym. Lett. Ed.*, **22**, 301, (1984)

79 H. Suhr, J. Bald, L. Deutschmann, E. Feurer, H. Holzschuh, J. Messelhausser, C. Oehr, S. Reich, R. Schmidt, B. Waimer, A. Weber, H. Wendel, *Int. Symp. Plasma Chem.* 9, **3**, 1287, (1989)

80 C. Oehr, H. Suhr, *Appl. Phys.*, **A45**, 151, (1988)

81 H. Nomura, S. Meikle, Y. Nakanishi, Y. Hatanaka, *J. Appl. Phys.*, **69**(2), 990, (1991)

82 J. G. Eaves, Ph. D. thesis, Durham University, (1986)

83 E. Feurer, H. Suhr, *Appl. Phys.*, **A44**, 171, (1987)

84 H. Abe, T. Tsuruoka, T. Nakamori, *Jap. J. Appl. Phys.*, **27**(3), L1473, (1988)

85 Matsushita Electric Co., Eur. Patent Appl., 86 300 848.8, (1986)

86 D. M. Brewis, D. Briggs, *Polymer*, **22**, 7, (1981)

87 G. Schaefer, P. F. Williams, K. H. Schoenbach, J. T. Moseley, *IEEE Trans. Plasma Sci.*, **11**, 263, (1983)

88 A. VonEngel, "Electronic Plasmas, their Nature and Uses", Plenum Press, New York, (1972)

89 G. M. Porta, J. D. Rancourt, L. T. Taylor, *Polym. Mater. Sci. Eng.*, ACS, Washington D. C., **63**, 87, (1990)

90 K. Fujimoto, Y. Ueda, Y. Takebayashi, Y. Ikeda, *Polym. Mater. Sci. Eng.*, ACS, Boston, **62**, 284, (1990)

91 N. Nakayama, T. Takahagi, F. Soeda, K. Hatada, S. Nagaoke, J. Suzuki, A. Ishitani, *J. Polym. Sci., Polym. Chem. Ed.*, **26**, 559, (1988)

92 a D. T. Clark, A. Dilks, *J. Polym. Sci., Polym. Chem. Ed.*, **15**, 15, (1977)

b D. T. Clark, A. Dilks, *J. Polym. Sci., Polym. Chem. Ed.*, **15**, 2321, (1977)

c D. T. Clark, A. Dilks, *J. Polym. Sci., Polym. Chem. Ed.*, **17**, 957, (1979)

d D. T. Clark, A. Wilson, *J. Polym. Sci., Polym. Chem. Ed.*, **21**, 15, (1983)

93 H. Yasuda, A. K. Sharma, *J. Polym. Sci., Polym. Phys.*, **19**, 1285, (1981)

94 S. Walker, PhD Thesis, Durham University, (1990)

95 H. S. Munro, D. I. McBriar, *Polym. Mater. Sci. Eng.*, ACS, Denver, **56**, 337, (1987)

96 J. R. MacCallum in "Comprehensive Polymer Science", Eds. G. Allen, J. C. Bevington, Pergamon, Oxford, **6**, 529, (1989)

97 M. Suzuki, A. Kishida, H. Iwata, Y. Ikada, *Macromol.*, **19**, 1804, (1986)

98 S. Kaizerman, G. Mino, L. F. Mienhold, *Text. Res. J.*, **32**, 136, (1962)

99 T. O. Glaseby, private communication

100 H. Yasuda, M. O. Bumgarner, H. C. Marsh, N. Morosoff, *J. Polym. Sci., Polym. Chem. Ed.*, **14**, 195, (1976)

101 A. R. Westwood, *Eur. Polym. J.*, **7**, 377, (1971)

102 N. Morosoff, B. Crist, M. Bumgarner, T. Hsu, H. Yasuda, *J. Macromol. Sci. Chem.*, **A10**, 451, (1976)

103 A. Dilks, S. Kaplan, A. VanLaeken, *J. Polym. Sci., Polym. Chem. Ed.*, **19**, 2987, (1981)

104 S. Kaplan, A. Dilks, *J. Polym. Sci., Polym. Chem. Ed.*, **21**, 1819, (1983)

105 L. F. Thomson, K. J. Mayhan, *J. Appl. Polym. Sci.*, **16**, 2991, (1972)

106 H. Kobayashi, M. Shen, A. T. Bell, *J. Appl. Polym. Sci.*, **18**, 885, (1973)

107 M. Seeger, R. J. Gritter, J. M. Tibbet, M. Shen, A. T. Bell, *J. Polym. Sci., Polym. Chem. Ed.*, **15**, 1403, (1977)

108 S. Kaplan, A. Dilks, R. Crandall, *J. Polym. Sci., Polym. Chem. Ed.*, **24**, 1173, (1986)

109 R. M. Richardson, M. J. Grundy, S. J. Roser, G. Beamson, W. J. Brennan, J. Howard, M. O. Neil, R. C. Ward, J. Penfold, C. Shackleton, *Int. Symp. Plasma Chem.* 9, **3**, 1450, (1989)

110 C. Till, Ph. D. Thesis, Durham University, (1986)

111 H. Yasuda, H. C. Marsh, M. O. Bumgarner, N. Morosoff, *J. Appl. Polym. Sci.*, **19**, 2845, (1975)

112 Y. Haque, B. D. Ratner, *J. Polym. Sci., Polym. Phys.*, **26**, 1237, (1988)

113 M. Klausner, I. H. Loh, *ACS Polym. Mater. Sci. Eng.*, **56**, 227, (1987)

114 M. Niionomi, H. Kobayashi, A. T. Bell, M. Shen, *J. Appl. Phys.*, **44**, 4317, (1973)

115 A. Nagata, M. Nakano, H. Kawamoto, M. Hirose, Y. Horiike, *Int. Symp. Plasma Chem.* 9, **3**, 1377, (1989)

116a R. Patil, S.-J. Kim, E. Smith, D. H. Reneker, A. L. Weisenhorn, *Polym. Comm.*, **31**, 12, 455, (1990)
b D.H. Reneker, J. Schreir, B. Howell, H. Harary, *Polym. Comm.*, **31**, 5, 167, (1990)
c R. Pirer, R. Reifenberger, D. C. Martin, E. L. Thomas, R. P. Apkarian, *J. Polym. Sci., Polym. Lett. Ed.*, **28**, 13, 399, (1990)

117 A. Brown, J. C. Vickerman, *Surf. Interface Anal.*, **8**, 75, (1986)

118a D. T. Clark, D. Shuttleworth, *J. Polym. Sci., Polym. Chem. Ed.*, **16**, 1093, (1978)
b D. T. Clark, A. Dilks, D. Shuttleworth in "Polymer Surfaces", Eds. D. T. Clark, W.J. Feast, Wiley, London, (1978)

119 K. Siegbahn, C. Nordling, A. Fahlman, R. Nordberg, K. Hamrin, J. Hedman, G. Johansson, T. Berkmark, S. E. Karlsson, I. Lidgren, B. Lindberg in "ESCA, Atomic, Molecular and Solid State Structure Studied by means of Electron Spectroscopy", Almquist and Wiksells, Uppsalla, (1967)

120 J. P. Coad, M. Getting, J. G. Riviere, *Farad. Disc. Chem. Soc.*, **60**, 269, (1975)

121 D. T. Clark, A. Dilks, *J. Polym. Sci., Polym. Chem. Ed.*, **14**, 533, (1976)

122 K. Siegbahn, C. Nordling, G. Johansson, J. Hedman, P. F. Heden, K. Hamrin, U. Gelius, T. Berkmark, L. D. Werme, R. Manne, Y. Baer in "ESCA Applied to Free Molecules", North Holland Pub. Co., Amsterdam, (1969)

123 D. T. Clark, A. Dilks, *J. Polym. Sci., Polym. Chem. Ed.*, **15**, 2321, (1977)

Chapter 2

Plasma Polymerisation of some Highly Fluorinated Monomers

2.1 Introduction

The polymerisation of some fluorinated monomers within a glow discharge has received attention previously. Clark *et. al.* studied deposits from a series of fluorinated monomers including benzene derivatives, and some other perfluorocyclic compounds. The highly electronegative nature of fluorine atoms enables such plasma polymers to be very effectively examined by XPS[1]. The C_{1S} region is easily deconvoluted into differing carbon atom environments. Many other perfluorocarbons have been used as starting compounds for plasma polymerisation, such as perfluorotoluene[2], perfluoropropane[3], tetrafluoroethylene[4], and a range of perfluoroalkanes[5]. In the cases of tetrafluoromethane and hexafluoroethane the ablation rate is higher than the rate of polymerisation with the result that these gases are often used as etchants.

The compositions of the products shows that considerable rearrangement of the monomer occurs during the plasma polymerisation process. For instance, the plasma polymer of perfluorobenzene will often contain a considerable density of CF_2 and CF_3 groups (as shown by XPS)[1] which are not present in the monomer. Yasuda attributes the major mechanism of perfluorocarbon plasma polymerisation to the reaction of difunctional or multifunctional activated species[6] (cycle 2 in figure 1.5). The detachment of fluorine atoms from the monomer results in reactive fluorine species being generated which will participate in further reactions with species in the gas phase. The generation of molecular fluorine is disfavoured energetically due to the low F-F bond strength (157 kJ mol^{-1}, compared with C-F bond strength ≈ 490 kJ mol^{-1}). Other work has shown[7] that CF_x radicals play a major role in the production

of polymer forming intermediates. However, the similarity of plasma polymers and photopolymers of highly unsaturated systems such as perfluorobenzene and perfluorotoluene imply that the major route of polymer formation for these compounds is through electronically excited intermediates, and that ion chemistry is not involved to a significant degree[8].

In general, plasma polymerised fluorocarbon films exhibit high chemical stability, low surface energies and low coefficients of friction, their main disadvantages compared to hydrocarbon plasma polymers is their poor adhesion to substrates and their softness[3]. Adhesion can be improved by cleaning the substrate thoroughly, although the formation of inorganic fluorides at the interface between substrate and polymer[9] may have an effect. The surface energy of a typical perfluoro plasma polymer is similar, but often not as low as conventional polytetrafluoroethylene (PTFE), whereas coefficients of friction for such materials are quite a lot larger than PTFE (typically 0.12 against steel[10], compared with PTFE; 0.04 against steel[11]). The reason for the difference in frictional properties is most likely due to the ability of PTFE chains to orientate and "slide" over each other[12], which is not possible for highly cross-linked plasma polymers (or polymers with bulky side groups).

The production of waterproof fabrics by plasma polymerisation of perfluorocarbons relies upon the low surface energies of the coating[5]. The advantage of processing fabrics in this way is that cheap materials can be waterproofed by an easy one step method, and have permeability to water vapour, a property that most conventional waterproof fabrics lack. Hexafluoropropene has been plasma polymerised to produce gas separation membranes[13], the monomer showing an affinity for oxygen (it is well known that oxygen is highly

soluble in perfluorocarbon liquids, and these have been used as blood substitutes). When plasma polymerised by itself or with methane, the films formed have a greater permeability to oxygen than to nitrogen. Plasma polymers from tetrafluoroethylene are used to coat tubes through which blood passes, the aggregation of platelets on such surfaces is minimal and they are considered relatively nonthrombogenic[14].

In this chapter, plasma polymers of perfluorinated monomers are investigated and by comparison between different monomers the proposed mechanisms of polymerisation (i.e. excited state *versus* fragmentation) are considered. The effects of power and flow rate are examined with two structurally dissimilar monomers. In chapter 3 the effect of the site of deposition within the reactor is investigated. Analysis of the surfaces produced was carried out using XPS, SIMS and contact angle measurements.

2.2 Experimental

2.2.1 Plasma Polymerisation

All plasma polymerisations were carried out in a cylindrical glass reactor (21.5 cm. long, 5 cm. diameter) inserted into an all glass, grease free vacuum line. The system is shown schematically in figure 2.1. Flanged joints were sealed with viton O rings, and all other connections were made with Cajon ultra torr couplings. Vacuum taps were sealed with PTFE stoppers. The whole apparatus was evacuated to a pressure of $\sim 3 \times 10^{-2}$ mbar using an Edwards E2M2 two stage rotary pump, protected by a cold trap. The pressure of the system was measured using an Edwards PR10-S pirani gauge. The plasma was

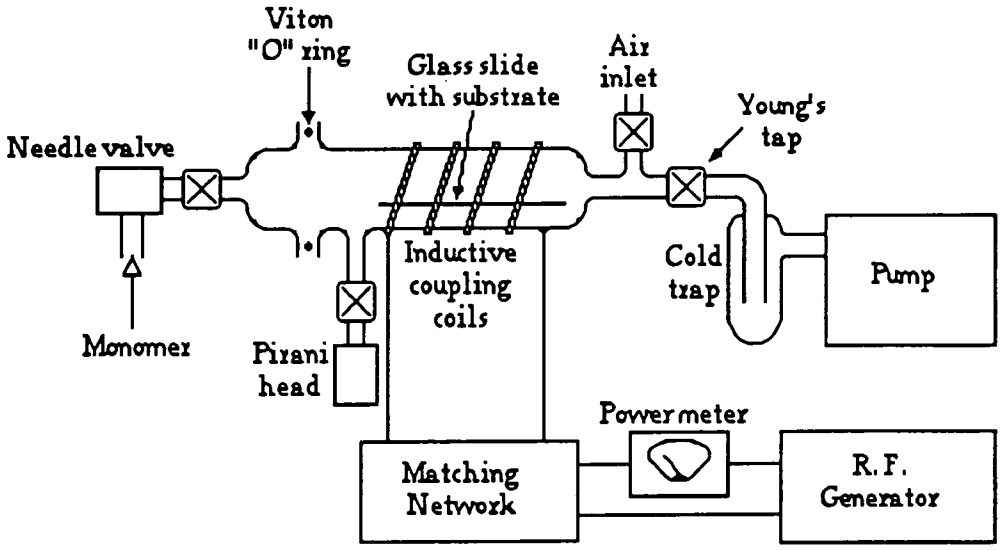

Figure 2.1 Schematic of equipment used for plasma polymerisation

generated by a 13.56 MHz R. F. generator inductively coupled to the reactor through an eight turn copper wire.

At the start of each experiment, the leak rate of the system was checked by isolating the pump from the reactor and measuring the time for a given pressure rise to occur. A high leak rate can lead to oxygen incorporation into the plasma polymer. If the leak rate was acceptable, then the monomer was introduced into the reactor through the needle valve. The flow rate of the monomer was measured in the same way as the leak rate. The pirani head was then shut off from the reactor before igniting the plasma to prevent damage to it. After ignition the plasma was balanced using an L-C matching network to give as low a standing wave ratio as possible. The power meter was employed to monitor the the R. F. power and the standing wave ratio. (Standing wave ratio (SWR) = Total power generated / Power transmitted to plasma.) The plasma polymer was collected on aluminium and glass substrates placed on the glass slide within the coil region of the reactor. Deposition was allowed to occur for 15 to 20

minutes. The reactor was then let up to atmosphere and the samples transported through air to be analysed.

The monomers used in this study were perfluorobenzene (PFB; 99% purity), perfluorohexane (PFH; 99%), perfluorodecalin (PFD; mixture of cis and trans isomers, 95%), perfluorocyclohexene (PFCH; 99%) and hexafluoropropene (HFP; 99+%). These were supplied by Aldrich and used without further purification. All monomers (with the exception of hexafluoropropene) were degassed before use by alternating freeze thaw cycles.

2.2.2 Analysis

XPS analyses were collected on either a Kratos ES200 or ES300 spectrometer in fixed retarding ratio mode using Mg K $\alpha_{1,2}$ X-rays of 1253.6 eV energy. Samples were mounted on a probe tip approximately 17 mm. by 8 mm., using double sided adhesive tape and, unless otherwise stated, a take off angle of 30° was used. C_{1S} component peaks were assigned by reference to the experimentally determined binding energies of various functionalities in standard samples[1c], and are constant to within ± 0.3 eV.

Contact angles of the plasma polymers with water were measured using the sessile drop technique.

Positive SIMS analysis was performed in a Perkin Elmer 5400 surface analysis instrument, using the static mode with a 4 keV Xe^+ ion source and a beam current of 1 nA.

2.2.3 Calculation of Flow and Leak Rates

At the pressures used for plasma polymerisation gases and vapours can be considered to behave according to the ideal gas law, see equation 2.1

$$PV = nRT \qquad \text{Eq. 2.1}$$

Where P is pressure, V is the volume of the reactor, n the number of moles of gas, R is the gas constant and T is the temperature in degrees Kelvin. Based on this, the flow rate and the leak rate can be calculated from the rate of pressure increase in the system when pumping is closed off.

$$\text{flow rate} = \frac{dn}{dt} = \frac{dP}{dt} \cdot \frac{V}{RT} \quad \text{mol sec}^{-1} \qquad \text{Eq. 2.2}$$

At STP one mole of gas occupies 22414 cm^3. Converting time to minutes and volume to litres, this leads to equation 2.3.

$$\text{flow rate} = 74.4\ V \frac{dP}{dt} \quad cm^3_{STP} / \text{min} \qquad \text{Eq. 2.3}$$

Leak rates can be calculated using the same formula; for accurate measurement of flow rates the leak rate should be subtracted from the measured flow rate, but in all cases the leak rate was very small compared to the flow rate and considered negligible.

2.3.1 Fluorocarbon Plasma Polymers from Monomers of Varying Unsaturation

Plasma polymers of perfluorobenzene (PFB), perfluorocyclohexene (PFCH), perfluorodecalin (PFD), hexafluoropropene (HFP) and perfluorohexane (PFH) were made at conditions of 20 W power, and flow rate of 0.5 cm^3 sec^{-1}. XPS analysis showed that all monomers formed a fluorocarbon film under these operating conditions. Some of the polymers exhibited small peaks in the O_{1S} (oxygen) region; oxygen incorporation occuring either during plasma polymerisation (due to the small leaks), or reaction of free radicals in the film with atmospheric oxygen upon exposure to air. No signal was found in the Al_{2P} (aluminium) region indicating that the films were uniformly at least 70 Å thick.

In all cases the C_{1S} spectra contained signals corresponding to a wide range of carbon environments. The component peaks and their binding energies[1] are shown with the relevant intensities of that peak for a given monomer in table 2.1. The peaks were assumed to be gaussian in shape, and the intensities and width were altered to give the best fit, an example is shown in figure 2.2. A shake up peak due to π-π^* transitions was sometimes observed at a binding energy of 295.2 eV, which is indicative of a degree of unsaturation in the plasma polymer. A small amount of hydrocarbon was found on all samples, probably present as contamination on the surface of the film.

The fluorine to carbon ratio was determined in two ways, firstly by dividing the total F_{1S} peak area by the C_{1S} area, taking into account

		% Contribution to C_{1S} Area				
Assigned Peak	Binding Energy	PFB	PFCH	PFD	HFP	PFH
$\underline{C}H$	285.0 eV	7.3	1.0	1.8	3.7	2.5
$\underline{C}$-CF_n	286.6 eV	18.0	15.0	13.4	14.0	14.7
$\underline{C}F$	288.3 eV 289.5 eV	41.7	30.2	27.9	30.5	24.2
$\underline{C}F_2$	291.2 eV	24.6	30.2	32.3	28.6	33.2
$\underline{C}F_3$	293.3 eV	7.5	23.0	24.2	23.2	25.4
π-π^*	295.2 eV	0.9	0.6	0.4	0.0	0.0

Table 2.1 Composition of plasma polymers of some perfluorocarbons

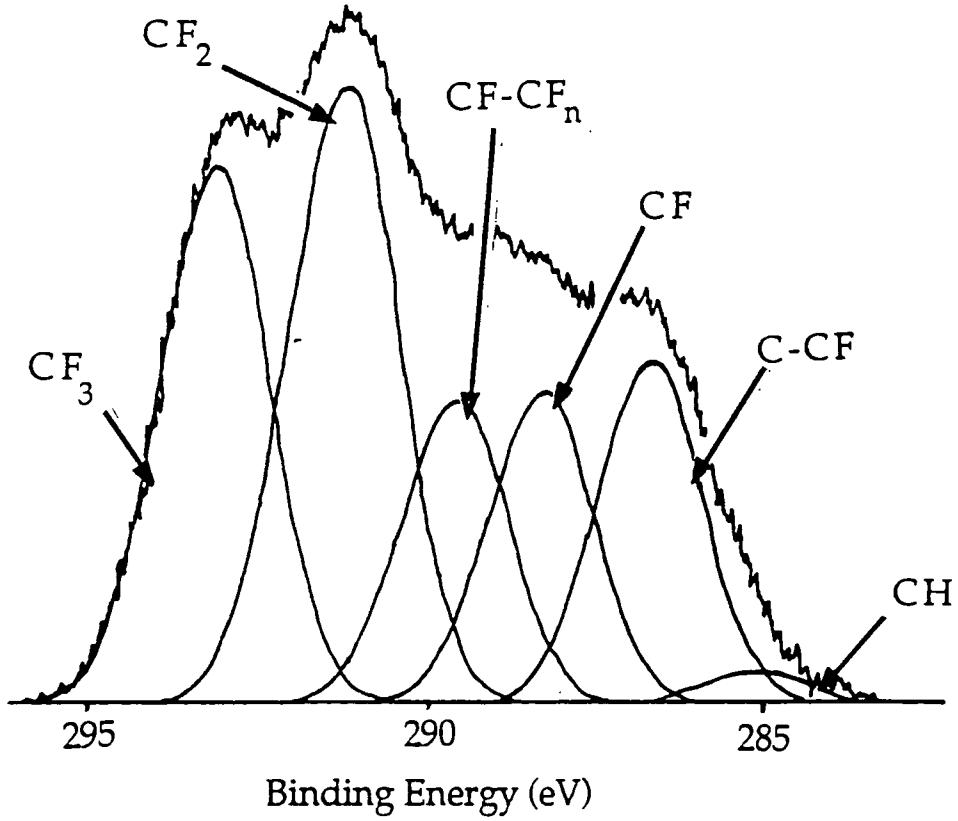

Figure 2.2 Peak fit of an hexafluoropropene plasma polymer made at 20W power and 0.5 ml/min flow rate

the relative sensitivity factors for each element (0.53 for fluorine and 1.00 for carbon on the XPS apparatus used for these analyses). Secondly, analysis of the component peaks of the C_{1S} envelope gave a fluorine to carbon ratio because it is possible to tell the number of fluorine atoms bound to a certain proportion of carbon atoms. The areas of each carbon peak [x] are treated as a number of fluorine atoms per carbon, as in equation 2.4. There was good agreement between the two methods, with less than 5% difference in the fluorine to carbon ratio between the first and second method.

$$\frac{F}{C} = \frac{3[CF_3] + 2[CF_2] + [CF]}{\text{Total } C_{1S} \text{ Area}} \qquad \text{Eq. 2.4}$$

Figure 2.3 shows the F:C ratio of the monomer plotted against that of the polymer. It was found that although the proportion of fluorine in the polymer rises as a result of an increased saturation of the monomer, the more saturated starting materials tended to produce polymers with similar stoichiometries of approximately $CF_{1.55}$. This seems to indicate that under these experimental conditions the film formed has a maximum F:C ratio, and this cannot be increased by changing the monomer. The results also show that a substantial loss of fluorine occurs during the plasma polymerisation of highly saturated monomers.

Deconvolution of the C_{1S} spectra (see table 2.1) also shows little difference between the more saturated monomers. A slight increase in CF_2 and CF_3 content is evident as the F:C ratio of the monomer increases. Hexafluoropropene does not seem to fit into this trend almost certainly because of a structural difference to the compounds it is being compared to. The other monomers comprise mainly of CF_2

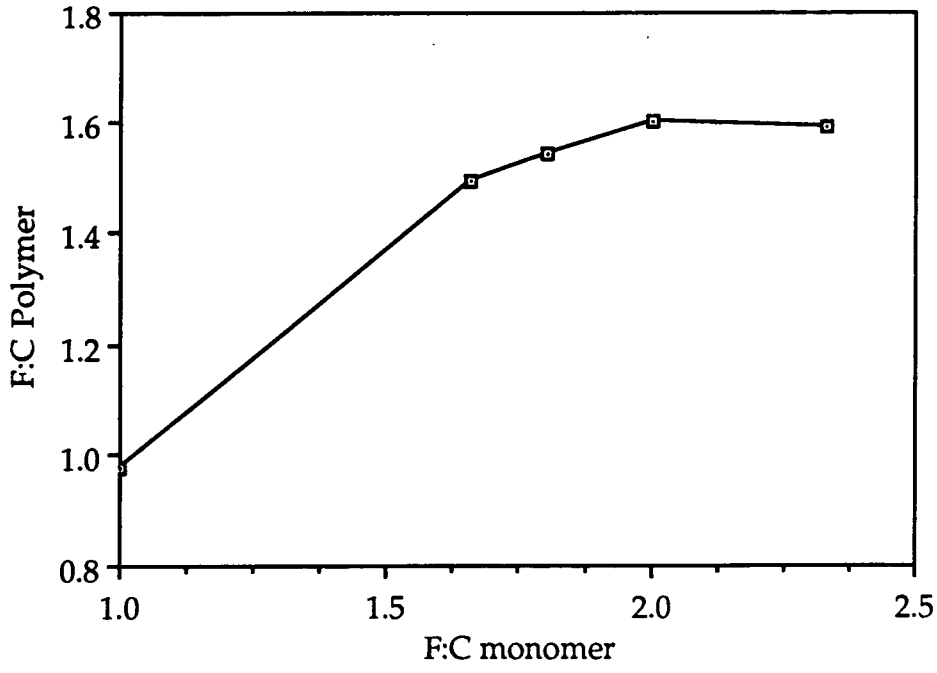

Figure 2.3 Plasma polymers of various monomers made at 20W and 0.5 ml min^{-1}

units (excluding PFB), whereas this reactant has CF, CF_2 and CF_3 groups initially in equal numbers. The resulting plasma polymer has a more even spread of functionalities which suggests that under the experimental conditions used the structure of the monomer has an influence upon the resulting polymer. The shake up peak intensity diminishes as the monomers become more highly saturated. This is indicative of a reduction in unsaturated sites in the plasma polymers, and also implies that the monomeric structure is not entirely lost during the deposition process.

Figure 2.4 shows the contact angle of water with the plasma polymers. Once again there is a large difference between perfluorobenzene and the more saturated monomers, with the more highly fluorinated surfaces showing high contact angles with water.

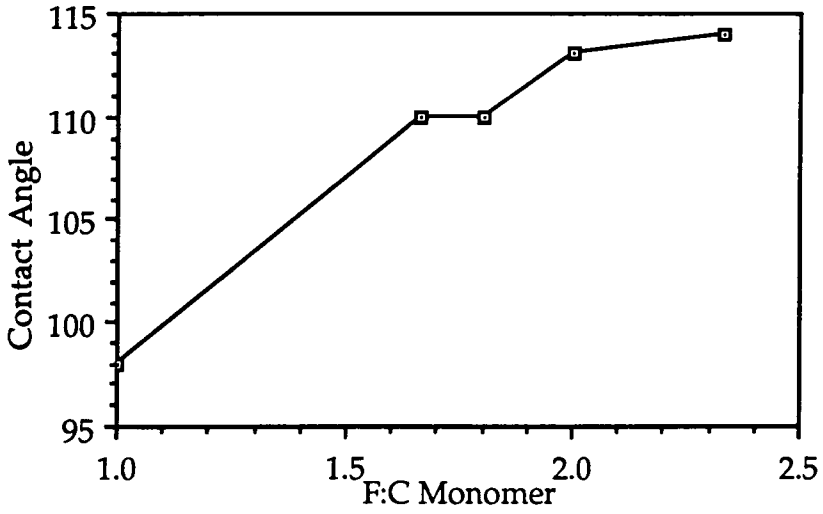

Figure 2.4 Contact angles of water with plasma polymers of perfluorocarbons

The contact angles are slightly higher than that of water on teflon (which is 110°[15]) even though the F:C ratio is lower by XPS analysis. The prescence of surface roughness could increase the measured contact angle, Wenzel's law[15,16] states that wettable surfaces ($\theta < 90^\circ$) will become more wettable when roughened, and non-wettable surfaces ($\theta > 90^\circ$) more non-wettable.

2.3.2 Plasma Polymers of Hexafluoropropene

The compositional changes of plasma polymerised hexafluoropropene films as the power and flow rate parameters were varied was studied, see figures 2.5 and 2.6. Hexafluoropropene plasmas produce polymers that tend to have C-CF, CF_2, CF_3 and CF groups present in comparable quantities (20 to 30 per cent). The presence of C-CF groups in such a large proportion indicates that fluorine

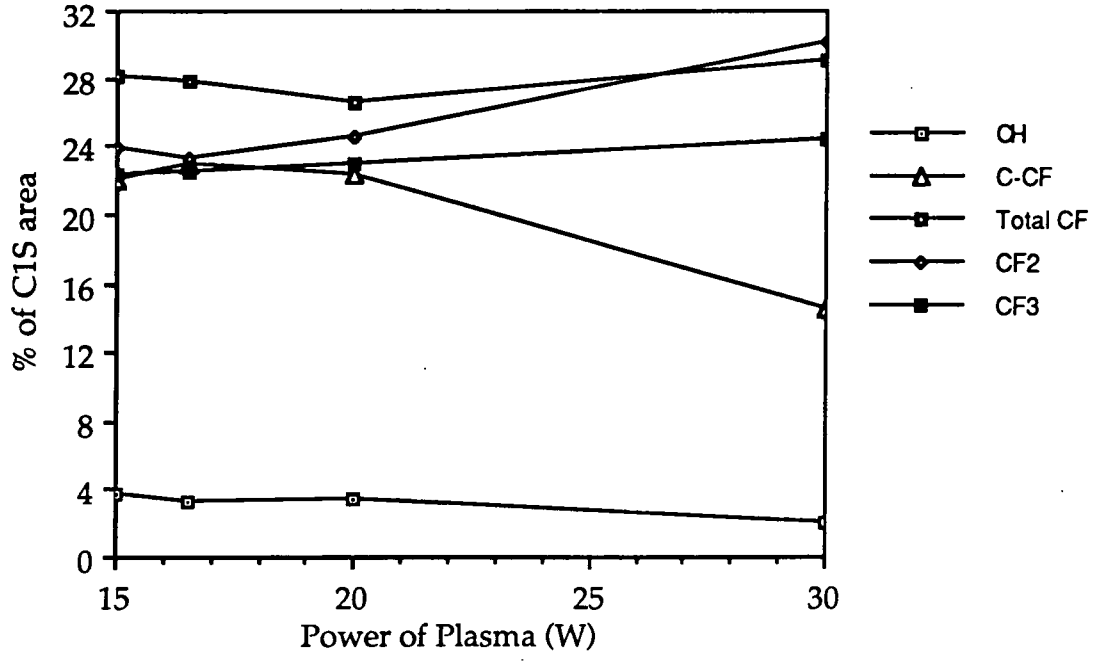

Figure 2.5 Change in composition of hexafluoropropene plasma polymerised films with varying power (flow rate = 0.5 ml / min.)

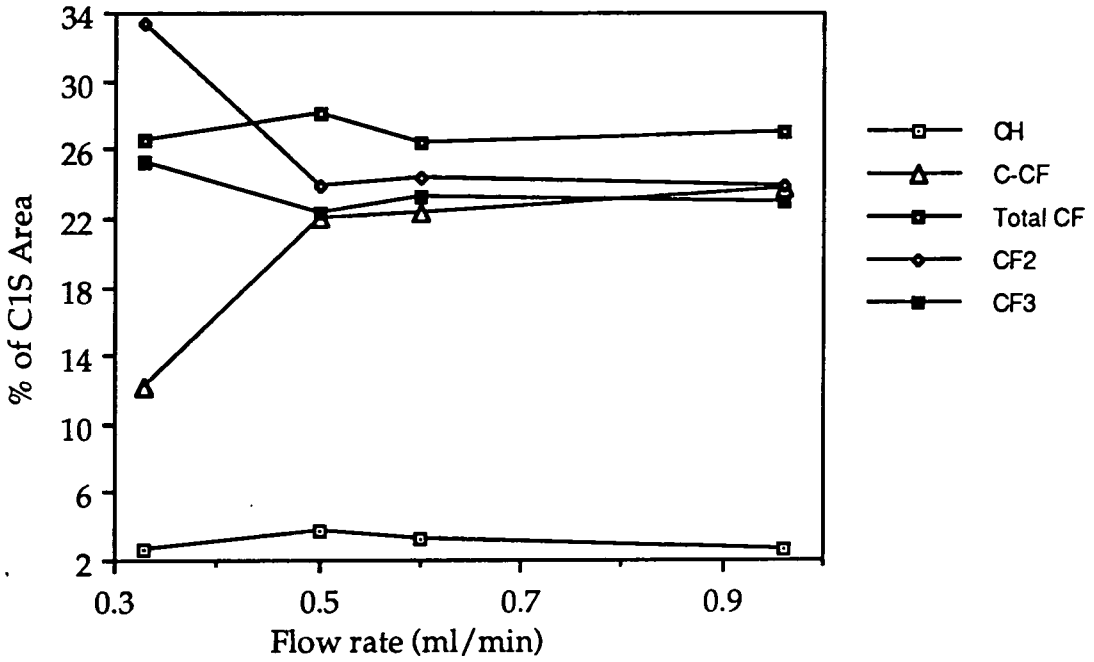

Figure 2.6 Change in composition of hexafluoropropene plasma polymerised films with varying flow rate (power = 15 W)

detachment plays an important part in the polymerisation process, since this group is not present in the monomer. The polymer made at the highest power in figure 2.5, and the lowest flow rate deposit in figure 2.6 both show an increased number of CF_2 groups in comparison to the other plasma polymers of this monomer, and a corresponding drop in $\underline{C}$-CF groups. Under these conditions, with an high $\frac{W}{F}$ parameter (see reference 6), an alternate polymerisation process appears to be occuring, with less elimination of fluorine on going from the monomer to the polymer. At low $\frac{W}{F}$ conditions (i.e. when there is a small amount of power per molecule) the major polymer forming reaction involves fluorine detachment, whereas at high $\frac{W}{F}$ this detachment is not as evident although significant molecular rearrangement takes place.

The close correlation between the CF, CF_2 and CF_3 intensities suggests that conventional polymerisation of this monomer occurs to a large extent during the deposition. This, however cannot be the case, because very high pressures are needed to produce polyhexafluoropropene[17]. The propagation step for free radical polymerisation through the double bond is sterically hindered by the bulky CF_3 group. Molecules of HFP can be incorporated into the growing film by reaction with unhindered radicals;

$$\text{Surface—}CF_2\cdot + \text{HFP} \rightarrow \text{Surface—}CF_2\text{–}CF_2\text{–}CF\cdot\text{–}CF_3$$

Which would account for the higher presence of these functional groups compared to the other monomers in section 2.3.1.

The deposition at low power input or high flow rate occurs then via removal of fluorine from the parent molecule and reaction of the

remaining fragments, and at higher power to flow rate ratio there seems to be a breakdown to polymer forming species not so typical of the monomer.

2.3.3 Plasma polymers of Perfluorohexane

Figures 2.7 and 2.8 show the effect of varying the power and flow rate parameters for the plasma deposition of perfluorohexane. At low powers and low flow rates perfluorohexane plasma polymers exhibit a high degree of fluorination with a large (30+%) content of CF_2 groups, the number of CF_3 groups is also large, reflecting the highly fluorinated nature of the monomer. Presence of CF and C-CF groups indicate that fluorine detachment occurs in the plasma, and given the

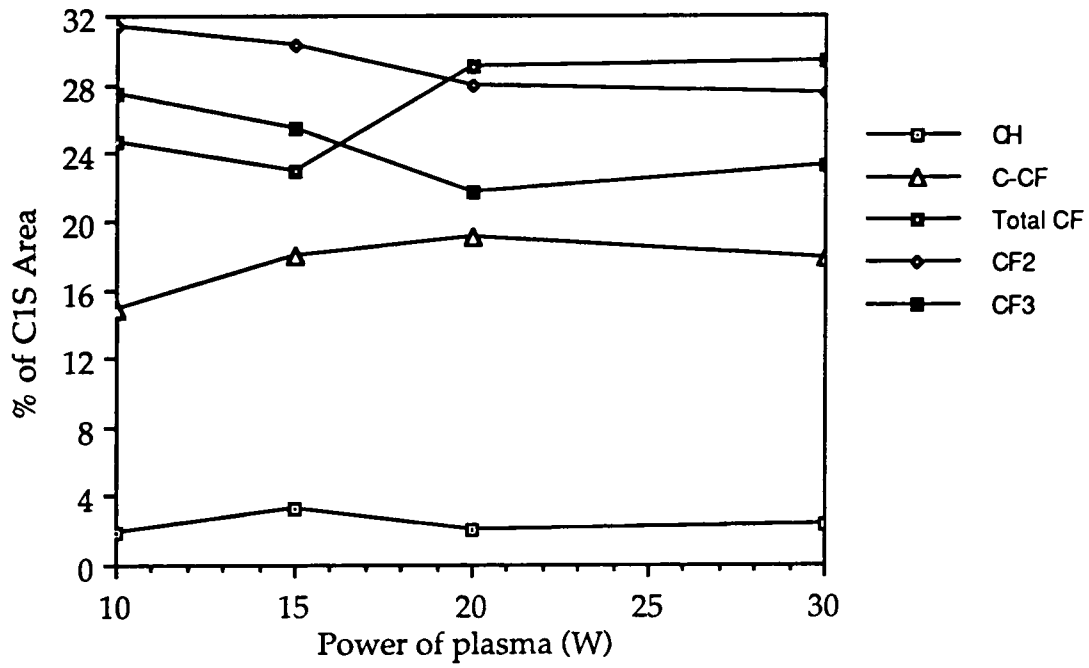

Figure 2.7 Change in composition of perfluorohexane plasma polymers with power (flow rate = 0.33 ml/min.)

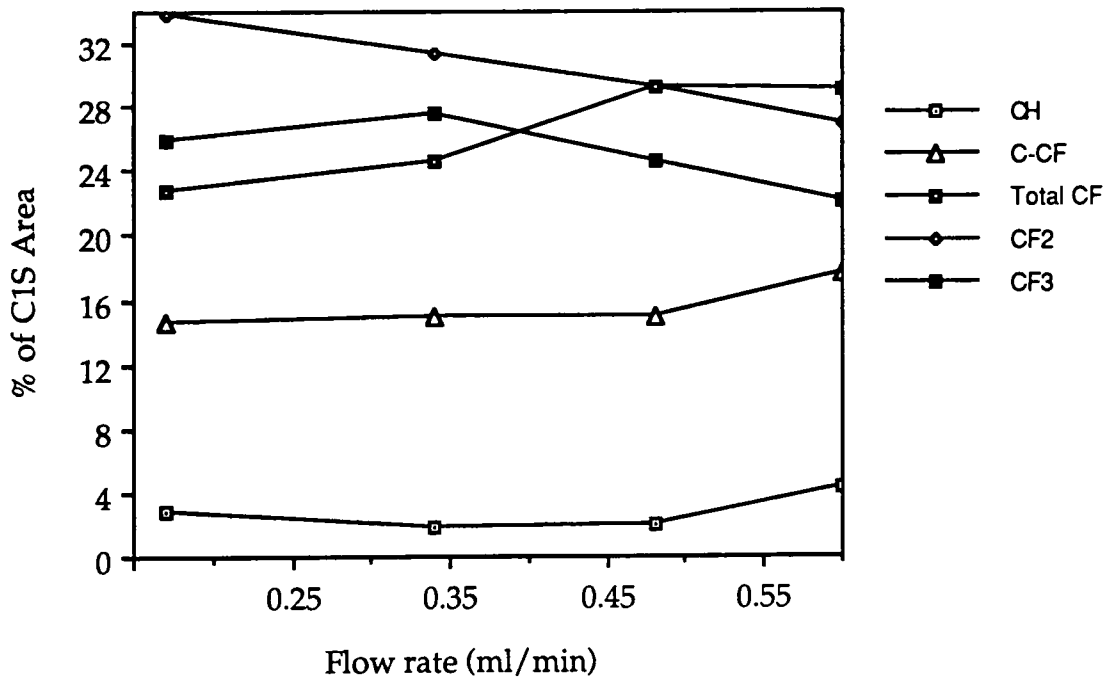

Figure 2.8 Change in composition of perfluorohexane plasma polymers with flow rate (Power = 10 W)

unsaturated straight chain structure of the monomer is probably necessary for any form of polymerisation. At high powers and also at high flow rates, the proportion of CF groups in the plasma polymer increases and the content of CF_2 and CF_3 groups tend to decrease, figure 2.9 shows two perfluorohexane plasma polymers made at high and low powers for comparison. Usually polymers formed at high flow rates are similar to those formed at low powers, as in the case of hexafluoropropene. Over the range of powers and flow rates studied here it appears that increasing power or flow rate in a perfluorohexane plasma produces similar chemical changes in the deposited film. No attempt was made to examine deposition rates, which may well follow the $\frac{W}{F}$ dependence outlined by Yasuda[6]. A plot of the fluorine to carbon ratio of perfluorohexane films against power multiplied by the

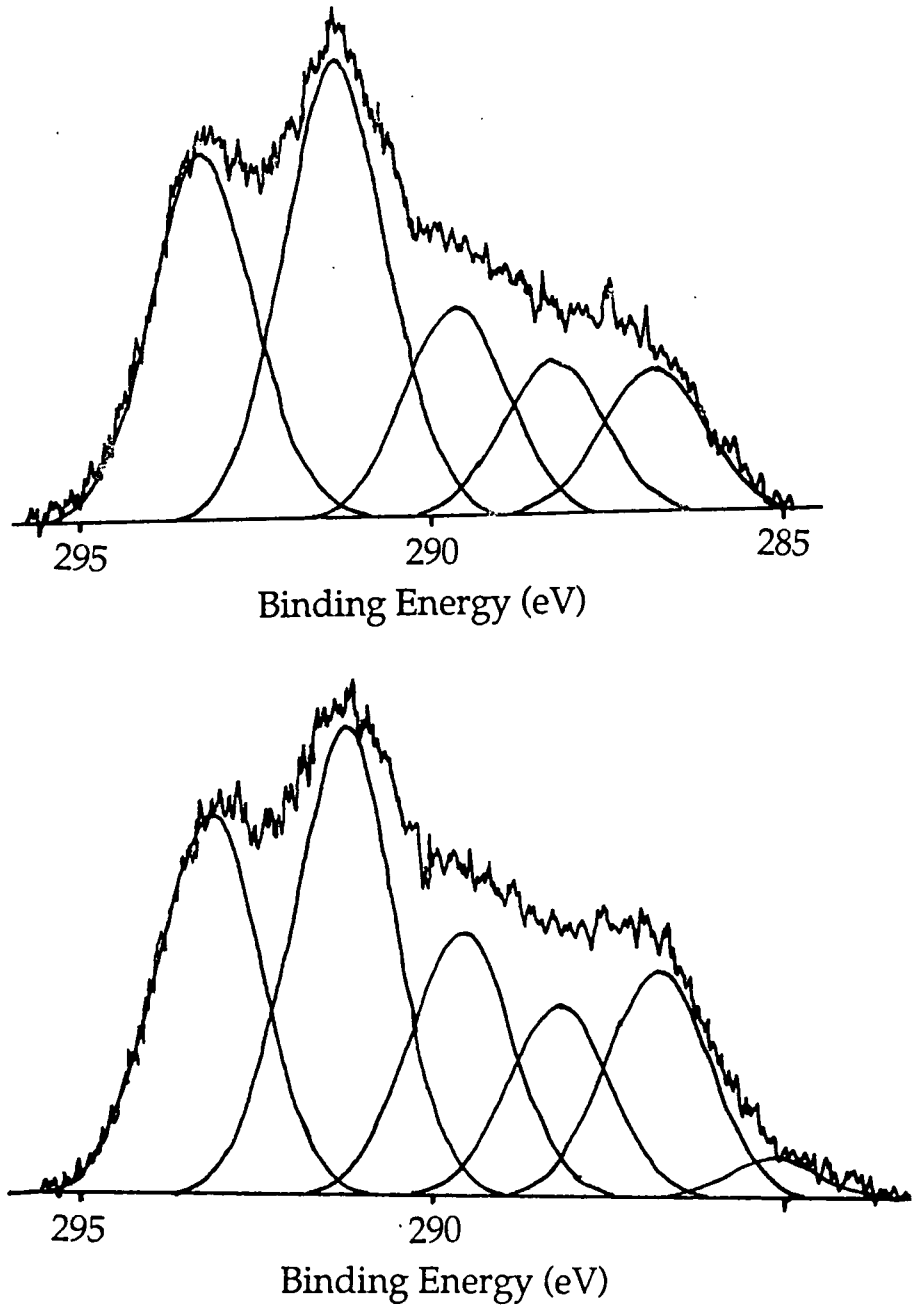

Figure 2.9 Plasma polymers of perfluorohexane made at 5W (top) and 20W (bottom) showing decrease in highly fluorinated carbon

flow rate showed a steady decrease in fluorine content with increasing W x F, see figure 2.10.

The compositions of the polymers formed at high powers and high flow rates imply that they have more cross linking than those formed at low powers and flow rates. It is known that exposure of

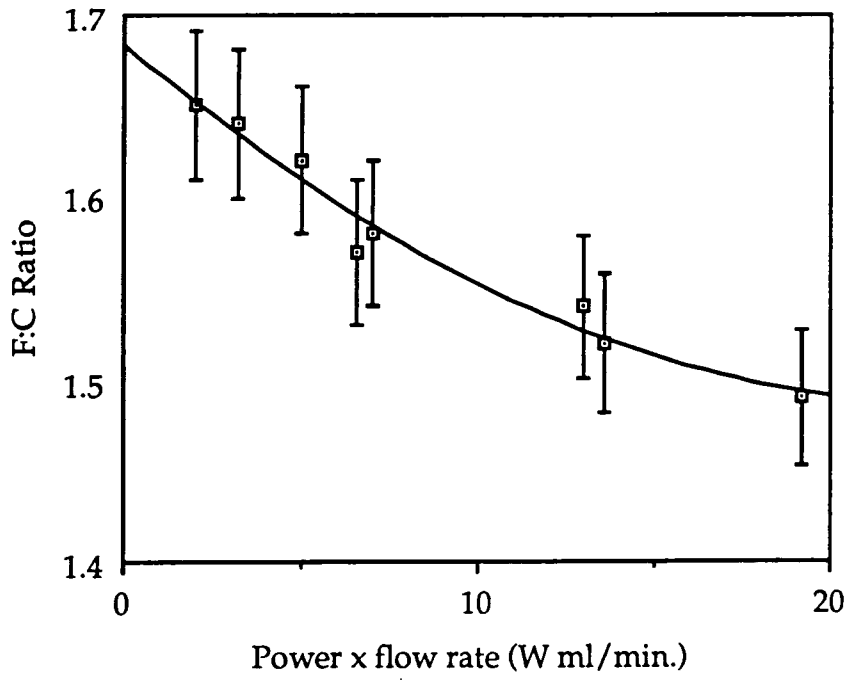

Figure 2.10 Fluorine content against reaction conditions for perfluorohexane plasma polymers

conventional polymers to an inert gas plasma induces cross linking at the surface of the polymer[18]; a similar effect could happen at the surface of the growing plasma polymer as it forms. The amount of cross linking would depend upon the flux of active species bombarding the surface and an increase in power would increase the number and energies of such species. A rise in pressure would also increase the flux of such species and in the reactor used in these experiments a rise in flow rate was accompanied by a rise in pressure, since the pumping speed was not variable. Cross linking would probably occur by elimination of volatile fluorocarbons or fluorine from the surface (see figure 2.11).

The positive SIMS spectrum of a film formed at a flow rate of 0.2 ml min-1 and a power of 15 W is shown in figure 2.12. This has

similarities to the SIMS spectra of PTFE[19] and plasma polymerised perfluorocyclohexane[20]. The main peaks are concentrated below 150 atomic mass units, which is indicative of a high degree of cross linking in the fluorocarbon substrate. The dominant fragment from the film is the CF_3^+ ion, which although present in the SIMS spectrum of PTFE is not as intense as the CF^+ peak. The presence of the CF_3^+ ion in SIMS analysis of PTFE is attributed to rearrangement of sputtered species before mass analysis occurs (PTFE consists solely of $-CF_2-$ units). The most intense peak in the SIMS spectrum of plasma polymerised perfluorocyclohexane is also CF^+. Although instrumental factors may alter the relative heights of peaks, the large CF_3^+ peak is probably due to a significant $-CF_3$ group concentration at the surface of the plasma polymer. The other peaks present in the spectrum are common fragments from a saturated perfluorocarbon surface, with most peaks in common with the SIMS spectrum of PTFE. The large $C_2F_5^+$ peak could indicate the presence of short, pendant aliphatic chains.

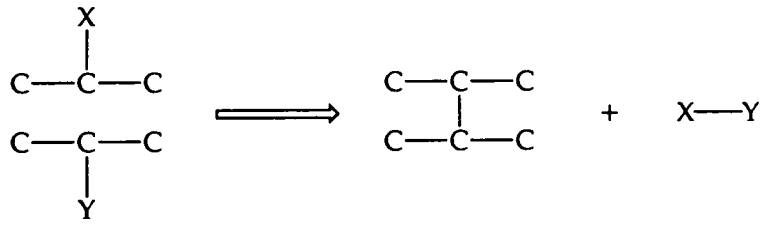

X.Y = F, CF_3, C_2F_5

Figure 2.11 Elimination of small molecules from a surface to form cross linking bonds

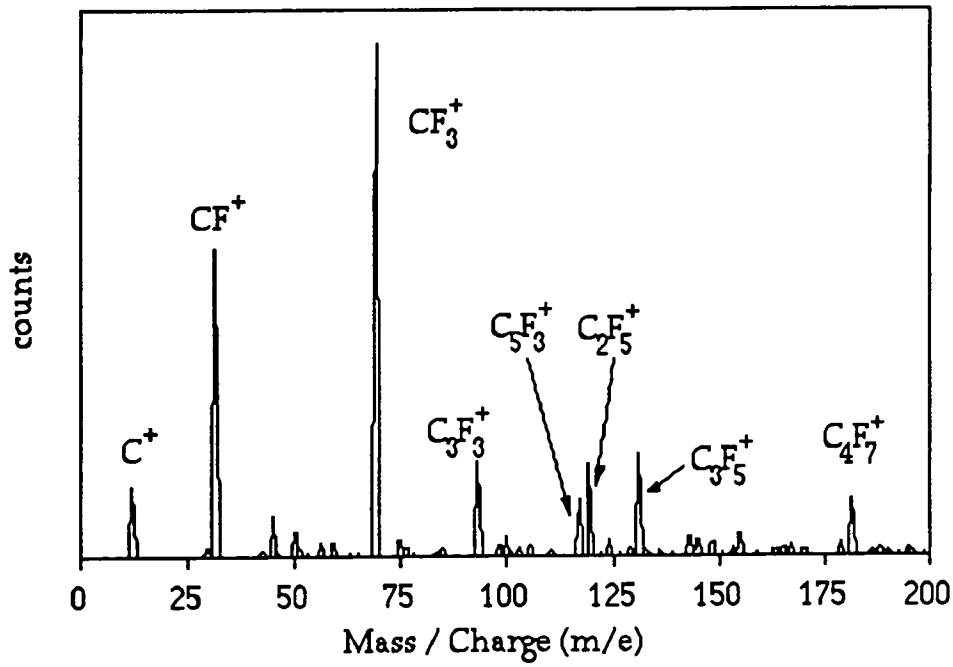

Figure 2.12 Positive SIMS spectra of 15 W, 0.2 ml/min plasma polymer of perfluorohexane

2.3.4 Contact Angles with Water

The contact angles with water of some of the plasma polymers were measured as a test of hydrophobicity. All the films examined exhibited contact angles similar to that of PTFE. Figure 2.13 shows that there is a tendency for the films to become more hydrophobic with an increasing F:C ratio (as measured by XPS). There is substantial variation from a straight line graph, which is larger than the error in measuring contact angles (about $\pm 2^{\circ}$). This demonstrates that it is not solely the fluorine content of the surface that determines the hydrophobicity of the surface. As mentioned previously surface roughness has a large effect, also the time between the formation of the film and the contact angle measurement can be important as the surface energy of highly fluorinated surfaces formed by plasma deposition can change with time[21].

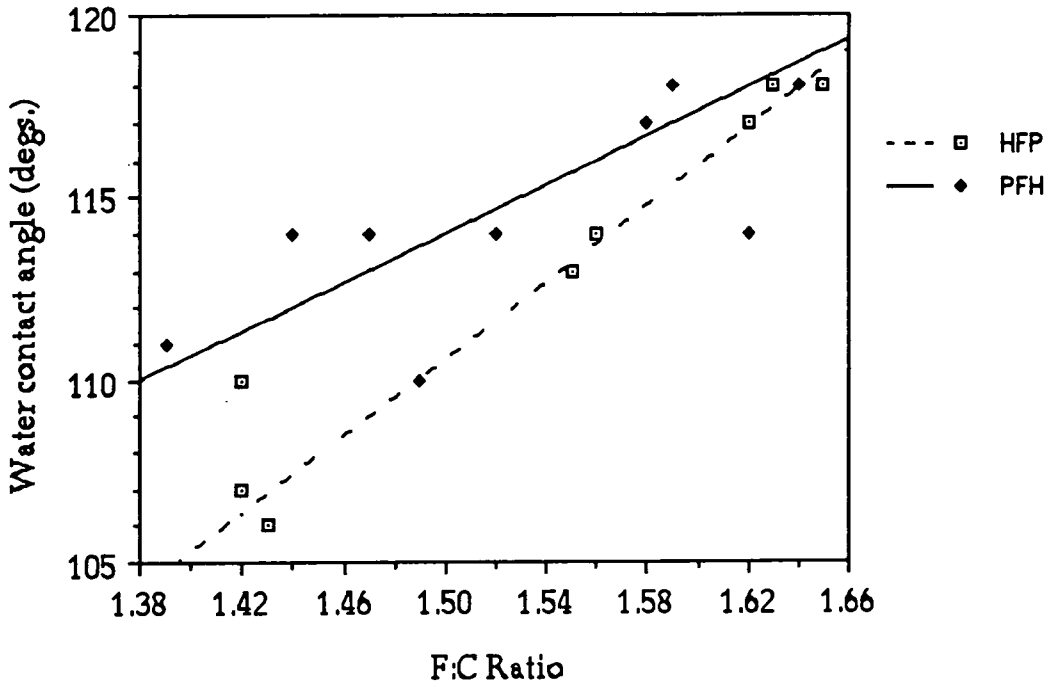

Figure 2.13 Contact angle of water on plasma polymers against fluorine content

2.4 Conclusions

Low energy surfaces with an high fluorine content can be formed by plasma polymerisation of perfluorocarbons. The contact angle of water with the surfaces deposited shows some degree of dependence on the fluorine to carbon ratio of the polymer as determined by XPS. Choice of starting material is important as monomers with high saturation will produce plasma polymers containing more fluorine than those of lower saturation.

The deposition characteristics of hexafluoropropene and perfluorohexane have been examined. At high powers and low flow rates hexafluoropropene forms a polymer with a larger CF_2 content than at low powers and high flow rates. Perfluorohexane on the other

hand forms a polymer with a high fluorine content at low power and low flow rate conditions, whereas at high powers and flow rates fluorine content diminishes. SIMS analysis shows that the perfluorohexane plasma polymer comprises of short alkyl chains with little or no unsaturation, and this is confirmed by the XPS results.

When these results are compared to studies carried out in similar reactors with differing monomers[1d] some interesting trends emerge. Perfluorocyclohexene follows a similar process to perfluorohexane, with high pressures and powers producing a film with a lower fluorine to carbon ratio. Although this molecule contains a double bond, it is hindered by bulky groups at both ends and cannot readily undergo addition to radicals in the growing film. The two perfluorocyclohexadiene isomers examined tended to higher fluorine contents at higher powers and low flow rates. This is similar to the results obtained with hexafluoropropene, although the power ranges in the two studies are not directly comparable. Polymer structure in these cases is not greatly influenced by ion bombardment, perhaps due to a high deposition rate. Perfluorobenzene also has a slightly increased fluorine content at higher powers[1c], and it has been demonstrated that it's polymerisation mechanism proceeds via excited states[8]. It is likely that electronically excited intermediates play an important role in the polymerisation of hexafluoropropene and perfluorocyclohexadiene possibly through [2+2] Diels-Alder reactions. For significant polymerisation to occur in this way there must be a significant number of excited states in the gas phase, which means that the polymerisation rate (and hence fluorine incorporation) will be enhanced by an increase in power.

The major plasma polymerisation mechanism of perfluorocarbons is highly dependent upon the monomer used and the

choice of operating parameters. Deposition of highly unsaturated systems is mainly through excited states, whereas saturated systems deposit polymers as a product of bond scission followed by recombination. Intermediate monomers polymerise via a combination of both processes and the precise operating conditions determine which predominates.

References

1 a D. T. Clark, D. Shuttleworth, *J. Polym. Sci., Polym. Chem. Ed.*, **16**, 1093, (1978)

b D. T. Clark, D. Shuttleworth, *J. Polym. Sci., Polym. Chem. Ed.*, **17**, 1317, (1979)

c D. T. Clark, D. Shuttleworth, *J. Polym. Sci., Polym. Chem. Ed..*, **18**, 27, (1980)

d D. T. Clark, D. Shuttleworth, *J. Polym. Sci., Polym. Chem. Ed..*, **18**, 407, (1980)

e D. T. Clark, M. Z. AbRahman, *J. Polym. Sci., Polym. Chem. Ed..*, **19**, 2129, (1981)

f D. T. Clark, M. Z. AbRahman, *J. Polym. Sci., Polym. Chem. Ed..*, **19**, 2689, (1981)

g D. T. Clark, M. Z. AbRahman, *J. Polym. Sci., Polym. Chem. Ed..*, **20**, 1717, (1982)

h D. T. Clark, M. Z. AbRahman, *J. Polym. Sci., Polym. Chem. Ed..*, **20**, 1729, (1982)

i D. T. Clark, M. M. Abu-Shbak, *J. Polym. Sci., Polym. Chem. Ed..*, **21**, 2907, (1983)

2 N. Inagaki, T. Nakanishi, K. Katsuura, *Polym. Bull. (Berlin)*, **9**, 10-11, 502, (1983)

3 S. F. Diaz, R. Hernandez, *J. Polym. Sci., Polym. Chem. Ed.*, **22**, 1123, (1984)

4 N. Morosoff, B. Crist, M. Bumgarner, T. Hsu, H. Yasuda, *J. Macromol. Sci., Chem.*, **A10**, 451, (1976)

5 Y. Iriyama, T. Yasuda, D. L. Cho, H. Yasuda, *J. Appl. Polym. Sci..*, **39**, 249, (1990)

6 H. Yasuda, "Plasma Polymerisation", Academic Press Inc., (1985)

7 R. d'Agostino, S. De Benedictis, F. Cramarossa, *Plasma Chem. Plasma Process.*, **4**, 1, (1984)

8 H. S. Munro, C. Till, *J. Polym. Sci., Polym. Chem. Ed.*, **26**, 11, 2873, (1988)

9 Y. Haque, B. D. Ratner, *J. Polym. Sci., Polym. Phy.*, **26**, 1237, (1988)

10 H. Biederman, S. M. Ojha, L. Holland, *Thin Solid Films*, **41**, 329, (1977)

11 CRC Handbook of Chemistry and Physics, Ed. R. C. Weast, (1982)

12 B. J. Briscoe, C. M. Pooley, D. Tabor in "Advances in Polymer Friction and Wear", Ed. L.-H. Lee, Polymer Science and Technology 5A, 191, Plenum, (1974)

13 N. Inagaki, J. Ohkubo, *J. Membr. Sci.*, **27**, 63, (1986)

14 H. Biederman, Y. Osada in "Advances in Polymer Science", **95**, 57, Springer-Verlag, (1990)

15 M. Klausner, I. H. Loh, R. F. Baddour, R. E. Cohen, *A.C.S. Polymeric Mater. Sci. Eng.*, **56**, 227, (1987)

16 B. D. Washo, *Org. Coat. Appl. Polym. Sci. Proc.*, **47**, 69, (1982)

17 R. E. Putman in "Comprehensive Polymer Science", Eds. G. Allen, J. C. Bevington, **3**, 321, (1989)

18 a D. T. Clark, A. Dilks, *J. Polym. Sci., Polym. Chem. Ed.*, **15**, 2321, (1977)

b D. T. Clark, A. Dilks, *J. Polym. Sci., Polym. Chem. Ed.*, **16**, 911, (1978)

19 J. C. Vickerman, A. Brown, D. Briggs, "Handbook of Static Secondary Ion Mass Spectroscopy", Wiley, Chichester, (1989)

20 R. Ward, PhD Thesis, University of Durham, (1989)

21 T. Yasuda, T. Okuno, K. Yoshida, *J. Polym. Sci., Polym. Phy. Ed..*, **26**, 1781, (1988)

Chapter 3

Deposition of Perfluorocarbon materials from Plasmas in Non-Glow Regions

3.1 Introduction

Deposition of polymeric materials in the non-glow regions of plasmas has been observed previously[1-4]. In the case of perfluorocarbon monomers, workers have characterised films formed in the downstream non-glow regions of perfluorobenzene, perfluorocyclohexane[1] and tetrafluoroethylene[2,3]. In this region tetrafluoroethylene can polymerise as a film consisting approximately of 95% CF_2 units (as determined by XPS)[2]. The deposition rate of such polymers was found to be typically 100 to 1000 times slower than in the glow region. Similar experiments[3] demonstrated that reactor design plays a crucial part in the deposition of these films, and such films are probably formed by conventional polymerisation of unaltered monomer. However, it was found that deposits could be formed in the non-glow region from other monomers which have no conventional polymerisation route available[1]. These polymers often had a large variance in structure from both the monomer and the deposit formed in the glow region. The results suggested that the downstream deposit in the non-glow region of perfluorocarbon plasmas is a result of long lived polymer forming species produced in the plasma, and not necessarily dependent upon the structure of the monomer.

The use of a Faraday cage within the plasma region itself to produce a field free zone has been shown to produce polymers from tetrafluoroethylene that are similar in structure to non-glow region products[4]. In these studies the polymers with high CF_2 content were formed only near the inlet of the reactor and can be attributed to conventional polymerisation of tetrafluoroethylene before the monomer has suffered rearrangement in the plasma.

Most of these studies have concentrated upon tetrafluoroethylene which conventionally polymerises to form material solely containing CF_2 groups. The position of substrates for collection of deposits were often distinguished only by being situated either within the glow or non-glow region. Studies carried out in this chapter show that such an approach is inadequate. In a flowing system such as those used in most studies, distance from the monomer inlet can have a profound influence on the chemical structure of the polymer both within and out of the glow region.

The monomers discussed in this chapter are hexafluoropropene, and perfluorohexane. Conventional polymerisation of these compounds will not occur under the conditions used in these experiments and for substantial deposits to form in the non-glow region, rearrangement or activation to produce long lived polymerisable species must occur.

3.2 Experimental

The experiments in this section were carried out in a cylindrical glass reactor 39.5 cm by 5.0 cm as shown in figure 3.1. A steel mesh cage, with 2 mm gaps and wire thickness of 2mm, which was capable of being earthed could be inserted into the downstream half of the reactor (figure 3.2), to act as a faraday cage, and no visible glow discharge occured within it at the powers used. It was found that the deposition rate in the cage and the non-glow region was low and the reactions were allowed to occur for 2 to 3 hours to build a layer which, by XPS, no substrate showed through. The plasma polymers were collected on aluminium foil placed at different points along the reactors. In reactor one, four pieces of aluminium foil were placed on the glass slides at

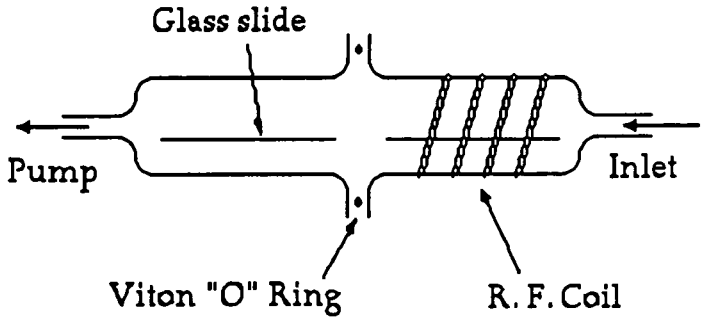

Figure 3.1 Reactor one, used for deposition of materials in the downstream region of the reactor.

distances of approximately 10 cm, 20 cm, 28 cm and 39 cm from the inlet end of the reactor. Because of the slight vibration of the reactor due to its connection to the pumping system there was often some initial movement of the substrates within the reactor. The positions were measured for a second time at the end of the experiment and these values were taken as the position of the substrate during actual deposition. In reactor two one piece of foil was placed inside the metal cage, at a distance of 28 cm from the inlet, and one outside, at 10 cm.

Analysis was carried out as described in chapter 2. The intensive

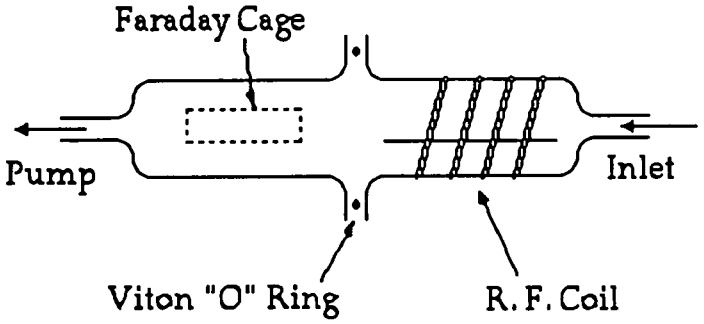

Figure 3.2 Reactor two, used for deposition of material within a field free zone

XPS study in section 3.3.1 was performed in a Perkin Elmer 5400 surface analysis instrument. In addition to water, the contact angle of diiodomethane with the surface was measured. The combination of water and diiodomethane contact angles could be used to determine the contribution to surface energy of the polar and dispersive components[5]. The approximate value of the surface energy of the sample can be found by adding the polar and dispersive components together, which are calculated from equations 3.1 and 3.2.

$$\gamma^p = \frac{(2.15\ \cos\theta w - \cos\theta CH_2I_2 + 1.15)^2}{0.127} \qquad \text{Eq. 3.1}$$

$$\gamma^d = \frac{(\cos\theta w - 0.193\sqrt{\gamma^p} + 1)^2}{0.016} \qquad \text{Eq. 3.2}$$

Where γ^p is the polar component and γ^d the dispersive component of the surface energy and θw and θCH_2I_2 are respectively the contact angle between water or diiodomethane and the surface.

3.3 Results and Discussion

3.3.1 Deposition of Perfluorohexane in the Non-Glow Region

Figures 3.3 and 3.4 are the result of an intensive XPS study of material deposited on a long aluminium foil strip laid along reactor 1. The conditions used for this experiment were 15 W power and 0.2 ml/min flow rate. Figure 3.3a illustrates the variation in chemical character of the polymeric film from the inlet end to the centre of the reactor (the glow region). Figure 3.3b shows in the foreground the furthest downstream deposit, and in the background the polymer

formed in the middle of the reactor (the non-glow region). It can be easily seen that peaks corresponding to the CF_2 functionality increase

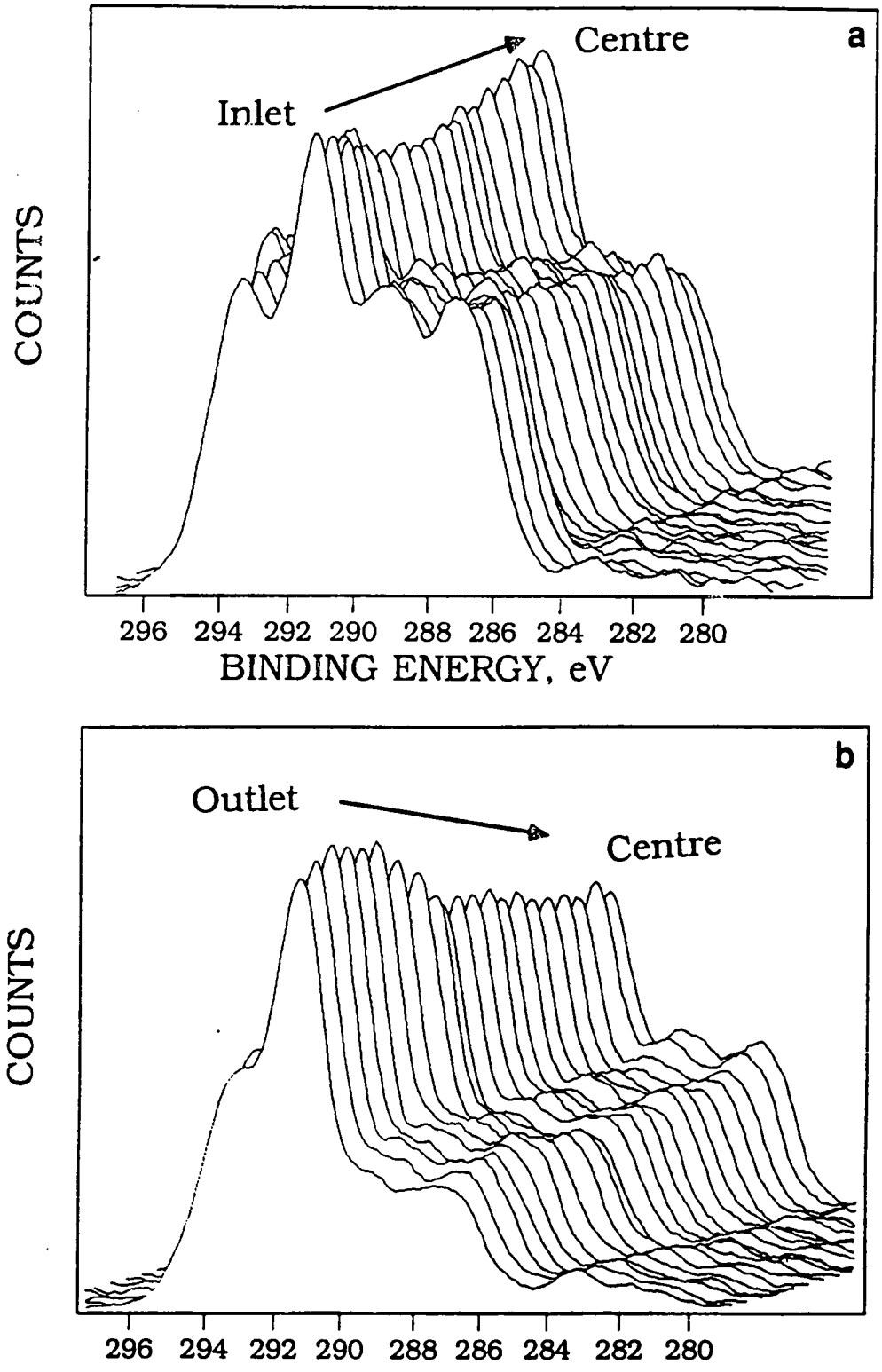

Figure 3.3 XPS C_{1S} spectra (a) from the inlet to the centre of the reactor, (b) from the outlet to the centre of the reactor

in relation to the other groups present in the polymers on moving toward the outlet. A comparison of elemental peak areas (F_{1S} and C_{1S}, see chapter 2) shows that the F:C ratio of the deposited film increases toward the outlet region of the plasma reactor. In the vicinity of the inlet the stoichiometry is $CF_{1.58}$ which increases to $CF_{1.91}$ at the furthest downstream site.

The deconvolution of the C_{1S} envelopes for the downstream deposits is summarised in figure 3.4. The growth of the CF_2 peak area appears to be almost linear with distance from the plasma region, and the other functionalities contribute less to the overall C_{1S} intensity as

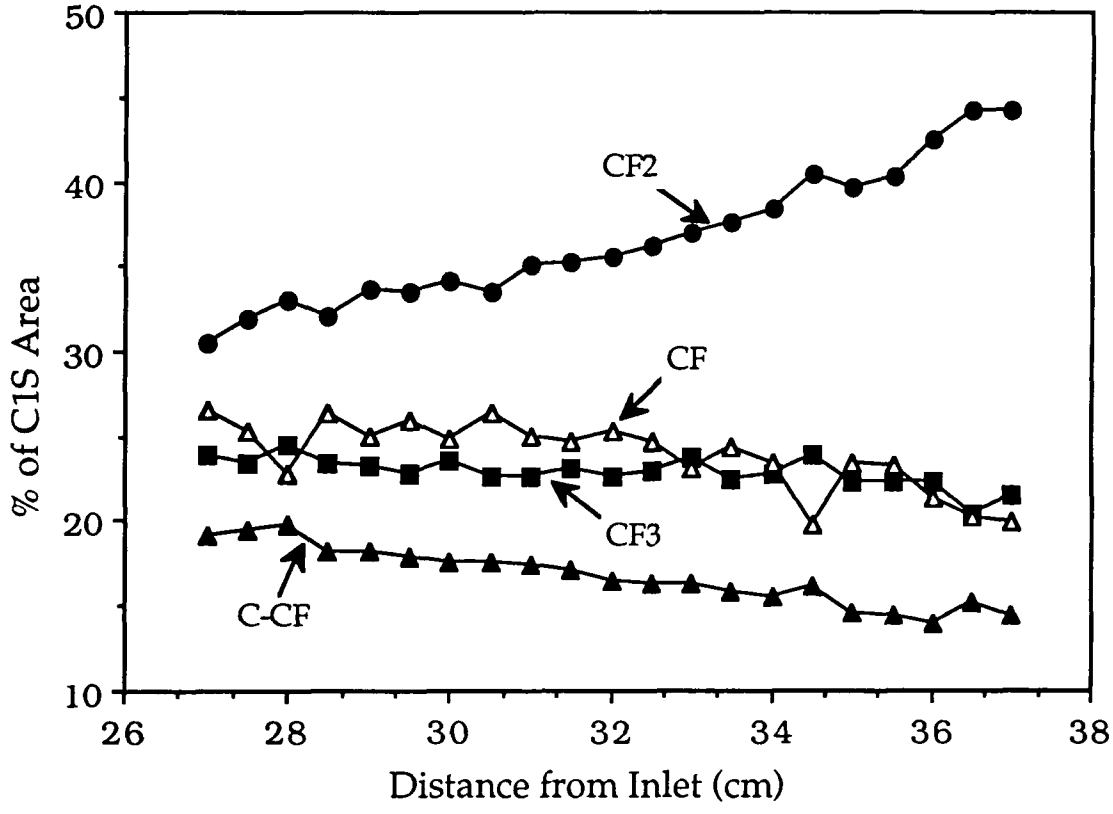

Figure 3.4 Composition of downstream deposits from a 15 W, 0.2 ml/min perfluorohexane plasma

their content in the film diminishes. There is a slight increase in CF_3 intensity relative to the CF and C-CF peak areas, but not as marked as the rise in CF_2 functionality. Variable take off angle XPS studies[6] demonstrated negligable chemical change with depth within the topmost 70 Å, which indicates that the films are reasonably homogenous throughout their bulk.

Table 3.1 shows the change in composition of the plasma polymers as a function of both power and position in reactor one. At 10W and 20W power the substrate furthest from the inlet failed to collect enough material to obscure the Al_{2P} signal. This meant that C_{1S} deconvolution could not be carried out in a meaningful way as

Distance from Inlet	% of C_{1S} Area						Contact Angles	
	CH	C-CF	CF	CF_2	CF_3	CF2/CF3	H_2O	CH_2I_2
10W power, 0.5 ml/min flow rate								
14 cm	2.3	17.5	29.4	27.9	22.9	1.22	112	75
20 cm	2.6	19.1	29.0	27.6	21.7	1.27	114	79
29 cm	6.0	16.0	21.9	32.7	23.4	1.40	119	83
38 cm	*	*	*	*	*	2.37	*	90
20W power, 0.5 ml/min flow rate								
10 cm	1.6	16.2	29.8	27.9	24.5	1.14	108	80
20 cm	1.8	19.9	28.3	26.7	23.3	1.15	114	87
29 cm	2.5	18.6	26.3	28.6	24.1	1.19	118	93
39 cm	*	*	*	*	*	1.90	*	91
30W power, 0.5 ml/min flow rate								
16 cm	2.8	17.5	29.2	27.4	23.2	1.18	117	95
22 cm+	5.4	19.6	30.4	24.8	19.9	1.25	111	89
28 cm	1.7	18.0	27.8	28.2	24.4	1.16	117	95
38 cm	1.6	17.4	23.5	31.3	26.2	1.19	118	90

* Reading not taken, due to low film thickness or instability to water

+Substrate fell from glass slide to base of reactor

Table 3.1 Perfluorohexane plasma polymers, effect of power and position in reactor

hydrocarbon material present on the surface of the aluminium foil was also visible by XPS. Peaks with chemical shifts assignable to both CF_2 and CF_3 groups were noted and since the intensities of such peaks should be unaffected by any contribution from the hydrocarbon layer, the ratio of the area under these peaks was taken as characteristic of the material deposited during plasma polymerisation. This ratio can be seen as an indication of the extent of cross linking in the polymer, with a large $\frac{CF2}{CF3}$ value indicating mainly a straight chain structure.

The measurement of the contact angle of water with some of the downstream samples proved difficult due to the apparent instability of such deposits to water. Initially very high contact angles were observed, but after a few seconds the drop of water spread to give low contact angles of about 10 to 15 degrees. Diiodomethane exhibited no spreading on these surfaces indicating that the polymers were stable to contact with some solvents other than water. This phenomenon is discussed further in section 3.3.3.

The most marked changes in the nature of the plasma polymers occurs at the boundary between the plasma region and the non-glow region. At 10W the plasma extended from the inlet to about 15 cm. downstream, at 20W it extended to about 25 cm. and at 30W power the plasma filled the reactor. Plasmas struck at below 10W in this reactor at 0.50 ml/min flow rate were unstable. At 30W power there is a slight increase in both CF_2 and CF_3 content in the downstream deposits, this is accompanied by a drop in CF groups, but virtually no change in the C-CF group concentration. One of the substrates (22 cm.) fell from the glass slide to the bottom of the reactor. The deposit on this substrate had a strong CF contribution, low F:C ratio and a comparitively high surface energy which does not appear to be typical of the other polymers formed on other substrates. This result shows that the radial

position of the substrate is also important in determining the character of the polymer. It is possible that the less fluorinated nature of this film is caused by ion bombardment. The walls of the reactor are negatively charged with respect to the plasma[7], and positive ions within the sheath region are accelerated toward the wall. The result of this impinging flux of ions could cause cross linking and elimination of fluorine, as described in chapter 2. Alternatively, the higher temperature of the walls in comparison with the glass slide (caused by close proximity to the induction coils) may result in volatilisation of low molecular weight, highly fluorinated species with a resulting drop in fluorine content.

The polymer formed at 20 cm. downstream in the 20W plasma has a slightly lower concentration of CF_2 and CF_3 groups compared

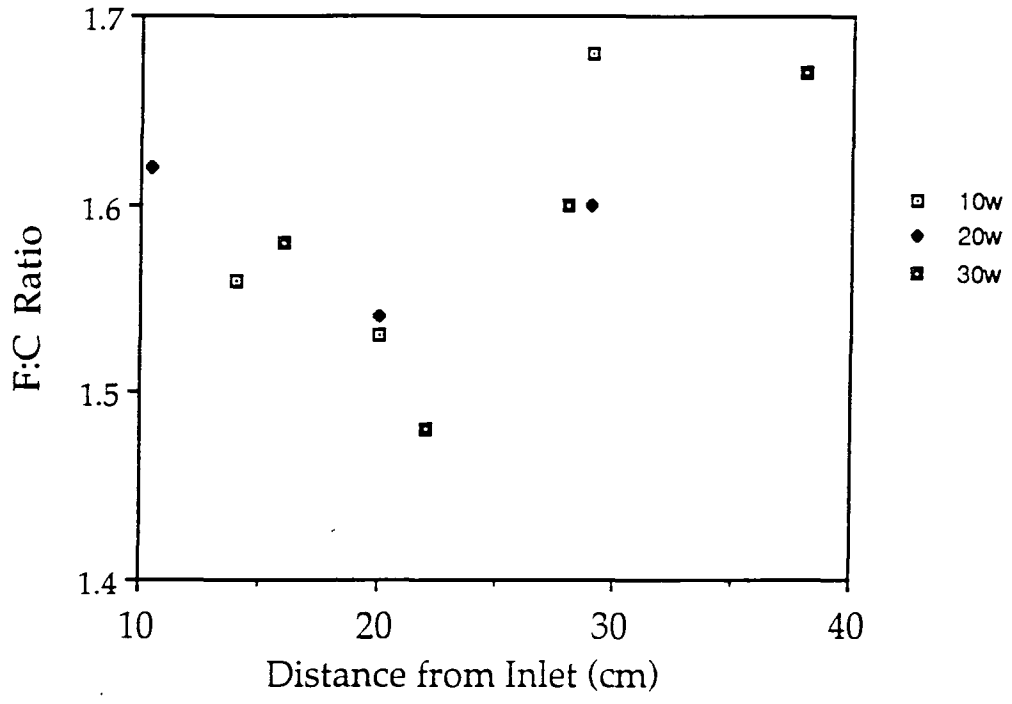

Figure 3.5 Stoichiometry of polymers as a function of position in reactor

with the deposit at 10 cm., coupled with an increase in the C-CF intensity. This change is mirrored in the 10W plasma polymer, figure 3.5 shows that there is a slight drop in the F:C ratio at this point followed by a rise. This change can result from fragmentation of the perfluorohexane monomer into smaller species, the deposits being typical of the species present in the plasma at that point. At ~20 cm. more fragmentation has occured than at ~10 cm. and hence the polymer has a structure less like that of the monomer. Further downstream (at ~30 cm.) there is a rise in CF_2 content in the polymer, a smaller rise in CF_3 content and a marked drop in CF content. The deposits at ~40 cm. were too thin for a meaningful peak fit to be carried out, but the ratio of the CF_2 area to the CF_3 area was very large in this region indicating a mainly straight chain polymer with a degree of

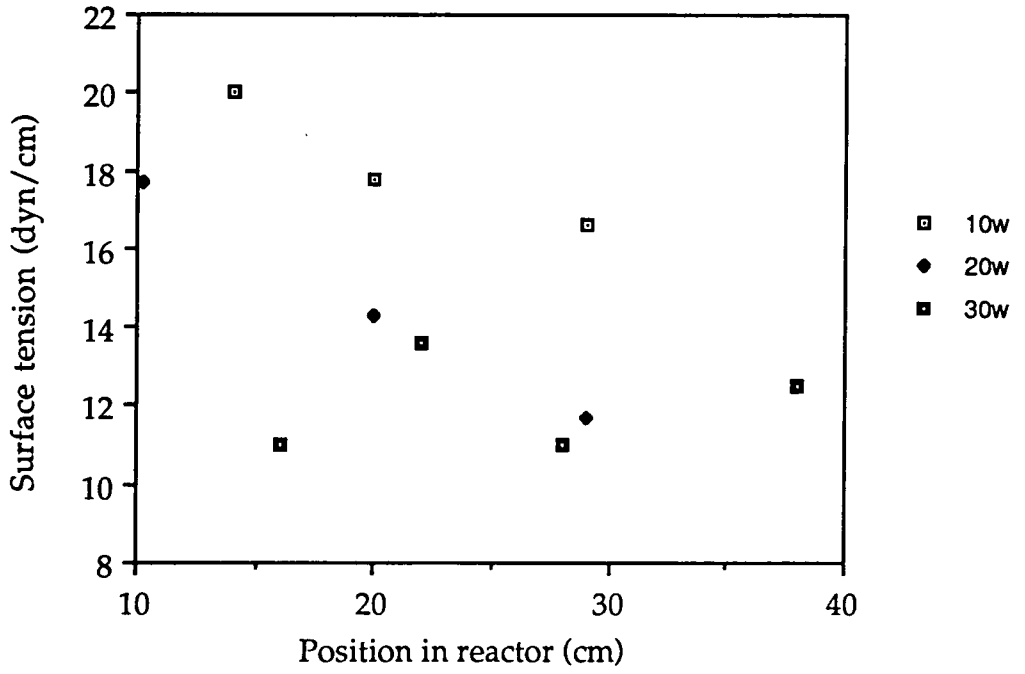

Figure 3.6 Surface energies of perfluorohexane plasma polymers as a function of power and position in reactor

crosslinking and branching.

The surface energies calculated from the contact angles in table 3.1 are shown in figure 3.6. Polar surface energies tend to be very low (of the order of 1 dyn/cm), most of the surface energy consisting of dispersion forces. The values obtained for surface energy of these materials are often lower than that of teflon (18 dyn/cm), this is probably because the surface of the plasma polymers is not ideally flat (see section 3.4). Downstream samples appear to have a lower surface energy than upstream samples, which may be a result of the higher fluorine content of the downstream samples. Surface energy also appears to decrease with an increase in the power of the plasma. This effect is almost certainly due to surface roughness, as there is little difference in the XPS data between polymers formed at different powers in upstream sites. The furthest downstream deposits at low powers demonstrated instability to contact with water, so no surface energy calculations were possible using this method. These deposits did show stability to diiodomethane and the contact angle exhibited was very large, about the same as the 30W plasma polymers.

Table 3.2 shows the change in the chemical nature of perfluorohexane plasma polymers with flow rate and position in reactor. The upstream deposits show a decrease in fluorine content with increasing flow rate, as expected from chapter 2. At ~20cm. there is a rise in the proportion of C-CF content coupled with a slight decrease in CF_2 and CF_3 content. This effect was noted when the power was altered (see table 3.1), and appears to occur at roughly the same distance from the inlet regardless of power and flow rate. Figure 3.7 illustrates both the decrease in fluorine to carbon ratio with increasing flow rate and the slight dip at about 20cm. The rise in the proportion of CF2 in the polymers with increasing distance from the inlet is hardly noticable at the lowest flow rates, and much more

Distance from Inlet	% of C_{1S} Area						Contact Angles	
	CH	C-CF	CF	CF_2	CF_3	CF2/CF3	H_2O	CH_2I_2
10W power, 0.3 ml/min flow rate								
15 cm	1.7	14.9	24.6	31.3	27.5	1.14	107	89
20 cm	3.1	16.2	23.5	31.2	26.0	1.20	112	89
31 cm	1.4	14.7	24.1	32.7	27.1	1.20	*	86
40 cm	*	*	*	*	*	1.52	*	84
10W power, 0.5 ml/min flow rate								
14 cm	2.3	17.5	29.4	27.9	22.9	1.22	112	75
20 cm	2.6	19.1	29.0	27.6	21.7	1.27	114	79
29 cm	6.0	16.0	21.9	32.7	23.4	1.40	118	83
38 cm	*	*	*	*	*	2.37	*	90
10W power, 0.8 ml/min flow rate								
12 cm	2.7	19.4	30.2	26.5	21.2	1.25	108	78
19 cm	3.0	21.3	29.5	26.3	19.9	1.32	110	77
28 cm	5.2	18.4	25.5	29.8	21.1	1.41	117	84
37 cm	*	*	*	*	*	2.05	*	87

Table 3.2 Plasma polymers of perfluorohexane, effect of flow rate and position in reactor

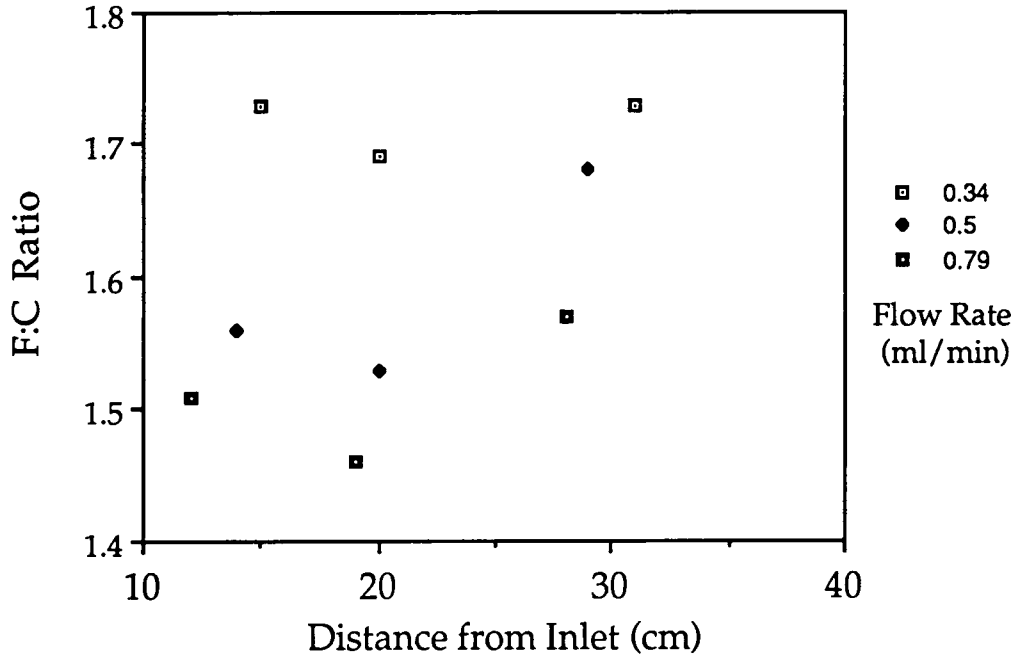

Figure 3.7 Stoichiometry of polymers as a function of flow rate and position in reactor

Figure 3.8 Surface energies of perfluorohexane plasma polymers as a function of flow rate and position in reactor

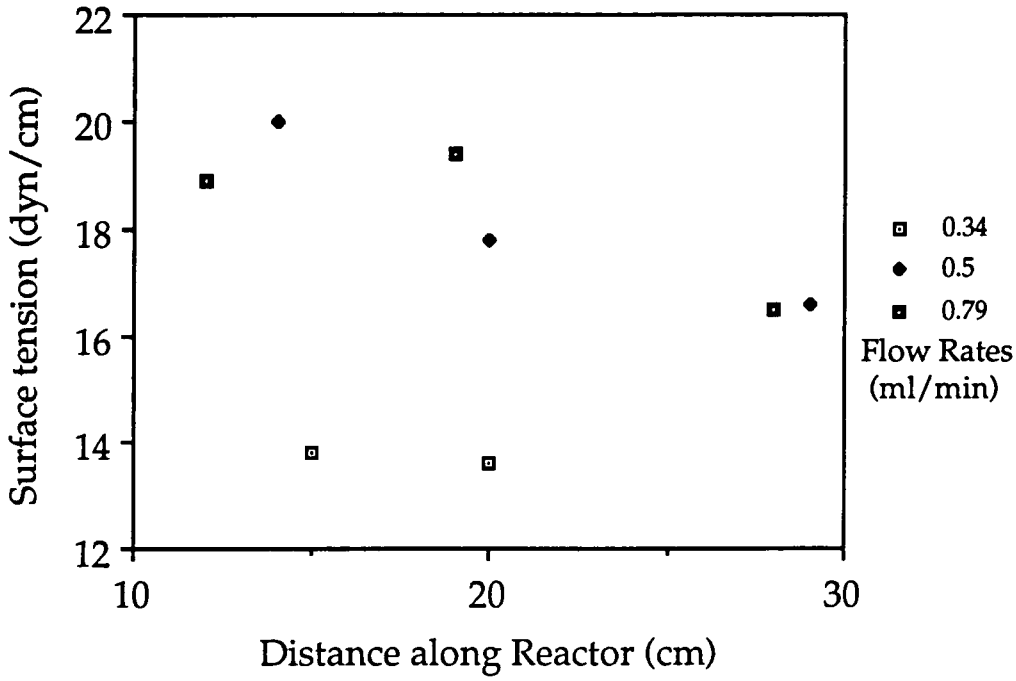

pronounced at higher flow rates. According to Yasuda's equation $\frac{W}{F}$ (see chapter 1) low flow rates are equivalent to high powers, and at high powers the deposits had similar chemical compositions throughout the reactor. However at 10 W power the glow region did not extend throughout the reactor and some change in the character of the polymers even at low flow rates was expected on going from the glow to the non-glow region. The differences in terms of chemical composition and surface energy between polymers formed at the higher flow rates are not as marked as the change on going to the low flow rate.

Figure 3.8 shows the surface energies calculated for polymers which were stable to contact with water. The low flow rate deposits demonstrating surface energies close to the 30 W plasma polymers, and

the higher flow rate deposits are similar to each other in terms of surface energy.

3.3.2 Deposition of Hexafluoropropene in the non-glow region

The deposition of hexafluoropropene at two different powers in reactor one is shown in table 3.3. The upstream deposits show the same dependence upon power for the chemical character of the polymer that was determined in chapter 2. At high powers, there is a larger CF_2 content in the polymer than at lower powers, the low power plasma polymers having a predominance of CF groups. The 30 W plasma polymers had a very uniform composition throughout the reactor, the glow region filling the whole vessel. This result is at variance with the 15 W polymers which show change in chemical nature within the glow region itself (this extended to 20 cm). The CF_2 content of the polymers formed at 15 W power show a large increase along the length

Distance from Inlet	% of C_{1S} Area						Contact Angles	
	CH	C-CF	CF	CF_2	CF_3	CF2/CF3	H_2O	CH_2I_2
15W power, 0.5 ml/min flow rate								
9 cm	2.8	22.7	27.4	22.8	22.3	1.02	113	*
19 cm	2.7	19.8	23.5	32.1	22.0	1.46	114	*
28 cm	1.8	16.0	21.3	39.3	21.7	1.81	118	*
30W power, 0.5 ml/min flow rate								
10 cm	2.3	15.1	27.9	30.3	24.4	1.24	109	93
19 cm	1.6	15.1	28.8	30.2	24.3	1.24	110	93
29 cm	1.7	15.0	28.1	30.6	24.6	1.24	113	96
37 cm	1.7	15.1	27.5	31.1	24.7	1.26	113	93

Table 3.3 Hexafluoropropene plasma polymers, effect of power and position in reactor

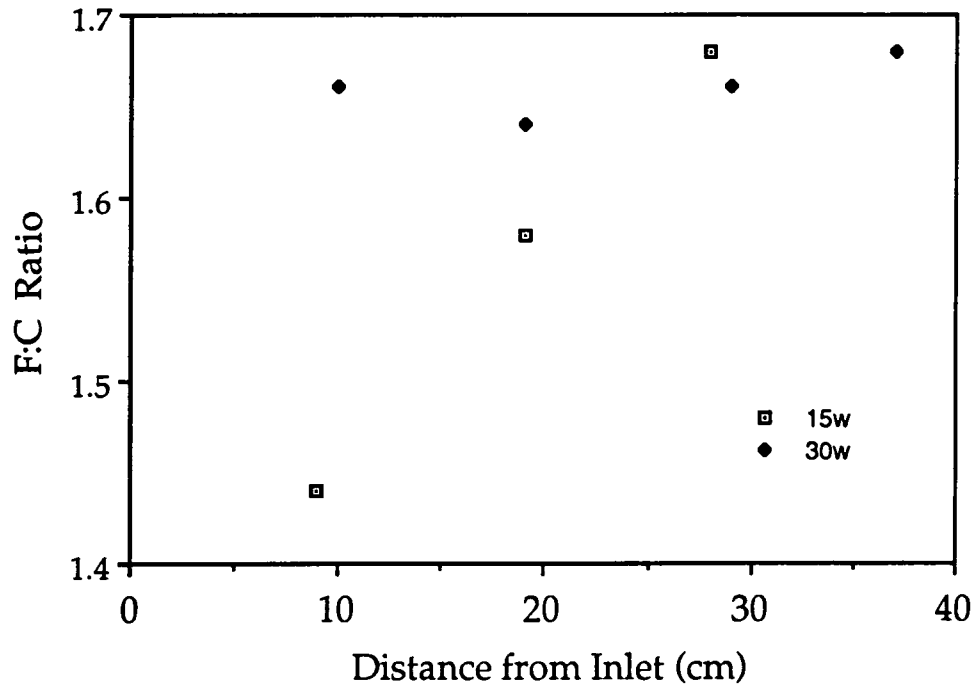

Figure 3.9 Stoichiometry of hexafluoropropene plasma polymers

of the reactor. The substrate at 28 cm. collecting a deposit with a larger proportion of CF_2 than any of the perfluorohexane plasma polymers at a comparable distance. The initial rise in CF_2 content within the glow region could be due to a change from the deposition process which occurs at low power to a process similar to that which occurs at high power, after substantial fragmentation or excitation of the monomer has occured. This is indicated by the deposit collected at 19 cm. under 15W power being closer to the 30 W polymers in structure and stoichiometry. The subsequent rise in the CF_2 intensity in the non-glow region would then be caused by a similar process to that occuring in the case of perfluorohexane. The structure of the deposits being typical of the polymer forming species exiting the glow region. Figure 3.9 shows the difference in fluorine incorporation at different powers and deposition sites in the reaction vessel. Unlike the perfluorohexane polymers which all followed a similar pattern of deposition

throughout the reactor, here there are clearly two differing processes at high and low power (see chapter 2).

The contact angles with diiodomethane were not measured for the 15 W plasma polymer. It was not possible therefore, to make an estimate of the surface energies of these samples. The surface energies of the 30 W samples are all between 11 and 12 dyn/cm, similar to the 30 W perfluorohexane plasma polymers.

3.3.3 Polymer Deposition in an Earthed Cage

Plasma polymerisation of both perfluorohexane and hexafluoropropene was carried out in reactor 2 (see figure 3.2). The earthing lead from the cage was attached internally to an earthed cajon joint at the outlet end of the reactor. The presence of this lead affected the pumping rate by occluding the outlet, with the result that flow rates were difficult to set precisely. The formation of films within the cage was slow due to low deposition rates and the polymers collected within the cage were often unstable to contact with water (as were some of the downstream deposits formed in the previous sections). Perfluorohexane plasma polymers are summarised in table 3.4, and hexafluoropropene plasma polymers in table 3.5.

In all cases, deposition within the cage resulted in a substantial increase in the CF_2 to CF_3 ratio. No underlying trend for the deposition of polymers with a high CF_2 content within the cage in terms of power and flow rate could be found from these results however. It can be noted that deposition rate in the cage using perfluorohexane is dependent upon high powers. Optimal conditions seem to exist for the production of these relatively unbranched polymers. In the case of perfluorohexane at 15 W power and 0.5 ml/min flow rate a very high

Position in reactor	% of C_{1S} Area						Contact Angles	
	CH	C-CF	CF	CF_2	CF_3	CF2/CF3	H_2O	CH_2I_2
10 W, 0.2 ml/min								
Plasma	2.5	14.1	22.2	33.2	25.4	1.31	*	*
Cage	*	*	*	*	*	1.82	*	*
10 W, 0.5 ml/min								
Plasma	1.9	16.2	26.3	30.8	24.8	1.24	*	*
Cage	*	*	*	*	*	1.97	*	*
15 W, 0.5 ml/min								
Plasma	3.3	17.6	22.6	29.9	25.3	1.18	106	78
Cage	0.0	6.6	8.0	72.9	12.5	5.83	*	75
20 W, 0.5 ml/min								
Plasma	2.4	17.9	28.1	26.9	24.7	1.09	111	85
Cage	1.5	16.2	21.3	38.8	22.2	1.75	*	82
20 W, 1.0 ml/min								
Plasma	1.3	19.0	29.1	27.8	21.5	1.29	114	88
Cage	2.0	17.8	24.0	30.9	24.0	1.29	*	92

Table 3.4 Perfluorohexane plasma polymers formed in the glow region and within a faraday cage

Position in reactor	% of C_{1S} Area						Contact Angles	
	CH	C-CF	CF	CF_2	CF_3	CF2/CF3	H_2O	CH_2I_2
10 W, 0.3 ml/min								
Plasma	2.6	12.1	26.4	33.0	24.9	1.32	106	*
Cage	1.1	11.8	24.8	36.6	24.4	1.50	108	*
10 W, 0.5 ml/min								
Plasma	1.9	18.5	28.7	27.3	23.6	1.15	107	72
Cage	*	*	*	*	*	1.90	*	79
15 W, 0.5 ml/min								
Plasma	3.6	22.0	28.1	24.4	22.3	1.08	106	65
Cage	*	*	*	*	*	1.97	*	75
20 W, 0.6 ml/min								
Plasma	2.5	14.0	27.9	28.6	23.2	1.23	110	87
Cage	0.0	11.7	21.2	41.6	24.2	1.71	*	90

Table 3.5 Hexafluoropropene plasma polymers formed in the glow region and within a faraday cage

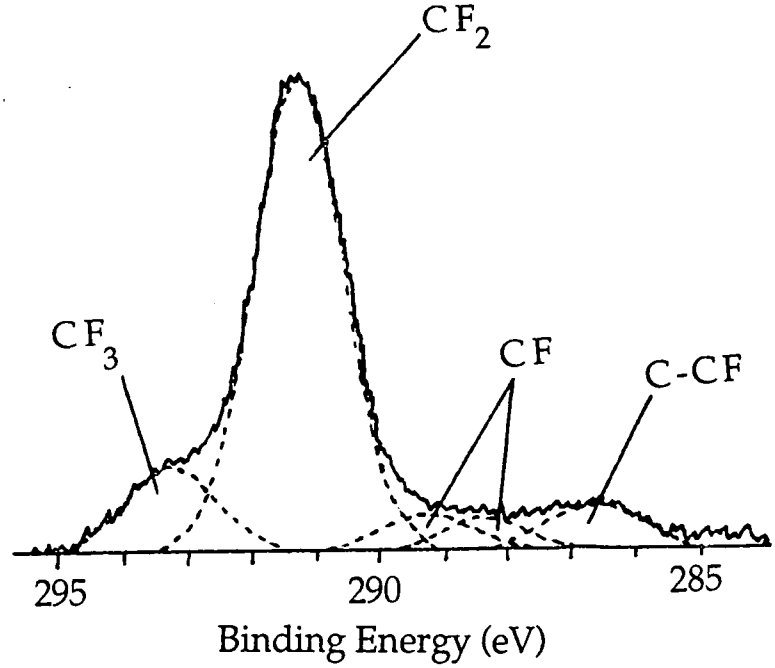

Figure 3.10 Polymer from faraday cage, perfluorohexane plasma 15 W

incorporation of CF_2 units was observed, the C_{1S} spectrum is shown in figure 3.10. The polymers formed within the faraday cage were all, with one exception unstable to contact with water, and so surface energy comparisons could not be made.

Figures 3.11 to 3.14 demonstrates the changes in the C_{1S} spectra of films after contact with water for one minute. Both plasma and faraday cage deposits of a perfluorohexane 20 W, 1.0 ml/min plasma were immersed in distilled water, dried and analysed by XPS. Both samples were shown to contain oxygen following wetting, (visible as a peak in the O_{1S} XPS region) the change to the plasma polymer being much less marked than the change in the faraday cage deposit. A comparison of elemental peak areas (with appropriate sensitivity factors) indicated that the stoichiometry of the plasma polymer changed from $CF_{1.49}$ to $CF_{1.47}O_{0.03}$, while the faraday cage deposit

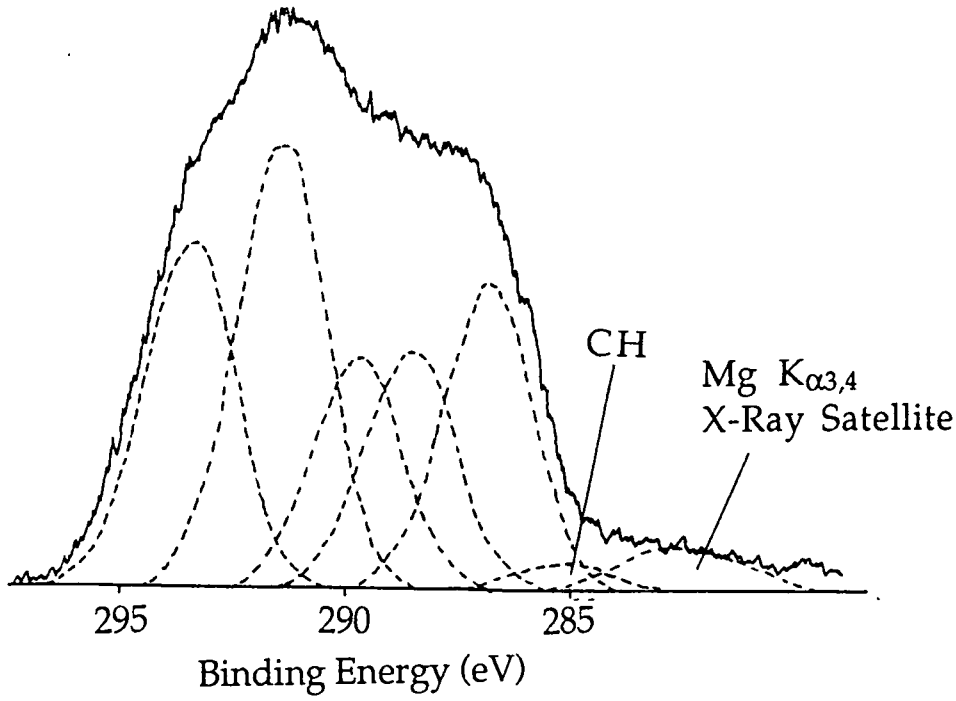

Figure 3.11 XPS C1S spectrum of plasma region perfluoro-hexane deposit at 20 W power

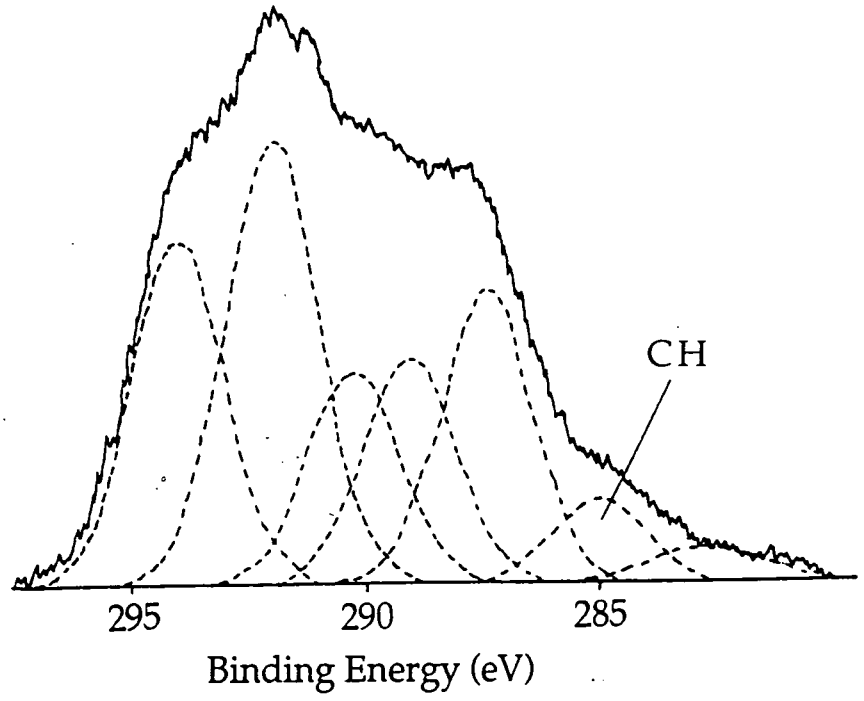

Figure 3.12 As above, immersed in water for one minute

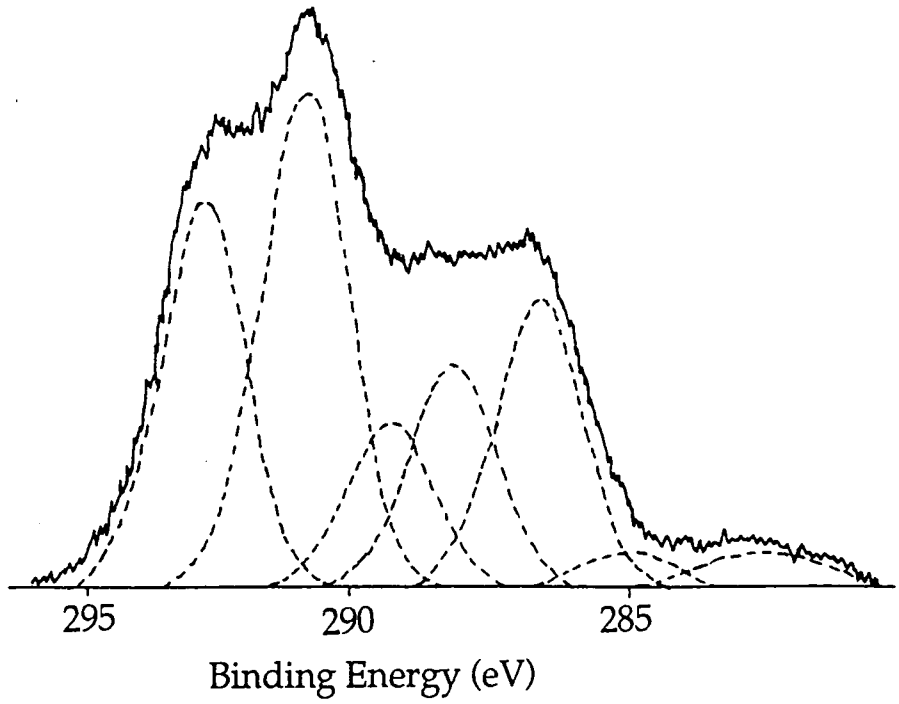

Figure 3.13 XPS C1S spectrum of faraday cage perfluoro-hexane deposit at 20 W power

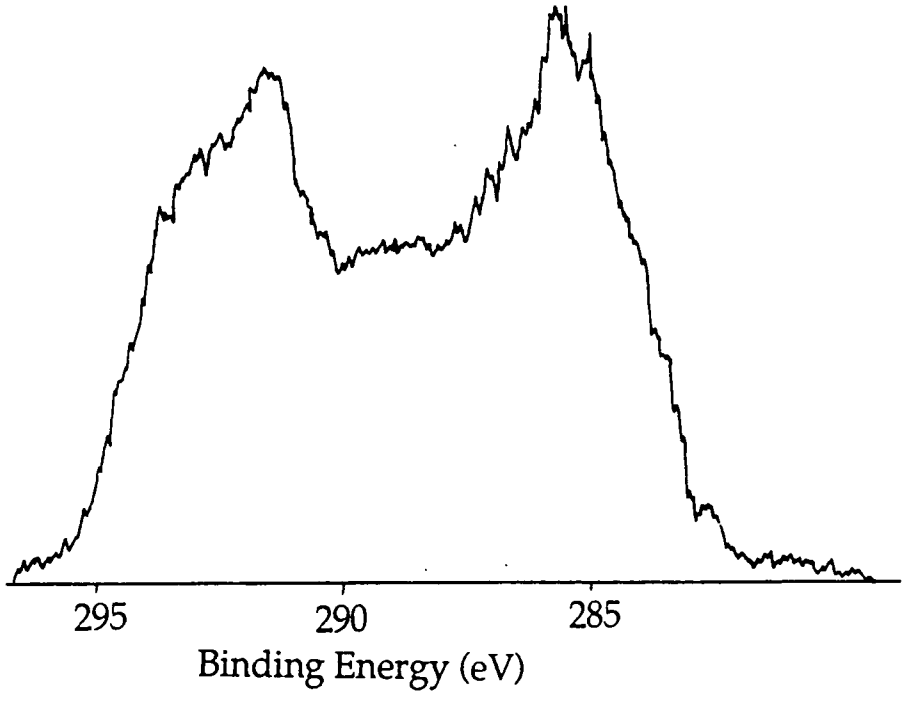

Figure 3.14 As above, immersed in water for one minute

changed from $CF_{1.58}$ to $CF_{1.32}O_{0.12}$. The increase in the low binding energy components of the C1S XPS region is more dramatic for the sample from the cage, but a meaningful peak fit was not possible for this sample due to the numerous possible carbon environments. Very thin cage samples with visible Al2P peaks were treated with water and no intensity change occured in the aluminium peak. This indicates that there is no change in the thickness of the film, and the phenomenon occurs either as a reaction at the surface of the film, or migration of oxygen containing hydrocarbon material to the surface. Some deposits from the cage were washed in perfluorohexane, which removed the polymer from the aluminium substrate. The fluorocarbon material was probably then of a low molecular weight and soluble in this liquid. None of the plasma region substrates were affected by washing in perfluorohexane. Cross linking of the plasma polymerised material renders it insoluble in perfluorohexane; this cross linking does not occur during non glow deposition possibly as a result of negligable ion bombardment during deposition (see chapter 2).

3.4 Discussion

In general it was found that material deposited in the down-stream non-glow region of a perfluorocarbon plasma contained a large amount of fluorine, and that the predominant group in such deposits was the CF_2 group. These and other results[1-4] suggest that the structure and to an extent the stoichiometry of the monomer does not affect the occurance of this phenomenon. Therefore certain polymer forming species which are produced in all perfluorocarbon plasmas must be responsible for these deposits. The gas phase downstream of the plasma contains only material which was not deposited within the plasma

region, in most cases the plasma polymer has a lower F:C ratio than the monomer and it follows that the spent gases will have an higher F:C ratio than the monomer. Material collected in this region will reflect this.

The production of CF_2 radicals and radical cations in a perfluorobenzene plasma has been noted previously by optical emission spectroscopy[8]. Mass analysis[9] of perfluorobenzene plasmas confirm the presence of these species along with such products as CF_3 radicals and tetrafluoroethylene. CF radicals are not prominent in the mass spectrum of a perfluorobenzene plasma, which could be due either to a low concentration or to a short lifetime. The presence of CF radicals in relatively high concentrations in perfluorocarbon plasmas[10] has been noted however, and therefore this species probably has a short lifetime. The CF radical will tend to react with fluorine radicals to form difluorocarbene species[11] which have good stability.

$$CF + F + M \rightarrow CF_2 + M$$

The production of CF_x radicals results from electron impact induced dissociations, these are shown below with the energy required for each bond cleavage[12]. It can be seen that following dissociation, the most stable radical species in this series is the CF_2 moiety.

$CF_4 + e \rightarrow CF_3 + F + e$	5.6 eV
$CF_3 + e \rightarrow CF_2 + F + e$	2.2 eV
$CF_2 + e \rightarrow CF + F + e$	6.1 eV
$CF + e \rightarrow C + F + e$	5.2 eV

CF_2 radicals combine to form tetrafluoroethylene and perfluorocyclopropane which are readily polymerisable[11].

$$2CF_2 \rightarrow C_2F_4$$

$$CF_2 + C_2F_4 \rightarrow \text{cyclo-}C_3F_6$$

CF_3 and F radicals are probably present in the non glow region, but cannot be considered polymer forming species, although their involvment in modifying and etching the growing film should not be discounted. Sputtering and cross linking of the film by ion impact will be negligable beyond the plasma region; free electrons will be rare and their energies insufficient to produce ionisation. Photons in the ultraviolet and vacuum ultraviolet regions are emitted from the glow region and electromagnetic radiation of this energy is able to cause electronic excitation in molecules and therefore could be important in gas phase reactions. The results in section 3.3.1 indicate that the longest lived polymer forming species have a $(CF_2)_n$ structure. Functionalities other than CF_2 become rarer further from the plasma region and may be formed by action of chemical etchants on the growing film, condensation of relatively large molecules produced in the plasma region or reaction with species such as CF radicals. The latter two processes would be expected to give the steady increase of CF_2 concentration away from the plasma region that was observed, though all three processes may contribute to the presence of CF and C-CF functionalities.

The instability of many of these films to water was unusual for plasma polymers, the films changed from being highly hydrophobic to being hydrophilic within a matter of seconds. A possible explanation is that some reaction is occuring at the polymer-liquid interface. Such

phenomena has been observed in plasma polymerised perfluoropyridine, and was attributed to surface hydrolysis[13]. If reaction occured between trapped free radicals in the film and water, highly fluorinated alcohols would be produced. The presence of such groups enhancing the hydrophilicity of the surface, very high and very low contact angles possibly being due to surface roughness in accordance with Wenzel's law[14]. However, if such radicals were present, some reaction with atmospheric oxygen on transport to the XPS analyser would be expected. A more likely explanation may be that hydrophilic contaminants present on the aluminium surface migrate through the fluorocarbon material and express themselves at the surface, drastically increasing the apparent surface energy. This would also account for the XPS results obtained in figure 3.14 were an enhancement of lower binding energy carbon is evident.

3.5 Conclusion

Two perfluorocarbon monomers were plasma polymerised, and a study of the nature of the polymer at different sites in the reactor was carried out. In both cases, despite the difference in structure of the monomers the deposit in the non glow region showed an enhanced content of CF_2 groups, indicating that the composition of the polymer in this region was more linear than in the plasma region. Perfluorohexane deposits were studied in detail and it was found that downstream of the plasma region the proportion of carbons with two fluorine atoms directly attached increased with distance from the plasma region. The removal of some of these films by washing with perfluorohexane indicates that they are soluble in this liquid and therefore probably of a relatively low molecular mass. The structure of

the downstream deposits suggests that the most stable polymer forming species produced within a perfluorocarbon plasma are $(CF_2)_n$ species.

References

1 D. T. Clark, D. Shuttleworth, *J. Polym. Sci., Polym. Chem. Ed.*, **18**, 27, (1980)

2 D. F. O'Kane, D. W. Rice, *J. Macromol. Sci., Chem.*, **A10**, 567, (1976)

3 H. Yasuda, J. Polym. Sci., *Macromol. Rev.*, **16**, 199, (1981)

4 P. D. Buzzard, D. S. Soong, A. T. Bell, *J. Appl. Polym. Sci.*, **27**, 3965, (1982)

5 B. W. Cherry, "Polymer Surfaces", Cambridge Solid State Science Series, Cambridge University Press, (1981)

6 D. Briggs, M. Seah in "Practical Surface Analysis by Auger and X-Ray Photoelectron Spectroscopy", Wiley, Chichester, 133, (1983)

7 B. Chapman, "Glow Discharge Processes, Sputtering and Plasma Etching", Wiley, New York, (1980)

8 C. Till, Ph.D. Thesis, Durham University, (1986)

9 R. Ward, Ph.D. Thesis, Durham University, (1989)

10 R. d'Agostino, S. De Benedictis, F. Cramarossa, *Plasma Chem. Plasma Process.*, **4**, 1, 1, (1984)

11 D. S. Y. Hsu, M. E. Umstead, M. C. Lin, in "Fluorine-containing Free Radicals", Ed. J. W. Root, ACS Symposium Series 66, (1978)

12 J. Bretagne, F. Epaillard, A. Ricard, *J. Polym. Sci., Polym. Chem. Ed.*, **30**, 2, 323, (1992)

13 D. T. Clark, M. M. Abu-Shbak, *J. Polym. Sci., Polym. Chem. Ed.*, **21**, 2907, (1983)

14 a M. Klausner, I. H. Loh, R. F. Baddour, R. E. Cohen, *ACS Polymeric Materials Science and Engineering*, **56**, 227, (1987)

b B. D. Washo, *Org. Coat. Appl. Polym. Sci. Proc.*, **47**, 69, (1982)

Chapter 4

Plasma and Vacuum Ultraviolet Oxidation of Polyethylene, Polystyrene and PEEK

4.1 Introduction

Controlled surface oxidation of polymers is an area of considerable scientific importance with regard to improving their wettability, printability and adhesion[1]. Many different processes have been used to acheive surface oxidation including hot pressing against aluminium foil[2], flame treatment[3], electrical corona discharge[4], glow discharge in oxygen[5], remote plasma treatment[6], surface ozonation[7] and photo-oxidation[8]. Oxidation is most severe at the surface of the polymer therefore an understanding of the surface chemistry is crucial.

Ultraviolet and plasma oxidation of polymers are known to generate a variety of surface species[6,9]. Precise mechanistic details are, however, a matter of much debate. In this chapter, the plasma and UV oxidation of polyethylene, polystyrene and poly (ether ether ketone) (PEEK) are compared (see figure 4.1). The role of different functionalities

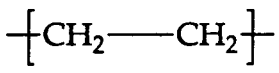

Polyethylene

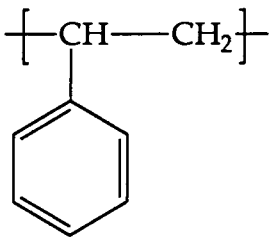

Polystyrene

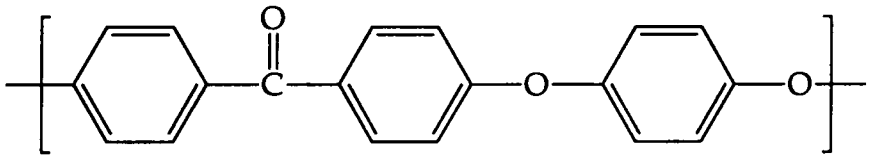

PEEK

Figure 4.1 Repeat units of polymers used in chapter 4

present in the polymers is examined in the production of an oxidised surface. In addition to oxygen, carbon dioxide and nitrous oxide are used as oxidising atmospheres.

4.2 Experimental

All reactions were carried out in the reactor shown in figure 4.2. Glow discharge treatments were carried out in the right hand side of the reactor. For glow discharge modifications, the reactant gases were introduced at a constant flow rate of 1.1 ml/min, and a power of 10W was used for three minutes. Longer treatments under these conditions produced no further changes (as shown by XPS) in the polymer surface.

For photo-oxidation the polymer was placed in the left hand side of the reactor which was isolated from the right hand side by a lithium fluoride window. Both sides were evacuated to a pressure of better than 5×10^{-2} Torr. A nitrogen glow discharge (50W, 1.1 ml/min) was struck

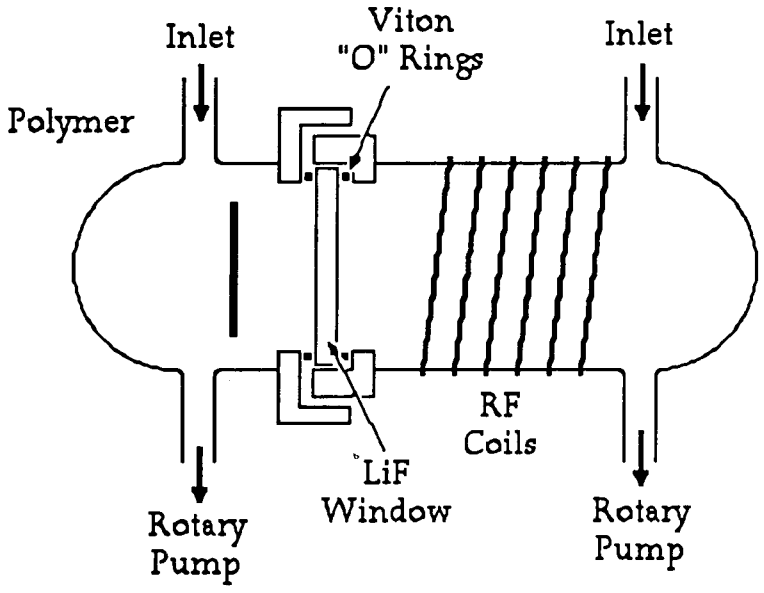

Figure 4.2 Schematic of reactor used in chapter 4

in the right hand side to generate ultraviolet radiation, the LiF window being transparent to the strongest lines at 174 and 149 nm. The left hand side contained the polymer to be modified under 25 Torr of oxidising gas. One hour exposures were found to yield constant XPS features.

In the absence of any form of excitation, none of the materials examined in this study were found to react with any of the gases.

Research grade oxygen, nitrogen, nitrous oxide and carbon dioxide were supplied by BOC. The low density polyethylene (LDPE), polystyrene and poly(ether ether ketone) (PEEK) were carefully washed with isopropyl alcohol and dried in air which was found to give a contaminant free surface (by XPS).

XPS spectra were acquired on the equipment described in chapter 2, take off angles of 30° and 70° were used, giving effective sampling depths of 35Å for C_{1S} and 25Å for O_{1S} electrons at the lower angle and 15Å and 10Å respectively at the higher angle[10]. Detailed chemical information about the modified polymer surfaces was obtained by peak

Assignment	Possible environments	Binding Energy
C-H	C-CH2-C, C-CH=C, etc.	285.0 eV
C-CO2-	C-CH2-COO-C-, C-CH2-CO2H etc.	285.7 eV
C-O	C-CH2-OH, C-CH2-O-CO-C, etc.	286.6 eV
C=O	C-CO-C, H-CO-C, C-OCH(OH)-C, etc.	287.9 eV
O-C=O	C-CO-O-C, C-CO2H, HCO-O-C, etc.	289.0 eV
-O-CO-O-	(Carbonate groups)	290.4 eV

Table 4.1 Typical C_{1S} Binding energies of oxygen containing structural features

fitting the C1S envelope to a range of carbon functionalities. Table 4.1 summarises the chemical shifts used during the deconvolutions[5]. A typical peak fit is shown in figure 4.3. Polystyrene and PEEK demonstrated a distinctive satellite to the main peak at ~291.6 eV, which is associated with low energy $\pi \rightarrow \pi^*$ shake up transitions in the aryl rings that accompany core level ionisation[11]. Instrumentally determined sensitivity factors are such that for unit stoichiometry, the C_{1S}:O_{1S} intensity ratio is ~0.55. By taking into account that the oxygen core level intensity and the deconvoluted carbon core level envelope are products of the actual groups present in the surface, an approximate idea of which functionalities make up the surface can be gained (e.g. carboxylic acids *versus* esters, alcohols *versus* ethers).

4.3 Results and Discussion

4.3.1 Polyethylene

The results of experiments carried out on polyethylene are tabulated below, the first column shows the percent loss in the hydrocarbon C1S peak area to other, more oxidised functionalities. The second column shows the ratio of oxygen atoms (O, from the O_{1S} peak area) to oxidised carbon atoms ($\Sigma(\underline{C},O) = \Delta(\underline{C}\text{-}H)$, from the C_{1S} peak area, subtracting any contribution from hydrocarbon environments). This ratio gives, for example, values of 2 for a surface containing only carboxylic acid groups, and 0.5 for a surface with only ether groups present. The distribution of oxidised carbon functionalities is given in the remaining columns (with $\Sigma(\underline{C},O) = 100\%$). The comparison of C_{1S} and O_{1S} data in this manner relies on some vertical homogeneity of the sample since these core levels produce electrons with differing mean free paths (see section 4.2).

Exposure to an oxygen plasma was found to yield highly oxidised

			Σ(C,O)			
Treatment	Δ(C-H)	O:Σ(C,O)	C-O	C=O	O-C=O	O-CO-O
O_2/Plasma	8	1.25	64	12	24	0
O_2/UV	19	0.90	44	30	26	0
CO_2/Plasma	14	0.86	44	19	31	6
CO_2/UV	15	0.80	59	18	23	0

Table 4.2 Results of oxidation reactions on polyethylene

functionalities at the LDPE surface, since the large O_{1S} peak (compared with the amount of oxidised carbon) indicates that carboxylic acid and alcohol groups rather than ester and ether linkages are present. A large

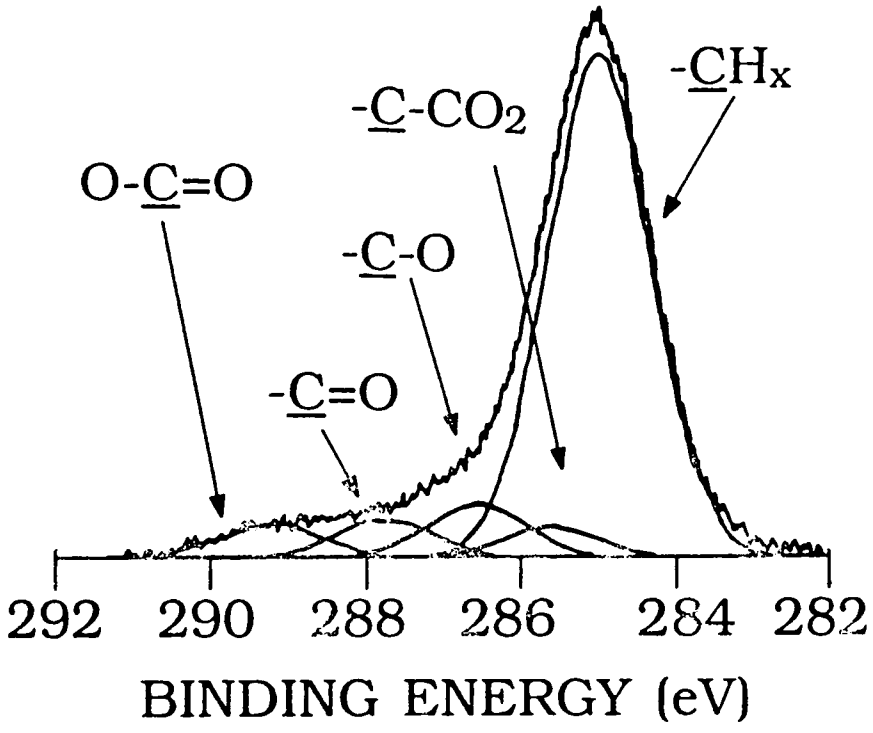

Figure 4.3 Peak fit of C_{1S} XPS spectrum for oxygen plasma modified polyethylene

amount of polyethylene remained unoxidised in this case, suggesting that there is significant ablation of the surface via sputtering and the desorption of gaseous products (for example CO_2 and H_2O), resulting in a continual unmasking of fresh LDPE. These observations are consistent with previous reports where the effects of glow discharge oxidation have been confined to the uppermost monolayers[5].

The other treatments, involving carbon dioxide and/or vacuum ultraviolet irradiation lead to more oxidised carbon atoms present at the surface with a tendency for ethers and esters to form, shown by a comparitively lower $O:\Sigma(\underline{C},O)$ ratio than the oxygen plasma experiment. The presence of more varied carbon-oxygen moieties in the CO_2 glow discharge[12] results in the creation of more ester and carbonate species than detected for ultraviolet modification with the same gas; the predominance of different reactant species from the differing modes of excitation being the most likely cause of this.

Previous workers[7] have photo-oxidised polyethylene at longer wavelengths (254 nm) under an oxygen atmosphere. The limiting values for the functional groups produced were 42:16:42 for the groups $\underline{C}$-O : $\underline{C}$=O : O-$\underline{C}$=O and an $O:\Sigma(\underline{C},O)$ of 0.90. Thus in this experiment (using higher frequencies) there is a tendency to favour carbonyl group formation rather than carboxyl groups.

A comparison of the oxygen and carbon dioxide ultraviolet experiments shows that under an oxygen atmosphere the formation of carbonyl groups is much more dominant than in a carbon dioxide atmosphere (where the production of ether linkages seems to be the main reaction). These observations can be explained on the following basis:

Photo-oxidation of polyethylene is mainly initiated by[13],

$$P\text{-}H + h\nu \longrightarrow P\cdot + H\cdot$$

Hydroperoxides intermediates are generated in the presence of molecular oxygen[14], these may then decompose to form ketones[15,16].

$$P\cdot + O_2 \longrightarrow P\text{-}OO\cdot$$

$$P\text{-}H + P\text{-}OO\cdot \longrightarrow P\cdot + P\text{-}OO\text{-}H$$

$$P\text{-}OO\text{-}H + h\nu \longrightarrow \text{ketones (+ esters)}$$

However, the reaction with CO_2 can be envisaged as:

$$P\cdot + CO_2 \Leftrightarrow P\text{-}CO_2\cdot \longrightarrow \text{esters + acids}$$

But there will also be photodissociation of CO_2:

$$CO2 + h\nu \longrightarrow CO + [O]$$

It has been illustrated previously through oxygen uptake measurements that the photo-oxidative process is controlled at low pressure by the availability of oxygen and at high pressure by the number of reactive centres produced in the polymer[17]. The carbon dioxide atmosphere is less oxidising than the oxygen atmosphere, making intermolecular reaction more likely;

$$2P\cdot \text{(close proximity)} + [O] \longrightarrow PO\cdot + P\cdot \rightarrow POP \text{ (ether)}$$

In many ways both the plasma and ultraviolet carbon dioxide treatments result in almost identical functionalisation. This similarity suggests that the main oxidation processes occuring in both cases are the same. The more highly oxidised moieties (especially the presence of

carbonate groups) produced in the plasma modification may be attributed to its more vigorous nature, and the formation of a greater concentration of free radicals in association with excited CO_2 species.

4.3.2 Polystyrene

Polystyrene consists of an alkyl chain polymeric backbone with pendant phenyl rings on alternate carbon atoms. There are two peaks observed in the C_{1S} region of the XPS spectrum for clean polystyrene; an hydrocarbon component (285 eV, 94% of total C_{1S} signal and a shake up satellite due to the $\pi \rightarrow \pi^*$ transition (~291.6 eV, 6%). The size

				Σ(C,O)			
Treatment	(C-H)	$\pi \rightarrow \pi^*$	O:Σ(C,O)	C-O	C=O	O-C=O	O-CO-O
untreated	94.0	6.0	*	*	*	*	*
O_2/Plasma	62.4	3.1	0.87	38	27	26	9
(70°)	(46.6)	(1.8)	(0.87)	(37)	(26)	(27)	(10)
O_2/UV	65.1	0.8	1.11	31	27	37	5
(70°)	(57.5)	(1.4)	(0.97)	(22)	(31)	(38)	(9)
CO_2/Plasma	63.2	3.1	0.97	41	22	28	9
(70°)	(58.1)	(2.3)	(1.01)	(34)	(26)	(31)	(9)
CO_2/UV	68.1	1.6	1.31	37	24	33	6
(70°)	(56.9)	(1.4)	(1.20)	(37)	(26)	(32)	(5)
N_2O/UV	87.8	4.2	0.88	84	16	0	0
(70°)	(85.4)	(4.4)	(0.75)	(80)	(20)	(0)	(0)

Table 4.3 Results of oxidation reactions on polystyrene

of this peak can be used as a measure of the retention of aromatic groups at the surface of the polymer after modification. Table 4.3 summarizes the results of plasma and ultraviolet experiments under various gases on polystyrene. XPS measurements at 70° have a higher surface sensitivity than the 30° results and can be used to examine how far the oxidation extends into the bulk.

Surface modification of polystyrene by a glow discharge yields a broad range of oxidised functionalities. Oxygen atoms within the plasma may be responsible for the large number of C-O groups, although peroxide groups (from oxygen molecules) could be responsible for some contribution to the C-O intensity. A relatively significant proportion of carbonate groups can be taken as an indication of the vigorous nature of the glow discharge treatment. At lower powers (0.1W) a diminished degree of surface ablation through sputtering leads to even more carbonate at the surface[5]. It should be noted that during plasma treatment the surface is continually renewed by the evolution of small volatile molecules[18], which confines oxidation mainly to the topmost layers. This can be seen by the smaller hydrocarbon component at 70° take off angle. The relative concentration of the various oxidised carbons remains essentially unaltered at both take off angles indicating that the oxidised species are at the surface of the polymer. The drop in the shake up component on going to an higher take off angle shows that there is a dramatic loss of unsaturated phenyl groups near the surface. Plasma oxidation of poly (p-xylylene) -[-CH_2-Ph-CH_2-]- (which is structuraly related to polystyrene) under similar conditions[19], results in a surface very similar to the one produced in these experiments. The structural components of the polymer being oxidised appear to be very important

in determining the functionalities produced at the surface following plasma or UV treatment.

Polystyrene undergoes extensive oxidation when excited with ultraviolet light in the presence of oxygen[20]. The nature of the changes induced at the polymer surface can differ from that in the solid. Oxidation of bulk polymer is highly dependent upon diffusion of oxygen into the polymer[21], whilst the surface is exposed to an abundant oxygen supply. It should be expected therefore that the mechanism of photo-oxidation and the final products formed in the two cases are different. At wavelengths shorter than 290 nm it has been postulated that photo-oxidative attack arises from excitation of the phenyl ring[22] to form either a charge-transfer complex between the phenyl rings and molecular oxygen[23] or a peroxy intermediate[24]. In experiments using vacuum ultraviolet (λ < 200nm), it is also possible for excitation of the alkane backbone to occur[25]. In addition the following photoexcitations in the gas phase may also be occuring[26]:

$O_2(X^3\Sigma_g^-) \longrightarrow O_2(A^3\Sigma_u^+)$	250-300 nm
$O_2(X^3\Sigma_g^-) \longrightarrow O_2(B^3\Sigma_u^-)$	175-200 nm
$O_2(X^3\Sigma_g^-) \longrightarrow O(^3P) + O(^3P)$	< 242 nm
$O_2(X^3\Sigma_g^-) \longrightarrow O(^3P) + O(^1D)$	<175 nm

Examination of the $\pi \rightarrow \pi^*$ shake up satellite reveals that upon exposure of polystyrene to vacuum ultraviolet radiation under a pure oxygen atmosphere, an enhanced attack on the phenyl ring occurs compared to irradiation at longer wavelengths[24,27]. Benzene is not detected as a product of photo-oxidation[20], therefore the loss in shake up intensity cannot be rationalised as a photolytic cleavage of phenyl

groups from the polymer backbone and must be attributed to loss of aromaticity by the formation of bonds to the ring carbon atoms. There is a concomitant decrease in the amount of carbon not directly bonded to oxygen and a rise in C-O, C=O and O-C=O functionalities. The extent of oxidative functionalisation and loss of shake up structure are indicative of oxidation of the aromatic rings.

A comparison of results from two take off angles shows that there is some change in composition with depth, oxidation occuring to some extent in the subsurface of the polymer and not just at the surface. At an high take off angle there is, as expected, a smaller contribution from the C-H component showing a larger degree of oxidation at the surface. Within experimental error there is little change in the shake up intensity, indicating that loss of aromaticity can occur at some depth within polystyrene under these conditions. There is a striking change in the relative concentrations of various oxidised groups with depth; the surface is composed mainly of carboxylate (mostly ester groups, given the O:Σ(C,O) ratio) and carbon atoms doubly bound to oxygen. With increasing depth, there is a rise in carbon atoms singly bound to oxygen and a slight drop in doubly bound atoms, but the relative concentration of carboxyl groups remains the same. The surface also appears to be richer in carbonate groups, demonstrating the high availability of oxygen at the surface. This contrasts with the oxygen plasma treatment where the oxidation appears to be confined to the outermost layers. Given that the glow discharge processes will also result in vacuum ultraviolet photo-oxidation of the polymer, these results demonstrate the degree to which surface ablation occurs during plasma treatment, although the

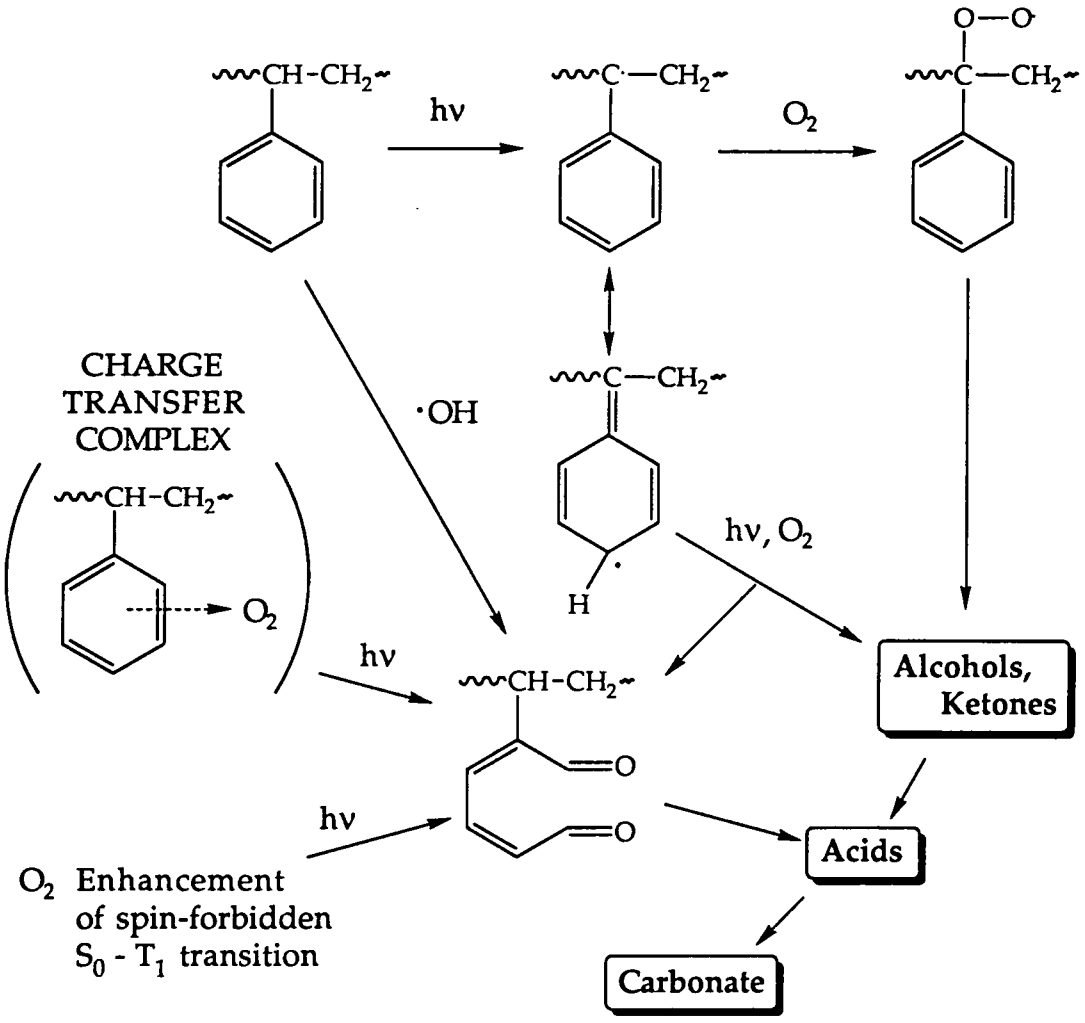

Figure 4.4 Scheme for some of the possible reactions occuring in the surface of polystyrene during photo-oxidation (ref. 28)

shorter experimental time may also have an influence if bulk oxidation is occuring.

Of particular note is the large proportion of oxidised carbon atoms as carboxylate groups, and the relative concentration of them throughout the surface and subsurface. It is probable that these groups are formed mainly through oxidation of the phenyl rings, see figure 4.4[28]. Formation of carboxyl groups from the polymer backbone is likely to result in scission of the polymeric chain; if such reactions were

common there would be a production of light molecules which would volatilise under the vacuum conditions used for XPS.

Both treatments involving carbon dioxide exhibit a greater oxygen and C-O content than their corresponding oxygen treatments. One possible explanation for this is that there is enhanced reactivity at the gas/polymer interface to produce:

$$CO_2 \longrightarrow CO + O$$

Since in the gas phase[26]:

$$CO_2 \longrightarrow CO + O(^3P) \qquad < 227 \text{ nm}$$
$$CO_2 \longrightarrow CO + O(^1D) \qquad < 167 \text{ nm}$$

Carbon monoxide would would be unlikely to participate in further reactions, whilst atomic oxygen reacts with the polymer substrate. As with polyethylene, there could be direct incorporation of CO_2 into the excited surface to produce carboxylate functionalities but photo-oxidation under oxygen seems to be more efficient at producing such groups.

Both carbon dioxide treatments appear to reduce the hydrocarbon components of the C_{1S} spectra by similar amounts, and the range of oxidised components following treatment correspond well. The similarity between the two C_{1S} deconvolutions is superficial however, because the larger oxygen content following the ultraviolet experiment points to mainly alcohol and acid groups whereas the plasma treatment produces more ether and ester groups. Upon changing the electron take off angle there is little change in the carbon dioxide photo-oxidised polystyrene except for a drop in the hydrocarbon component indicating that oxidation is confined mainly

to the surface. The plasma treated polystyrene shows an increase in the more oxidised functionalities at the surface, but the small drop in hydrocarbon content at higher take off angle coupled with the change in oxidised functionalities suggests that oxidation extends some way beneath the surface. These results point to carbon dioxide plasmas having a lower level of ablation than oxygen plasmas. Enhanced etch rate of polymers in oxygen plasmas has been shown to result from the high reactivity of neutral oxygen with excited sites produced by other processes, such as ion bombardment and UV activation[29]. The confinement of oxidation to the surface in the carbon dioxide photo-oxidation experiment is at odds with the oxygen results, where oxidation occurs to some depth using similar excitation. This is possibly due to a lack of oxidising species being available within the subsurface, as neutral carbon dioxide is unreactive compared to oxygen.

Further evidence for the preferential incorporation of atomic oxygen into the polymer surface as C-O bonds was found with nitrous oxide. N_2O dissociates readily below 200 nm[26] to form nitrogen and atomic oxygen:

$$N_2O \longrightarrow N_2 + O$$

On vacuum ultraviolet irradiation of polystyrene under nitrous oxide, there is exclusive incorporation of oxygen into the polymer surface; no N_{1S} XPS signal was detectable indicating that no reaction occured between the polymer and nitrogen. The dominant functionality formed was carbon singly bound to oxygen, with doubly bound carbon being the only other carbon species. On comparing the O:C ratio of 0.07 ± 0.01 with a decrease of approximately 8% in the non-oxidised carbon atoms, it can be concluded that this treatment results in mainly alcohol groups being formed rather than ether linkages. These

results contrast with the other photo-oxidation treatments where a variety of oxidised surface groups have been observed. The process occuring can be envisaged as a reaction between atomic oxygen and excited polystyrene centres to produce C-O linkages. Then a reaction with stray hydrogen radicals, or neighbouring carbon-hydrogen bonds to produce alcohol groups. There is a small loss in shake up intensity, but hardly as substantial as the other photo-oxidation experiments, possibly indicating that alcohol formation occurs by reaction with radicals formed on the polymeric backbone. The most likely site for this is at tertiary carbon atoms as these radicals will be stabilised by the phenyl ring (see figure 4.4). Results from different take off angles agree closely, suggesting that the modification produced extends at least to a depth of ~30Å. The extent of reaction was far less than that observed for treatment with oxygen and carbon dioxide under the same conditions.

4.3.3 Poly(ether ether ketone)

XPS analysis of clean PEEK shows three distinct peaks in the C_{1S} region typical of hydrocarbon, carbon singly bound and carbon doubly bound to oxygen. The O_{1S} region also has two peaks typical of oxygen in an ether environment and oxygen in a carbonyl environment, in the ratio ether : carbonyl 69%:31% (theoretically 67%:33%). The deconvolution of the C_{1S} envelope, see table 4.4, also agrees well with the theoretical values of (C-H); 70.4% (given a $\pi \rightarrow \pi^*$ contribution of 4.3%), and the expected 80:20 ratio between carbons in ether and carbonyl environments. The $O:\Sigma(C,O)$ ratio should be 0.63 which is also in very good agreement with the experimentally determined value.

				Σ(C,O)			
Treatment	(C-H)	π→π*	O:Σ(C,O)	C-O	C=O	O-C=O	O-CO-O
untreated	72.5	4.3	0.65	84	16	0	0
O_2/Plasma	60.5	2.4	1.00	46	26	25	3
(70°)	(49.9)	(3.2)	(0.96)	(40)	(27)	(27)	(6)
O_2/UV	50.8	1.2	1.08	38	22	37	3
(70°)	(35.7)	(1.0)	(0.90)	(31)	(24)	(44)	(1)
CO_2/Plasma	62.0	2.3	1.04	51	17	23	9
(70°)	(63.3)	(2.4)	(1.14)	(45)	(18)	(28)	(9)
CO_2/UV	55.6	2.1	1.02	50	19	26	5
(70°)	(47.4)	(1.0)	(0.87)	(40)	(26)	(29)	(5)
N_2O/UV	70.6	3.5	0.81	76	14	10	0
(70°)	(67.8)	(1.7)	(0.75)	(71)	(17)	(12)	(0)
N_2/UV	77.4	3.1	0.77	84	16	0	0
(70°)	(77.1)	(3.2)	(0.71)	(83)	(17)	(0)	(0)

Table 4.4 Results of oxidation reactions on PEEK

The benzophenone unit in PEEK (see figure Z.1) is a strong chromophore, and can be expected to undergo a Norrish type-I process[25], or an intermolecular hydrogen-atom abstraction process, see figure 4.5. Thus, excitation of the polymer surface will occur much more readily than with either polystyrene or polyethylene. Table 4.4 also shows the results of the modifications carried out on PEEK. Of note is the exposure of PEEK to the ultraviolet source under nitrogen. No incorporation of nitrogen was found by XPS, and an increase in hydrocarbon intensity was found to occur, although the shake up peak

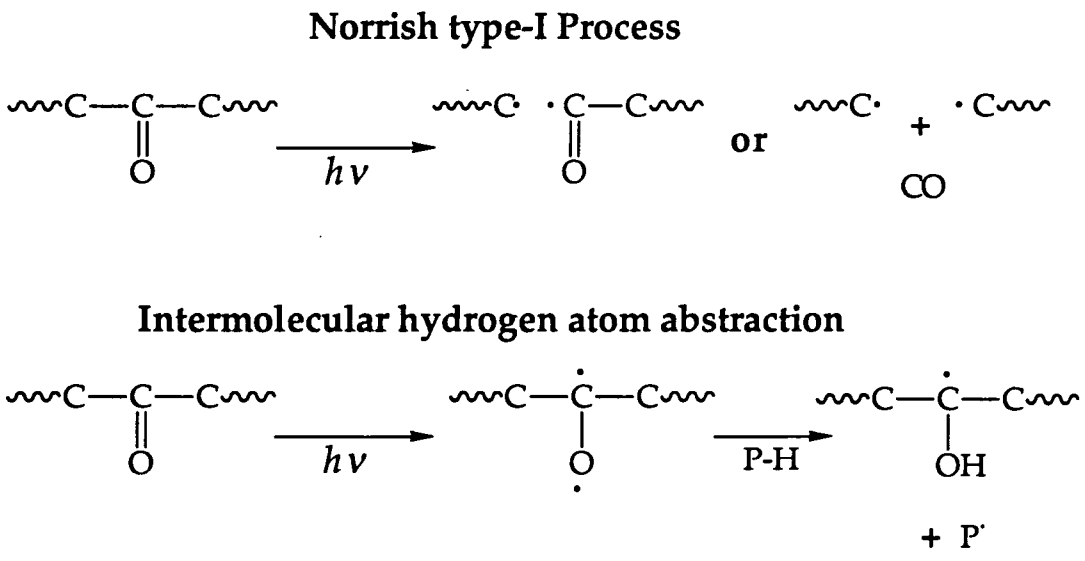

Figure 4.5 Formation of radical centres in PEEK by excitation of the carbonyl chromophore

decreased in intensity. The proportions of carbon doubly and carbon singly bound to oxygen remained constant, but the O_{1S} signal increased in proportion to the amount of carbon bound to oxygen. This implies that there has been some replacement of ether groups with alcohol groups. The actual ratio of carbon to oxygen remained constant at $CO_{0.15}$, suggesting that although some rearrangement had occured, any oxygen leaving the surface was equaled by the proportionate amount of carbon also leaving.

Norrish type-I reactions occuring consecutively along the length of a polymer chain would create volatile short chains which could leave the surface (into the gas phase or the bulk). The result of these reactions would be a slight decrease in the proportion of carbonyl groups to ether linkages. Intermolecular hydrogen abstraction occuring at the same time would create alcohol groups from carbonyl groups, decreasing the proportion of carbonyl carbons seen by XPS. The overall

effect would be a change from C=O functionalities to C-O groups, and some other process must be occuring to produce carbonyl functionalities. The increase in the hydrocarbon intensity may be explained by recombination of phenyl radicals following a Norrish type-I process.

Direct photolytic cleavage of the ether carbon-oxygen bonds to create alcohol groups is consistant with both the constant O:C ratio and the rise in the hydrocarbon component of the C_{1S} spectrum. The $\underline{C}$-O : $\underline{C}$=O ratio would not remain constant unless conversion of carbonyl to alcohol (as described above) was occuring as well. It has been shown[30] that cleavage of such bonds is one of the primary photochemical processes in polysulphones, and it seems likely that such a reaction is occuring here. The fall in intensity of the shake up satellite is probably due to isomerisation of the phenyl rings to give fulvene and benzvalene type structures[31] or cross linking between excited aryl rings.

Following all oxidation treatments, the O:$\Sigma(\underline{C},O)$ ratio is approximately unity, i.e. there is one oxygen atom for every oxidised carbon atom. This implies that in the cases where there is a high level of carboxyl groups they exist mainly as ester groups; free acid functionalities contain two oxygen atoms to one carbon, so if they exist a corresponding number of ether links must also be present.

Vacuum ultraviolet irradiation in the presence of oxygen gives a very similar surface to that found following photo-oxidation at longer wavelengths (> 290 nm)[32]. There is little actual intensity change in the $\underline{C}$-O component of the C_{1S} spectrum from unmodified PEEK indicating that the ether cleavage occuring without oxygen present is still in equilibrium with alcohol formation, or that it is unimportant compared to other reactions occuring during photo-oxidation. The

production of carboxylate groups is prominent during photo-oxidation, particularly at the surface. These groups are formed both by oxidation of the aryl rings as in polystyrene, and oxidation of the carbonyl group following a Norrish type-I process. The production of carbonyl groups further to those already present is due mainly to oxidation of the aryl rings as in polystyrene. Shake up intensity is low throughout the XPS sampling depth, giving evidence of a loss in aromaticity to a depth of about 30Å. This once again points to oxidation of the phenyl rings.

The glow discharge treatment of PEEK in oxygen results in a lower oxidation of the PEEK surface, and a more prominent shake up satellite than after photo-oxidation. This is probably due to the ablation of material from the surface during plasma oxidation to reveal unmodified PEEK as in the case of polystyrene. At 70° take off angle there is some decrease in the presence of carbon atoms singly bound to oxygen although this is still the dominant species. There is a large drop in the hydrocarbon component (as with photo-oxidation) at high take off angle, indicating that most oxidation is confined to the surface.

Carbon dioxide plasma treatment shows a similar contribution from the hydrocarbon component at both take off angles which implies that modification occurs to some depth beneath the surface. The surface shows more carboxylate groups and fewer singly bound carbons than the bulk, and fewer carbonyl groups than following oxygen plasma treatment. The carbon dioxide photo-oxidation process produces an higher degree of oxidation, particularly at the surface, but the predominant group is still carbon singly bound to oxygen. There seems to be little direct incorporation of carbon dioxide into the polymer to produce carboxylate functionalities, reaction with oxygen species following a degradation of CO_2 to carbon monoxide and oxygen appears to be the main reaction. $\pi \rightarrow \pi^*$ shake up intensity is virtually

identical for both processes at 30° take off angle, but at 70° the UV treated sample shows a drop in relative intensity of the satellite; attack on the aryl ring being, in this case, more severe at the polymer surface. Plasma modification does not show a drop in the integrity of aryl rings at the surface, the higher availibilty of reactive species in the subsurface possibly accounting for this difference.

Following UV oxidation under a nitrous oxide atmosphere modification appears to be confined to the outermost layers of the polymer. There was no evidence for incorporation of nitrogen into the polymer by XPS (i.e. no peak visible in the N_{1S} region). The results at 30° take off angle are not substantially different to the results after the nitrogen-UV treatment. In particular, the $\pi \rightarrow \pi^*$ intensity is roughly the same. At 70° take off angle, this intensity has dropped markedly, which does not occur in the N_2-UV modification. The implication is that some reaction is occuring between excited aryl rings and N_2O (or atomic oxygen) at the surface of the PEEK, but not within the bulk.

The ratio of $\underline{C}$-O : $\underline{C}$=O intensities at 30° is the same as unmodified PEEK (i.e. 84:16), at 70° it is roughly similar (81:19). The only other groups present are carboxylate functionalities, possibly produced by reaction of excited carbonyl groups with nitrous oxide or atomic oxygen. From these results it can be seen that atomic oxygen does not on its own play an important part in the oxidation of PEEK. The results from the carbon dioxide treatment which demonstrated a greater degree of oxidation could arise from production of molecular oxygen in the gas phase:

$$2CO_2 + h\nu \longrightarrow 2CO + O_2$$

The low partial pressure of oxygen following this reaction would produce a different result from that following treatment with pure

oxygen, particularly as competing reactions will occur between the surface and other species present in the plasma.

4.4 Conclusion

Surface modification of polymer films by glow discharge techniques can be modelled by vacuum-UV methods. Plasma treatments often result in competing etching/ablation processes which expose unreacted polymer. These reactions do not occur during UV irradiation where a greater depth of oxidation is often found to occur. The presence of aryl and carbonyl groups are found to enhance the reactivity of the polymer to oxidation, and a correlation between the generated oxidised functionalities and the structure of the polymer is found to exist. The nature of the oxidising process also plays an important part in determining the resultant groups and depth of modification.

Aliphatic components of a polymer are likely to form C-O linkages following oxygen treatments, whereas carbon dioxide treatments result in a greater incorporation of carboxyl groups. Oxidation of phenyl rings yield predominantly C=O and O-C=O species and carbonyls produce mainly carboxylate functionalities.

Carbon dioxide treatments do not result in a greater production of O-C=O groups when aryl rings are present, the formation of these functionalities during oxygen treatments are a result of processes peculiar to molecular oxygen attack on such rings. UV oxidation of polymers in a carbon dioxide atmosphere is confined mainly to the surface, subsurface oxidation does not occur probably due to a lack of reactive neutral species diffusing into the bulk.

Reaction of polymers with atomic oxygen produced by photolytic cleavage of nitrous oxide does not produce highly oxidised species. It is unlikely therefore that atomic oxygen plays a major role in plasma or UV oxidation of polymers. This process may have uses as a means of selectively functionilising polymers such as polystyrene to produce alcohol groups without carboxylic acid formation.

References

1 D. M. Brewis, D. Briggs, *Polymer*, **22**, 7, (1981)

2 D. Briggs, D. M. Brewis, M. B. Konieczko, *J. Mater. Sci.*, **11**, 1270, (1976)

3 D. Briggs, D. M. Brewis, M. B. Konieczko, *J. Mater. Sci.*, **14**, 1344, (1979)

4 D. Briggs, C. R. Kendall, *Int. J. Adhes.*, **2**, 13, (1982)

5 D. T. Clark, A. Dilks, *J. Polym. Sci., Polym. Chem. Ed.*, **17**, 957, (1979)

6 R. Foerch, N. S. McIntyre, D. H. Hunter, *J. Polym. Sci., Polym. Chem. Ed.*, **28**, 193, (1990)

7 J. Peeling, D. T. Clark, *J. Polym. Sci., Polym. Chem. Ed.*, **21**, 2047, (1983)

8 J. Peeling, D. T. Clark, *Polym. Degrad. Stab.*, **3**, 177, (1981)

9 a S. W. Bigger, O. Delatycki, *Polymer*, **29**, 1277, (1988)
b F. Gugumus, *Angew. Makromol. Chem.*, **182**, 85, (1990)
c H. S. Munro, H. Beer, *Polym. Commun.*, **27**, 79, (1986)

10 D. T. Clark, A. Dilks, *J. Polym. Sci., Polym. Chem. Ed.*, **16**, 1093, (1978)

11 D. T. Clark, A. Dilks, *J. Polym. Sci., Polym. Chem. Ed.*, **15**, 15, (1977)

12 F. Poncin-Epaillard, B. Chevet, J. C. Brosse, *Eur. Polym. J.*, **26**, 333, (1990)

13 H. H. G. Jellinek, *Appl. Polym. Symp.*, **4**, 41, (1967)

14 K. Tsuji, T. Seiki, *Polym. J.*, **2**, 606, (1971)

15 J. M. Ginhac, J. L. Gardette, R. Arnaud, J. Lemaire, *Makromol. Chem.*, **182**, 1017, (1981)

16 F. Gugumus, *Angew. Makromol. Chem.*, **158/159**, 151, (1988)

17 S. W. Bigger, O. Delatycki, *Polymer*, **29**, 1277, (1988)

18 C. Mayoux, A. Antoniou, B. Ai, R. Lascoste, *Eur. Polym. J.*, **9**, 1069, (1973)

19 A. Dilks, A. Vanlaeken in "Physicochemical Aspects of Polymer Surfaces", Ed. K. L. Mittal, Plenum, New York, 749, (1983)

20 T. Shiono, E. Niki, Y. Kamiya, *Bull. Chem. Soc. Japan*, **51**, 2390, (1978)

21 G. C. Furneaux, K. J. Ledbury, A. Davis, *Polym. Degrad. Stab.*, **3**, 431, (1981)

22 J. F. Rabek, B. Ranby, *J. Polym. Sci., Polym. Chem. Ed.*, **14**, 1463, (1976)

23 J. F. Rabek, J. Sanetra, B. Ranby, *Macromolecules*, **19**, 1674, (1986)

24 D. T. Clark, H. S. Munro, *Polym. Degrad. Stab.*, **8**, 213, (1984)

25 J. F. McKellar, N. S. Allen, "Photochemistry of Man-Made Polymers", Applied Science, London, (1979)

26 H. Okabe, "Photochemistry of Small Molecules", Wiley Interscience, New York, (1978)

27 N. A. Weir, K. Whiting, *Eur. Polym. J.*, **25**, 291, (1989)

28 H. S. Munro, Ph.D. Thesis, University of Durham, (1982)

29 C. H. Steinbruchel, B. J. Curtis, H. W. Lehman, R. Widmer, *IEEE Trans. on Plasma Sci.*, **14**, 2, (1986)

30 N. S. Allen, J. F. McKellar, *J. Appl. Polym. Sci.*, **21**, 1129, (1977)

31 J. F, Rabek, B. Ranby, *J. Polym. Sci., Polym. Chem. Ed.*, **12**, 273, (1974)

32 H. S. Munro, D. T. Clark, A. Recca, *Polym. Degrad. Stab.*, **19**, 353, (1987)

Chapter 5

Deposition Characteristics of Zinc acetylacetonate and Aluminium tri-*sec*-butoxide from non-Polymerisable gas Plasmas

5.1 Introduction

Plasma enhanced chemical vapour deposition (PECVD) has been discussed to some extent in chapter one. The production of thin films from glow discharges of organometallic precursors has been geared mainly to the formation of metals or metal oxides[1]. Less interest however has been shown in depositing metal/polymer[2] and metal nitride[3] films. The incorporation of metals or their oxides into polymers can alter the mechanical, electrical or thermal properties of the polymer[4]. Composite materials of this type can be easily formed by using PECVD.

TEM studies of metal/polymer films formed from a variety of precursors showed that two distinct phases of metal (or metal oxide) and organic polymer were created[5]. These results suggested that at some point a separation of the metal and organic components occured and followed separate aggregation processes relatively independent of each other. A general mechanism based on this concept is shown in figure 5.1, this chapter will demonstrate that this reaction scheme is not applicable in all cases.

Examples of metallic films created from glow dicharges of metal containing monomers have mostly employed a direct (resistive) coupling of the power source to the plasma. This method of coupling results in a higher flux of ion bombardment on the forming surface than in the case of inductive coupling[6], which may result in a comparative enhancement of metal content in the growing film due to ablation of the organic component. High sputtering rates at low ion energies (< 1 keV) is related to both low heat of vapourisation and a similarity in the size of the ion and atoms being sputtered[7]. Almost all metal oxides have heats of vapourisation in excess of common organic

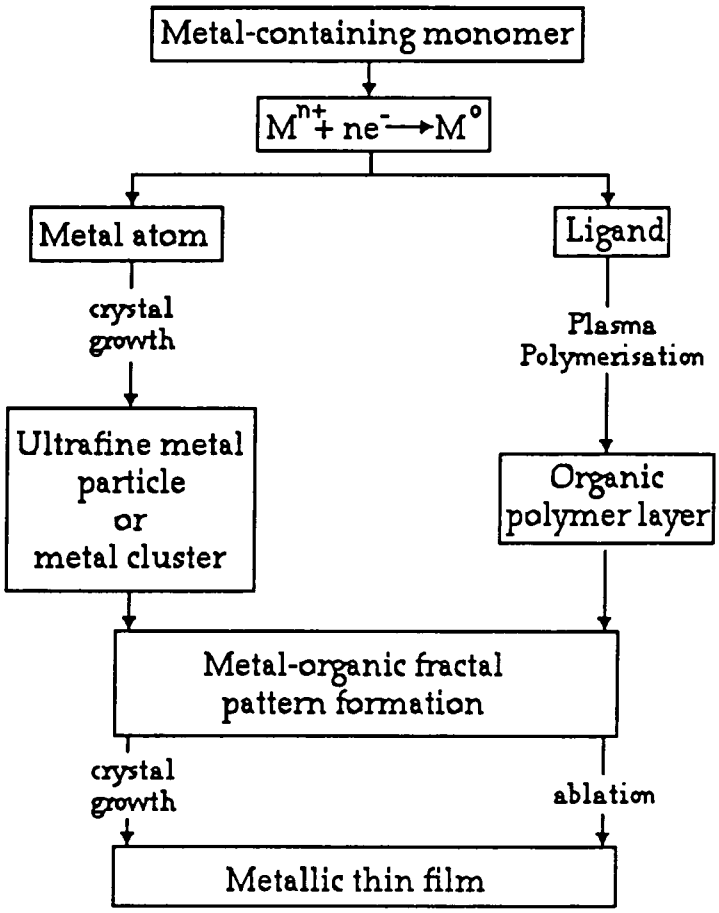

Figure 5.1 Proposed mechanism of formation of metal/polymer films (ref 5).

compounds[8], and the main sputtering species within the plasma are likely to be closer in mass to carbon than the metal.

Literature examples of PECVD also rely upon a small distance between the monomer inlet and the substrate to produce composites with a high metal content[1,2]. This is almost certainly due to the rapid degradation of the monomer and condensation of the metallic component. The use of inductive coupling, and its potential effect on substrate position dependency is investigated in this chapter.

The two metal containing compounds used in this chapter are shown in figure 5.2. Both contain oxygen in close proximity to the

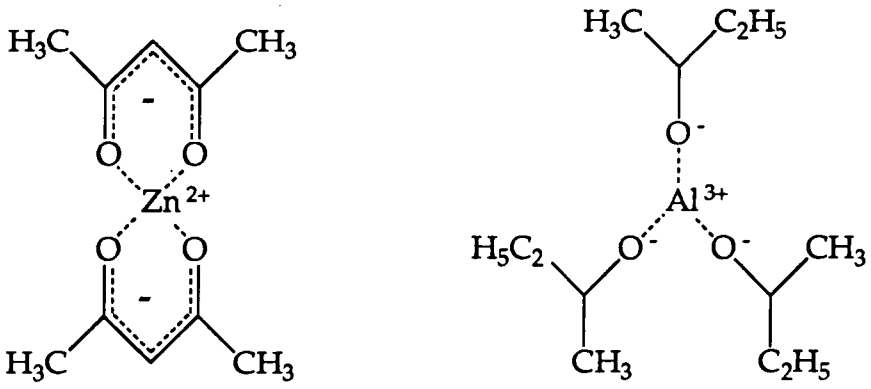

Zinc acetyl acetonate **Aluminium tri-*sec*-butoxide**

Figure 5.2 Monomers used in chapter 5

metal ion and are therefore likely to produce metal oxide containing products rather than unoxidised metal.

Zinc acetylacetonate [Zn(acac)2] has previously been used to deposite a thin metal oxide/polymer composite via a glow discharge route[5]. The properties of these films depended upon the relative ratios of zinc oxide to organic component. For instance, it is known that zinc oxide is an n-type semiconductor[9], and the electrical resistivity of the composite layer should fall with an increased metal oxide content. The electrical conductivity through zinc-oxide and organic thin films produced using similar techniques does indeed change with varying deposition conditions (which give products with differing amounts of organic component)[10]. Factors influencing the conductivity of the deposited layer were found to be the temperature of the substrate during deposition, the duration of the deposition, the temperature (vapour pressure) of the monomer and the discharge power.

Zinc oxide also displays other useful properties; it is used as an absorber of ultraviolet light (below 3655 Å), and also exhibits thermoluminescence and photoconductivity[9].

Plasma deposition of thin films of Aluminium tri-*sec* -butoxide [$Al(OCH(CH_3)C_2H_5)_3$] (see figure 5.2) has not been reported previously. It has a boiling point of 200°C under 30 torr pressure[11], and should be an ideal monomer for PECVD. It is, however, air sensitive and must be handled carefully. This compound has been used to incorporate small aluminium oxide particles within elastomeric polymers to change their mechanical properties; the aluminium oxide is produced following hydrolysis of the metal butoxide[12].

Aluminium containing films from plasma discharges have been created using other starting materials. Glow discharges of aluminium alkyls[13] and bromides[14] have been employed to produce aluminium nitride, a wide gap III-V compound with high electrical resistivity, thermal conductivity and chemical stability[15] which is of interest to the semiconductor industry. The formation of aluminium oxide films from glow discharges using trimethylaluminium has also been studied[16].

5.2 Experimental

Reactions were carried out in the cylindrical glass reactor (22 cm long by 5 cm diameter) illustrated in figure 5.3. A 13.56 MHz R. F. generator was inductively coupled to it via an externally wound eight turn copper wire. The non-polymerisable gases were introduced to the reactor through a needle valve to allow adjustability of the flow rate; no regulator was needed to control the flow of the metal-containing monomers due to their low volatility. Changes in evaporation rates of the metal compounds was achieved by warming the monomer tube with heating tape. It was also necessary to heat the connecting tubes between the monomer tube and the reactor to prevent condensation of

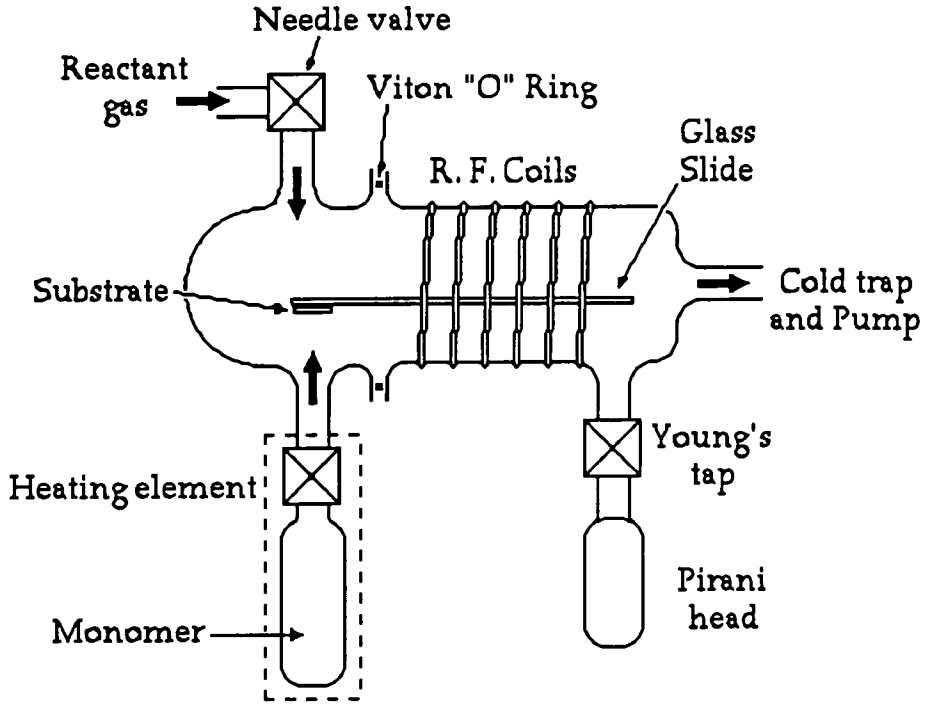

Figure 5.3 Reactor configuration used in chapter 5

the vapour before reaching the reactor. Measurement of the monomer flow rates was not possible using this reactor as condensation occured on the cooler reactor walls before reaching the pirani guage. The temperature of the monomer resevoir was measured via a chromel-alumel thermocouple inserted between the heating tape and the glass container. Control of the power supplied to the heating tape was acheived using a Variac transformer; it was possible by this method to maintain a constant temperature within ±5°C throughout the course of a reaction. The degree of heating depended upon the power supplied to the heating tape, but also varied between experiments because small differences in the rewinding of the tape changed the heat flow properties of the system. This became important when using aluminium tri-*sec*-butoxide, as this monomer's deposition characteristics are highly temperature sensitive.

Other details of the reactor system are identical to those in previous chapters. The reaction vessel was pumped to a pressure of better than 5×10^{-2} torr, and the non-polymerisable gas was allowed to enter at the desired flow rate. The plasma was ignited, in most of the reactions described in this chapter a power of 5W was used as higher powers gave negligable deposition rates of polymer. The monomer was then opened to the reactor and heated to the temperature required. Reactions were allowed to occur for one hour before shutting off the monomer from the reactor, cooling the connecting tubes and turning off the plasma.

The substrates used were glass and potassium bromide discs, which were attached to the glass slide with double sided scotch tape in a variety of positions, as shown in figure 5.4. Sites "a", "b" and "d" are on a glass slide inserted into the cylindrical reactor; respectively 2.5 cm directly above the monomer inlet, 15 cm downstream of "a" and 2.0 cm above the monomer inlet on the underside of the glass slide. Site "c" is located halfway up a vertical piece of glass which was fused to the top and bottom reactor walls 1 cm upstream of the monomer inlet. In experiments were the influence of the location of site of deposition

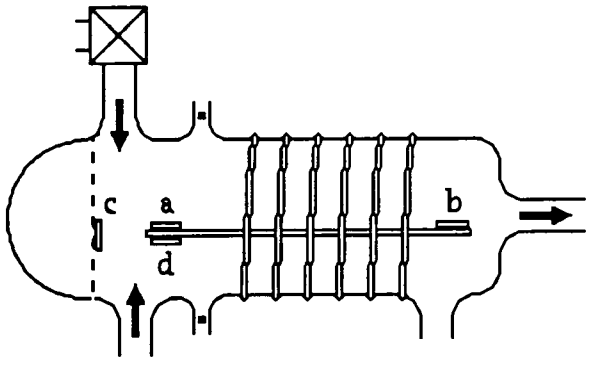

Figure 5.4 Schematic of Positions of Substrates within Reaction Vessel

within the reactor were not investigated, position "d" was exclusively used.

Research grade oxygen, argon, hydrogen and carbon dioxide were supplied by BOC. Aluminium tri-*sec*-butoxide (97%) was supplied by Aldrich and handled in a nitrogen atmosphere. Before each reaction it was degassed by consecutive freeze-thaw cycles and any volatile decomposition products were removed under vacuum. After the reaction had finished the vessel was flushed through with nitrogen and then let up to atmospheric pressure under nitrogen. Zinc acetylacetonate was provided by P. Coates (Chemistry Dept., Durham) and was analysed by infrared and found to give absorbances in agreement with the literature[17], although the presence of water was noted. The monomer was dehydrated by heating to 100°C under vacuum before use.

XPS spectra were acquired on a Kratos ES300 surface analysis instrument in the fixed analyser transmission analyser mode for deposits from $Zn(acac)_2$, and on a Kratos ES200 instrument in the fixed retarding ratio analyser mode for deposits from $Al(OBut)_3$. Experimentally determined sensitivity factors (which agree well with literature values[18]) were used to calculate surface elemental compositions. Infrared spectra were taken of deposits on KBr discs using a Mattson Polaris FT-IR spectrometer.

5.3 Treatment of Zinc Acetylacetonate

5.3.1 Site of Deposition

Substrates were placed at the four sites described in the experimental section. Oxygen was used as the modifying gas, and the zinc acetylacetonate was heated to evaporate it into the reactor. Following the reaction, these samples were analysed by X-ray photoelectron spectroscopy. The surface elemental compositions from the XPS results are shown in table 5.1. Temperature of the zinc acetylacetonate resevoir is shown in degrees centigrade for both reaction conditions; the oxygen flow rate was kept constant at 0.70 ml/min for each experiment. The Si_{2P} (~102 eV) region was examined also to see if the glass substrate is visible. The presence of a silicon signal gives a qualitative indication of low deposition rate.

In both cases there was negligable film formation at positions "a" and "b", the silicon peak indicates that thickness of any material is

Element : Carbon Ratio						
	110°C, 0.70 ml/min			140°C, 0.70 ml/min		
Position	Zn	O	Si	Zn	O	Si
a	0.00	1.18	0.35	0.00	1.21	0.32
b	0.00	1.36	0.24	0.00	1.40	0.30
c	0.19	1.23	0.12	0.22	0.75	0.00
d	0.30	1.02	0.00	0.24	0.60	0.00

Table 5.1 The dependence of position within reactor on film formation

small and the lack of a detectable zinc signal shows that predominantly organic material reached these sites. It is probable at site "a" that oxygen etching of material is the main reaction since substantial build up of carbonaceous matter is not occuring. Site "b" lies out of the visible plasma region, which approximately extended from the inlets toabout 10 cm downstream of them. Collection of material here was also negligable, oxidation of organic components within the glow precluding the production of polymer forming species. Site "d" is the position at which the zinc to carbon ratio is the greatest, it is also the closest to the monomer inlet. The other point of collection "c" is positioned obliquely to the monomer flow, whereas "a" and "d" are perpendicular to it. Although all three are roughly equidistant from the point of entry of zinc acetylacetonate, the film composition of films formed on these surfaces varies enormously. This shows that not only is distance from the inlet important but so is orientation towards it. The difference between the latter two suggests that zinc-containing material from the inlet condenses on the first surface that it contacts. Substrates placed close and in direct line of sight of the monomer inlet will collect material with a larger metal content.

5.3.2 Effect of Power

The collection of material from plasmas of 10W power was attempted at site "d" at various power and flow rates. Table 5.2 lists the XPS results of these experiments. None of the conditions resulted in significant deposition of material, this is evident from the large silicon signal. In section 5.3.3 a power of 5W was used at comparable flow rates and monomer temperatures, and significant coverage of the substrate

Oxygen flow rate (ml/min)	$Zn(acac)_2$ temperature	Zn : C ratio	O : C ratio	Si : C ratio
0.70	115°C	0.00	1.22	0.40
0.70	140°C	0.00	1.08	0.20
1.39	110°C	0.00	1.23	0.38

Table 5.2 Deposits formed at 10W from Zinc acetylacetonate in an oxygen plasma

was acheived. In the light of these results, powers of greater than 10W were not thoroughly investigated. It was noted that at 20W the glow region extended into the monomer inlet tube which would cause significant monomer disruption before entry into the reactor.

5.3.3 Results and Discussion

Typical XPS spectra of material formed from zinc acetylacetonate/oxygen plasmas are shown in figure 5.6. It should be noted that the data collection systems on the instruments is different to those used in previous chapters, and the binding energy scale increases to the right, and not the left. The films demonstrate zinc contents varying from 40 at.% to none. Inspection of the results reveal that a low monomer tube temperature at a constant oxygen flow rate (0.70 ml/min) will produce a film of high metal content. Figure 5.7 plots the relative concentrations of zinc and oxygen atoms against the temperature applied to the $Zn(acac)_2$ resevoir. Although deposition rate was not measured for these products it is probable that a lower

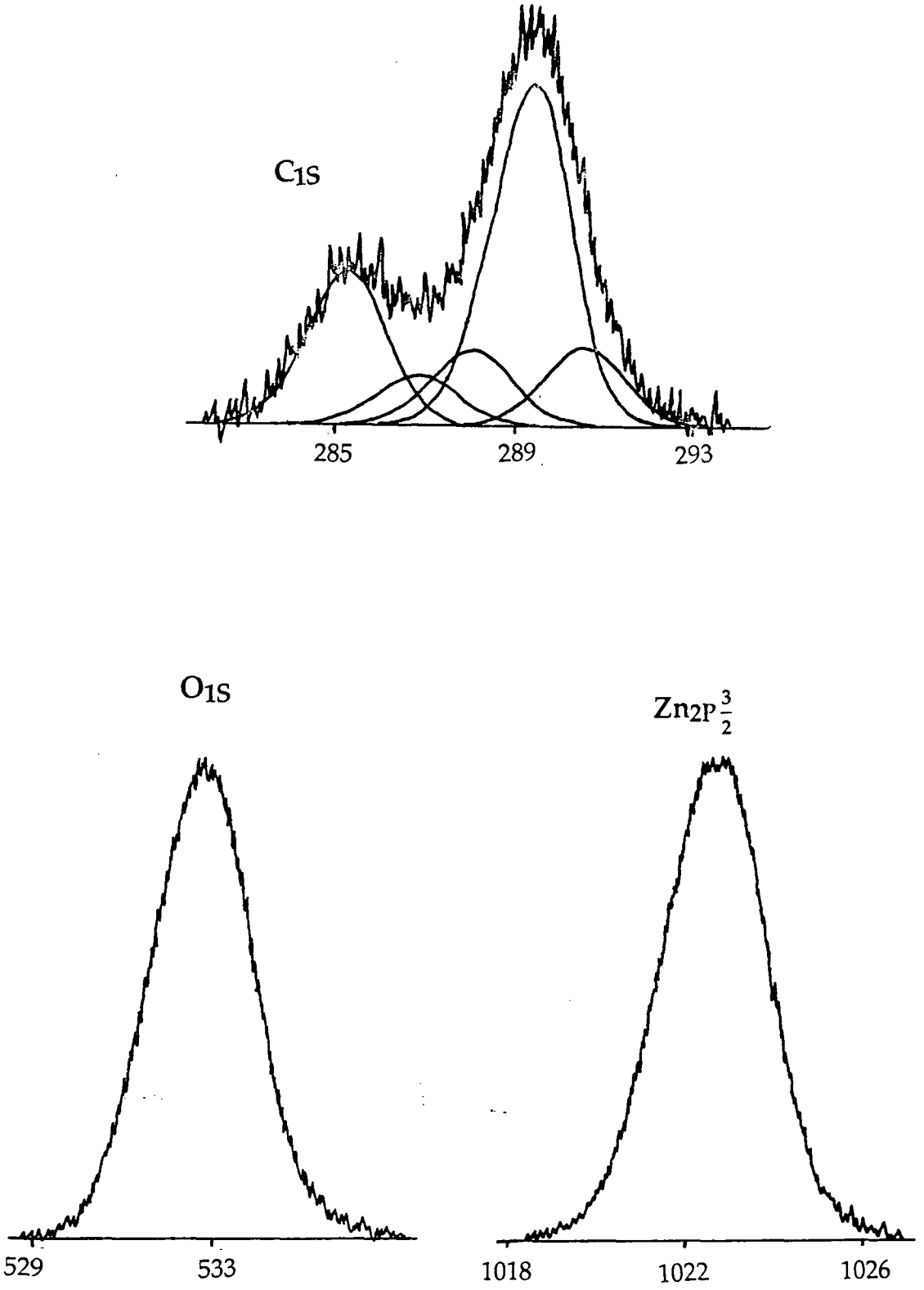

Figure 5.6 XPS spectra of a zinc containing film made at an oxygen flow rate of 1.39 ml/min., and a monomer temperature of 110°C

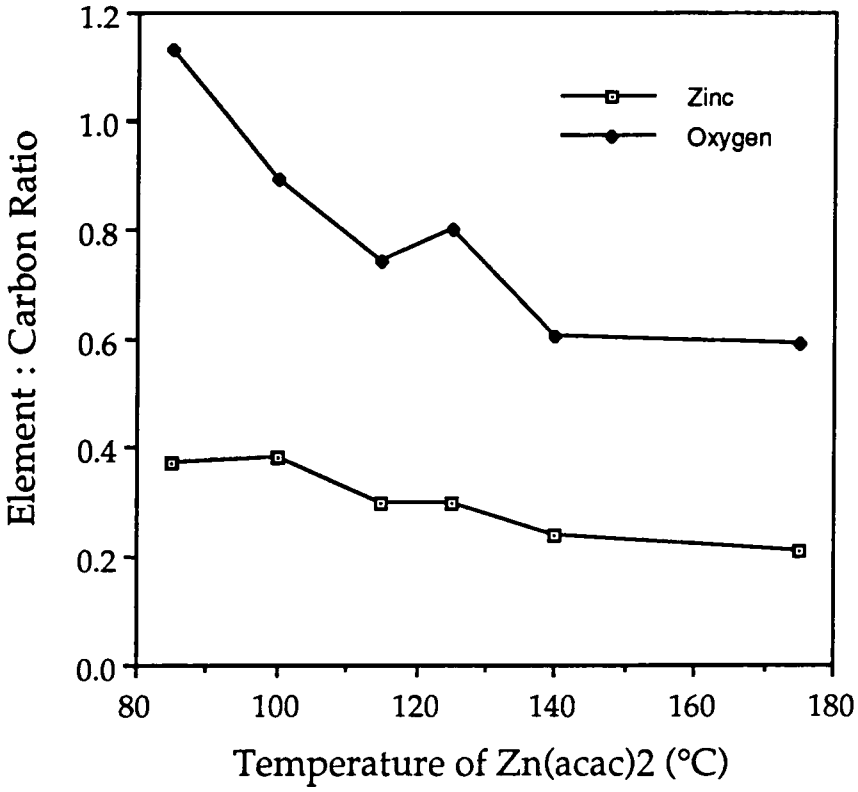

Figure 5.7 Elemental composition of films with monomer temperature (O_2 flow = 0.70 ml/min)

partial pressure of the monomer (i.e. less heating) will reduce the rate of film formation because deposition is dependent upon the amount of monomer able to reach the surface (see section 5.3.2). Indeed, when there is very little heating (45°C; Zn:C = 0.00, O:C = 1.24, Si:C = 0.41) XPS reveals that the glass substrate is uncoated. It is interesting to note that the oxygen to carbon ratio is larger when the percentage of zinc in the deposit increases, which could be an indication that oxygen becomes strongly associated with zinc ions during these processes. If the scheme shown in figure 5.1 applies, then free metal atoms will rapidly react to form zinc oxide. No splitting was visible in the O_{1S} spectra (see figure 5.6) which would indicate that oxide ions were being formed. The

binding energy of the main photoelectron peaks were typical of covalently bound oxygen although they were invariably broad, implying a wide range of environments.

High oxygen flow rates produced films through which glass could still be seen with X-ray photoelectron spectroscopy. In these cases there is some incorporation of metal, showing that the monomer is reaching the substrate, but the deposition and etching rates must be almost identical. The rise in Si2P intensity with increasing oxygen flow rate can be seen in figure 5.8. Zinc to carbon ratios remain relatively constant although there is slightly more metal at a low pressure of oxygen. The reason for this is unclear, since a reduction in oxygen concentration in the gas phase should result in a larger organic film

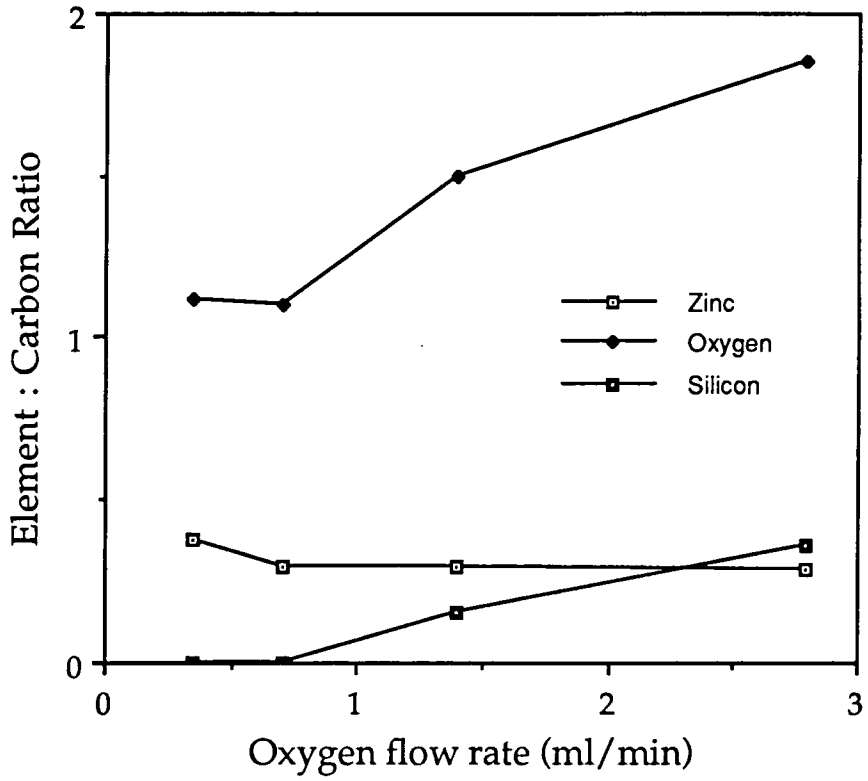

Figure 5.8 Elemental composition of films with oxygen flow rate (Monomer temperature = 110°C)

component. One of the main oxidation processes of hydrocarbons in pure oxygen plasmas is the reaction between activated organic species and neutral oxygen[19], a lower availability of oxygen should reduce the rate of this. It is possible then, that the limiting factor involved in this oxidation process is the activation of ligand species. More variance in the Zn:C ratio was found on changing the monomer temperature, with low evaporation rates increasing the zinc incorporation. This also indicates that the rate limiting step in the oxidation of the ligand is it's activation (by UV light, electron, or ion bombardment). High partial pressures of the monomer will result in a smaller proportion of excited species.

C_{1S} peak fits were carried out with the assumption that only carbon-oxygen species were present. The chemical shifts of such groups are given in chapter three. The possibility of forming zinc carbide or similar species in an oxidising atmosphere was considered negligable, and would have resulted in a peak to the low binding energy side of the C_{1S} hydrocarbon peak which was not evident. The dominant functionalities expressed in these products are carboxylic acid groups and hydrocarbon groups. The tendency for a higher percentage of carboxylic acid carbon atoms at a low monomer tube temperature is shown in figure 5.9. Formation of organic acids could result from a Norrish type I cleavage of methyl groups from the parent ligand followed by reaction of the remnant with oxygen.

High oxygen flow rates enhance the contribution of the more oxidised species to the carbon spectra. This tendency can be seen in figure 5.10. When the deposition rate is negligable (the Si_{2P} region visible) there is a substantial presence of carboxyl and carbonate groups

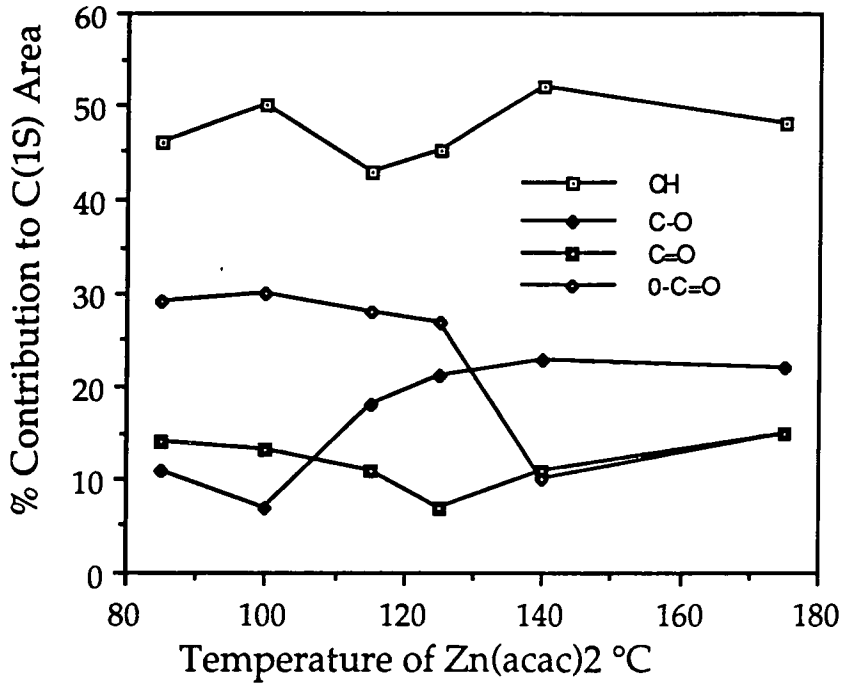

Figure 5.9 Carbon functionalities against monomer temperature

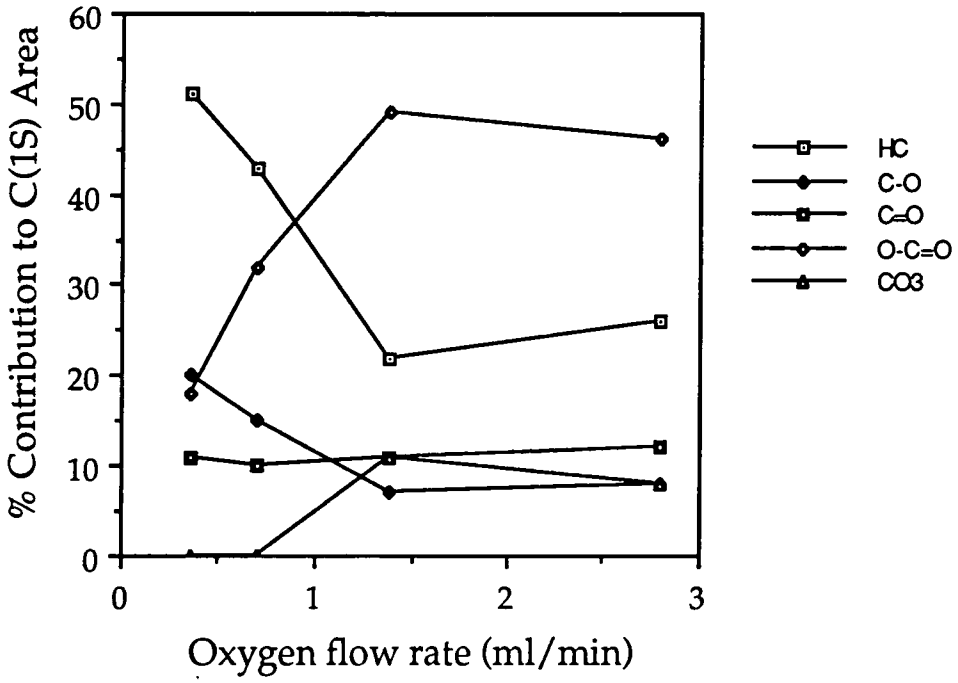

Figure 5.10 Carbon functionalities versus oxygen flow rate

with the exception of a film formed with $Zn(acac)_2$ temperature of 45°C, and an oxygen flow rate of 0.70 ml/min ($\underline{C}$-H 51%, $\underline{C}$-O 20%, $\underline{C}$=O 15%, O-$\underline{C}$=O 11%, $\underline{C}O_3$ 3%). In this case no zinc was detected in the product, implying that the metal ions are necessary for the retention of acid and carbonate species within the organic component.

Deconvolution of the carbon envelope suggests that carboxylic acid groups or carboxylate ions are one of the main organic products. This, and the lack of a shoulder to the low binding energy side of the O_{1S} peak (indicative of oxide ions) implies that almost all the oxygen is associated with the organic film component. If this is the case, then the oxygen to carbon ratio determined from core levels should be consistent with the results of the C_{1S} peak fit.

Equation 5.1 determines a theoretical oxygen to carbon ratio from carbon deconvolutions based on the following assumptions. Only alcohol groups are formed, no ether or peroxide groups. Only carbonyl groups, and only carboxylic acids or carboxylates, no esters or acid anhydrides. Carbonate groups were assumed to be in ionic form. This results in a maximum oxygen to carbon ratio consistent with the carbon peak fit (unless the hydroperoxy group concentration is exceptionally large). If the O1S intensity is much larger than expected from this formula then, since no other elements are present in the examples shown in table 5.3 there must be a direct association of zinc and oxygen, possibly as zinc hydroxide.

$$\text{Theoretical O:C} = (\underline{C}\text{-O}) + (\underline{C}\text{=O}) + 2 \times (\text{O-}\underline{C}\text{=O}) + 3 \times (\underline{C}O_3) \qquad 5.1$$

At high monomer tube temperatures the calculated and experimentally determined oxygen to carbon ratios are similar. It is likely, in these cases, that the carboxylic acid groups exist in the ionised

Oxygen Flow rate	$Zn(acac)_2$ Temp.	O:C from C_{1S}	O:C from peak areas	Zn:C ratio
0.70	175°C	0.67	0.59	0.21
0.70	140°C	0.54	0.60	0.24
0.70	125°C	0.82	0.80	0.30
0.70	115°C	0.85	0.74	0.30
0.70	110°C	0.89	1.02	0.30
0.70	100°C	0.80	0.92	0.38
0.70	85°C	0.83	1.13	0.37
0.35	110°C	0.67	1.12	0.38
1.39	130°C	1.03	1.33	0.24

Table 5.3 Comparison of C_{1S} peak fit with O_{1S} intensity

form in association with zinc ions, since there is insufficient O_{1S} intensity for the metal to exist only as the oxide or hydroxide and the C1S peak fit to be consistent. When the resevoir temperature is lower, the oxygen core level peak is significantly larger than can be accounted for from the carbon region. Since there were no other elements detected by XPS these conditions must result in the production of some zinc oxide or hydroxide. It is likely that the hydroxide is formed, since, as stated earlier, there was no peak to the low binding energy side of the O_{1S} peak.

Infrared spectroscopy performed on films collected on potassium bromide discs confirms that carboxylate ions are formed. The strong absorbances at ~1570 cm^{-1} and ~1400 cm^{-1} seen in figure 5.11 are assigned, respectively, to the asymmetric and symmetric stretches of the carboxylate anion[20]. The higher intensity of these bands at lower oxygen flow rates is due to a greater film thickness. The strong hydroxyl

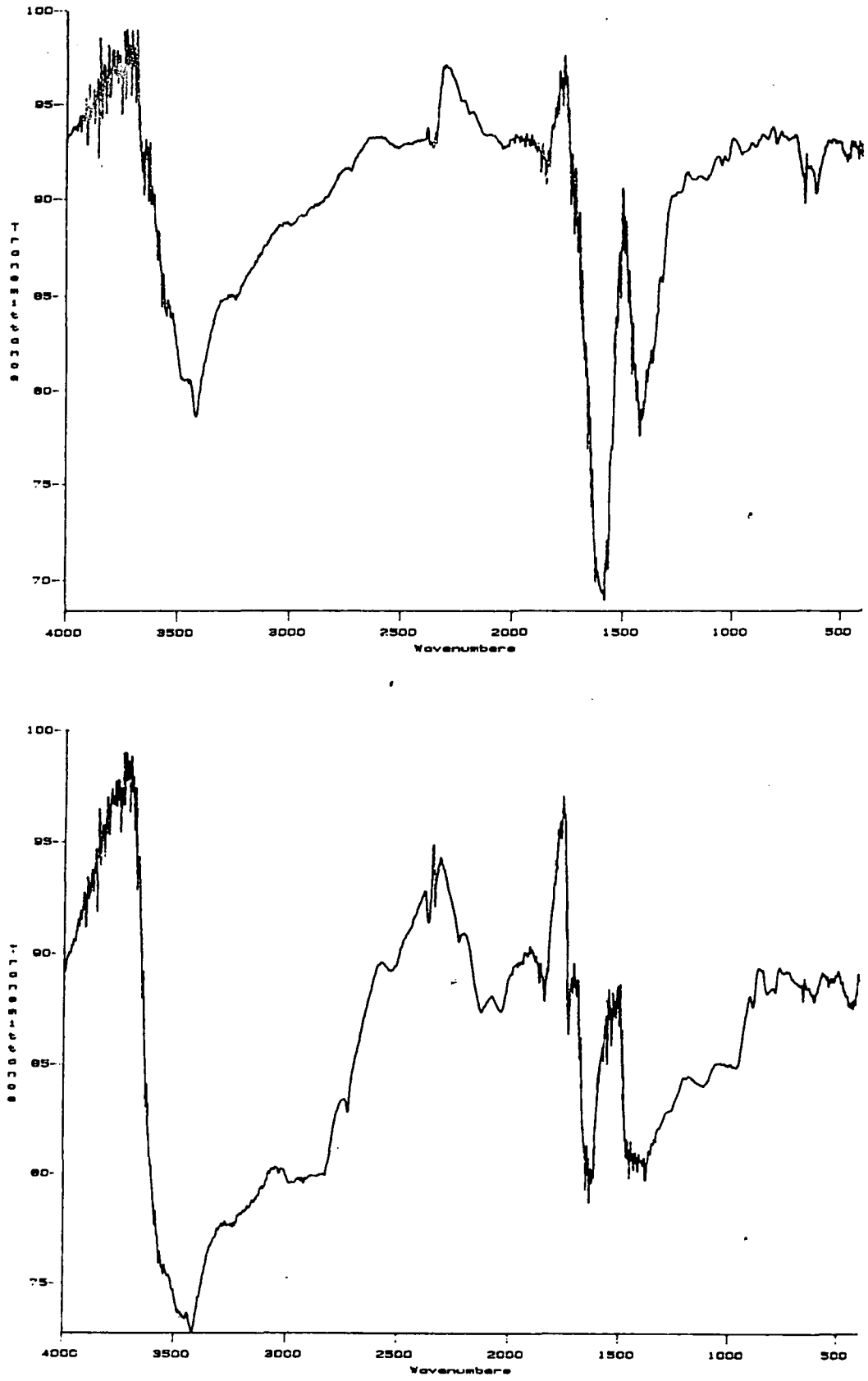

Figure 5.11 Infrared spectra of (top) 0.70 ml/min., 115°C and (bottom) 1.39 ml/min., 115°C deposits from $Zn(acac)_2$ and oxygen showing the strong carboxyl absorption

stretch at ~3460 cm^{-1} is broadened due to hydrogen bonding. Characteristic C=O stretches are not evident, but in the monomer this absorbance is shifted to 1592 wavenumbers[18], and so the carbonyl groups evident in the C_{1S} XPS spectra may still retain diketonate character.

5.3.4 Synopsis

The rapid condensation of metallic components from the monomer is evident from the critcal positioning of substrates. Deposition of material occurs only close to the monomer inlet, with oxygen etching occuring throughout the remainder of the reactor. Negligable film formation is also found when the flow rate of oxygen is high, or the zinc acetylacetonate resevoir receives insufficient heating.

The oxidation process does not seem to involve a dissociation of the monomer into metal ions and ligands (as outlined in figure 5.1). There is a loss of carbonyl functionality on going from the monomer to the product, from 40% to between 10 and 15%. Oxidation of these groups results in carboxylate anions, which are still associated with the zinc cations. Carbon singly bonded to oxygen will result from reaction of the hydrocarbon part of the acetylacetonate ligand, of which a substantial portion of the film is formed.

5.4 Treatment of Aluminium tri *sec* -butoxide

5.4.1 Results and Discussion

The most critical feature of reactions carried out with this monomer was found to be the temperature of the resevoir. Insufficient

heating produces virtually no film formation, whereas a higher temperature results in visible condensation of $Al(OBut)_3$ liquid on surfaces close to the inlet. The optimum temperature was 165°C ± 5°C, and all experiments described in this section were carried out within these limits. Plasma powers of 10W were again found to produce negligable deposition rates. Table 5.4 summarises the results of reacting this monomer in a variety of gas plasmas, and typical XPS spectra are shown in figure 5.12.

The most notable feature of the deposits collected is that the oxygen content is almost directly related to the amount of aluminium incorporation regardless of the reactant gas used. The O:Al ratios in each case are consistent at 1.9 ± 0.25. There is always significantly more

Gas	Flow rate	Al:C	O:C	$\underline{C}H$	$\underline{C}$-O	$\underline{C}$=O	O$\underline{C}$-O	$\underline{C}O_3$
none	no plasma	0.21	0.41	79	21	0	0	0
none	*	0.95	1.61	70	15	3	6	6
Ar	0.70	0.45	0.96	77	14	1	5	3
H_2	0.70	1.02	1.68	76	15	2	7	0
O_2	0.70	1.37	2.55	63	10	4	18	5
N_2	0.70	1.36	2.73	62	17	10	7	4
CO_2	0.70	0.99	1.75	67	9	3	15	5
CO_2	1.40	1.21	2.32	60	12	10	13	5

Table 5.4 XPS results of reaction of Aluminium tri-sec-butoxide with non-polymerisable gas plasmas. (Flow rates in ml/min., C_{1S} deconvolution results in per cent contribution.)

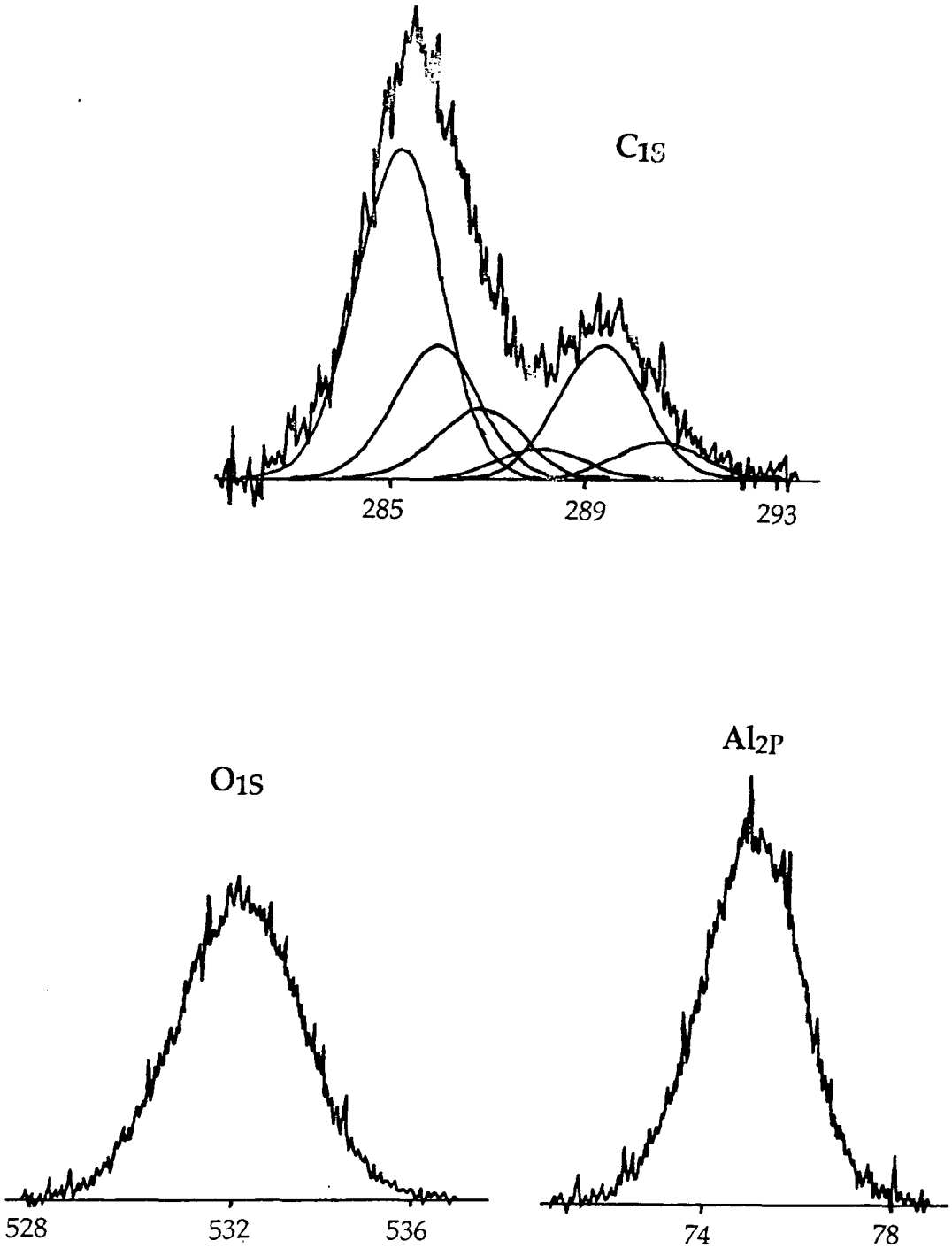

Figure 5.12 XPS spectra for the Al(OBut)3 and oxygen plasma reaction

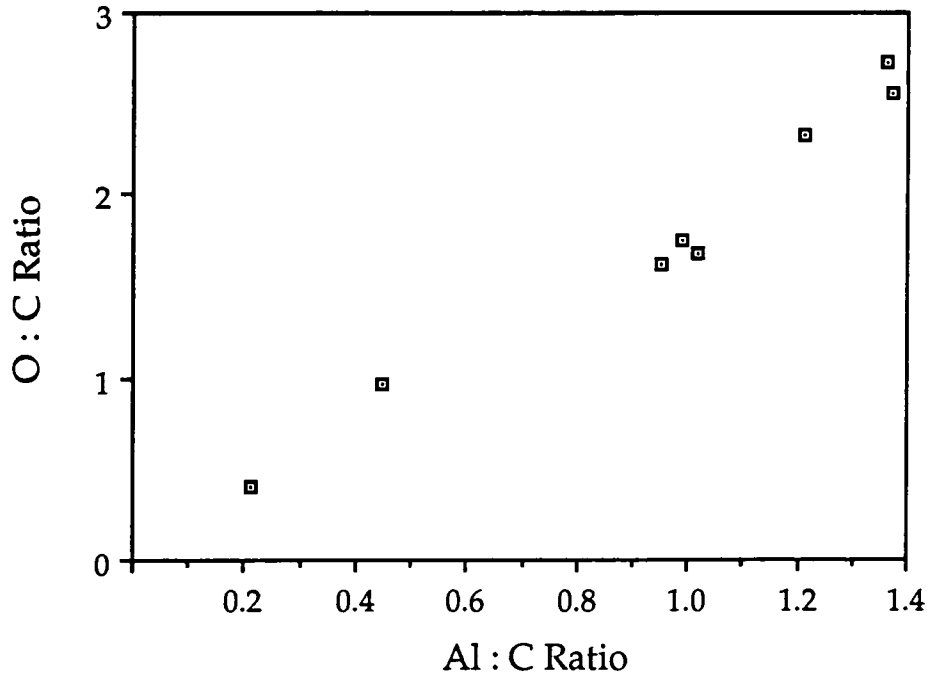

Figure 5.13 Relation between aluminium and oxygen intensity

oxygen than can be accounted for from the C_{1S} deconvolution (see equation 5.1). Therefore, all these films contain a substantial amount of aluminium oxide, hydroxide or a mixture of both. Figure 5.13 plots the oxygen:carbon ratio against the aluminium:carbon ratio and clearly shows a straight line relationship.

Neat aluminium tri-*sec* -butoxide evaporated onto a substrate without a plasma being struck undergoes some hydrolysis during exposure to air whilst being transported to the photoelectron spectrometer. All materials were treated in a like manner, the figures given here are therefore not necessarily representative of the freshly deposited films. Theoretically, without hydrolysis the Al : C ratio should be 0.08, and the O : C ratio 0.25. It is evident that when this compound reacts with air some loss of organic material (and hence drop in C_{1S} intensity) occurs. The carbon spectra resolves into two

component peaks with shifts typical of hydrocarbon and carbon singly bound to oxygen. Such groups arise from the butoxide ligand and can be assumed to come mainly from unhydrolysed aluminium tri-*sec* -butoxide either at the surface or just below it. 2-Butanol, the organic hydrolysis product is reasonably volatile (b.p. 100°C at 760 torr[21]) and would evaporate at the low pressure used for XPS. Although there may be some chemisorption, the O_{1S} intensity is too low to account forcomplete hydrolysis within the depth analysed. The results of deconvolution are close to the theoretical values with a slightly higher hydrocarbon component than expected. Butoxide ions should give a relative intensity of ~75% $\underline{C}H$ to ~25% $\underline{C}$-O, the larger unoxidised carbon component is probably due to a small degree of surface contamination.

A glow discharge of $Al(OBut)_3$ produces an higher aluminium content than does evaporation onto a substrate. The butoxide ligand suffers a degree of change during plasma treatment, the C_{1S} deconvolution shows a slight drop in hydrocarbon intensity, and more oxidised forms of carbon are present. Formation of the metal oxide or hydroxide is almost certainly occuring, the nearly equal numbers of aluminium and carbon atoms precluding any sensible scheme that involves retention of metal-ligand bonds. A breakdown of the compound into metal and organic parts followed by separate deposition processes, as outlined in figure 5.1 probably occurs. The higher content of aluminium being due to the faster condensation of this material from the gas phase.

The introduction of aluminium tri-*sec* -butoxide into the plasma of a non-polymerisable gas will affect the properties of the resultant film. These changes will be influenced predominantly by reactions occuring within the gas phase. Other effects will result from differences

in the transport of material to the substrate. Since the presence of another gas will result in a rise in pressure, the mean free path of species within the reactor will be reduced, see equation 5.2[22].

$$\lambda_{p,t} = \lambda_o \cdot \frac{Po}{P} \cdot \frac{T}{To} \qquad 5.2$$

Table 5.5 lists the mean free paths of gases used in this chapter at atmospheric pressure[22], the pressure at which they are introduced to the reactor (0.15 mbar), and the pressure at which the pure aluminium tri-*sec* -butoxide plasma operated (0.04 mbar). The mean free path of the metallic compound will be even lower than that of the gases due to its greater collisional cross section. This can be seen from equation 5.3 where r_1 and r_2 are, respectively, the effective collisional radii of the slower moving and faster moving components of a gaseous mixture[22].

$$\lambda = \frac{1}{\pi (r_1 + r_2)^2 N} \qquad 5.3$$

	Mean Free Path (metres) at T=288K		
Gas	1 bar	0.15 mbar	0.04 mbar
H_2	11.7×10^{-8}	0.78×10^{-3}	2.9×10^{-3}
N_2	6.28×10^{-8}	0.42×10^{-3}	1.6×10^{-3}
O_2	6.79×10^{-8}	0.45×10^{-3}	1.7×10^{-3}
CO_2	4.19×10^{-8}	0.28×10^{-3}	1.0×10^{-3}
Ar	6.66×10^{-8}	0.44×10^{-3}	1.7×10^{-3}

Table 5.5 Mean free paths of gases used in this section at various pressures

Film forming species will undergo, on average, many tens of collisions on moving 2 cm from the inlet to the substrate. On introduction of an unreactive gas such as argon, the frequency of collisions will increase. If there is no dissociation of the aluminium tri-*sec* -butoxide molecule then the film composition should remain relatively unchanged. This is not the case, because although the shape of the C_{1S} spectra is similar to that resulting from a pure plasma, the aluminium and oxygen content are almost halved.

This implies that there is a separation into aluminium/oxygen species and organic ligand species prior to deposition. Diffusion directly from the inlet to the substrate of these materials is less probable under the higher pressure. Condensation on walls closer to the inlet removes many more of the metal/oxygen clusters than organic components since re-evaporation or ablation is more likely in the latter case.

Using hydrogen as a feed gas, it can be seen that any effect from the reduction in diffusion is offset by its reactive nature. The elemental composition of this mix is close to that of the pure monomer. Formation of volatile products such as methane and water will reduce the carbon incorporation into the growing film, and the reducing atmosphere discourages generation of carbonate groups. The formation of metallic aluminium would not be detected in this experiment since it reacts rapidly with air to form aluminium oxide at least to the depth of the XPS experiment.

Oxygen and nitrogen plasmas both enhance strongly the aluminium content of the film, suprisingly there is no evidence in the N_{1S} XPS region for incorporation of nitrogen into the resultant film. The main difference between the two deposits is the greater production of organic acid groups following the oxygen treatment. It is unclear why if the butoxide ligand is unreactive toward a nitrogen plasma, the

film formed should not be similar to the one produced from an argon plasma. There could be reactivity toward the organic component to produce predominantly volatile products which would then not be expressed in the deposit. Alternatively, collisional activation and deactivation processes in the gas phase may be different with nitrogen because of it's smaller mass. Aluminium tri-*sec* -butoxide does not appear to be a suitable precursor for the formation of aluminium nitride by this method.

Treatment with carbon dioxide was carried out at two flow rates. At the higher flow rate a greater degree of oxidation of the organic component occured, resulting in a greater metal content in the film. A lower aluminium : carbon ratio was found with this gas in comparison to oxygen at the same flow rate. Carbon dioxide is a less vigorous oxidiser than oxygen in a glow discharge (see chapter 4), so the transport of metal/oxygen species plays a greater role in this reaction scheme.

5.4.2 Synopsis

PECVD of aluminium tri-*sec* -butoxide in the presence of non-polymerisable gases is influenced by both the decreased mean free path of the monomer, which adversely affects the metal content of the product, and the reactant nature of the gas which modifies the organic part of film. The type of gas used does not appear to change the chemical state of the deposited metal. Aluminium oxides and hydroxides are the main products, although the presence of carboxylic acids and carbonates suggest that some organic metal salts may also form.

5.5 Conclusions

Inductively coupled plasmas were used to produce metal containing thin films. It was found that pure metal oxide films were not formed using the reaction set up described here. Similar experiments carried out with titanium isopropoxide produced similar results, and showed that the organic component could be removed by heating[23]. In these experiments it was found that the monomer inlet into the reactor had to be in close proximity to the substrate in order to achieve a reasonable incorporation of metal into the film. Metal complexes from the heated inlet must condense rapidly on the colder glass surfaces within the reactor.

Factors influencing the metal content of these films were found to be the temperature of the monomer resevoir (and connecting tubes), the flow rate of the gas used for modification and the nature of the gas itself. High plasma powers were found to cause rapid breakdown of the monomer, and no metallic part of it could be collected on the substrate.

The two compounds used in this chapter appear to follow quite different mechanisms of film formation. Zinc acetylacetonate remains closely associated within the plasma, resulting in a mainly metal carboxylate film. Similar materials have been produced using glow discharge techniques to create solid polymer electrolytes with mobile cations[24]. Aluminium tri-*sec* -butoxide dissociates to give a metal/oxygen part, and an organic part which then follow differing reaction pathways. Even in plasmas where oxygen is not readily available, aluminium oxides and hydroxides are the dominant product. Although this may be a result of oxidation or hydrolysis upon exposure to air, it is more likely to be due to cleavage of the monomer

at carbon-oxygen bonds so that oxygen remains associated with aluminium ions.

It is important to note that a knowledge of the rate of entry of the monomer into the reaction vessel would be useful in understanding the processes which are occuring in the experiments described in this, and the subsequent chapter. The positioning of a pressure gauge on the inlet tube would give some idea of this rate, although experimental problems may occur due to this sensor having to be at the same temperature as the inlet tube. Alternatively, the vapour pressure can be related to the monomer tube temperature through the equation (adapted from ref. 8);

$$\log P = -(a/T) + b \qquad 5.4$$

Where P is the vapour pressure, T is the temperature (in Kelvin), and a and b are constants typical of the compound.

References

1 H. Suhr, J. Bald, L. Deutschman, E. Feurer, H. Holzschuh, J. Messelhauser, C. Oehr, S. Reich, R. Schmidt, B. Waimer, A. Weber, H. Wendel, *Int. Symp. Plasma Chem. 9*, **3**, 1287, (1989)

2 a H. Biederman, L. Martinu, D. Slavinska, I. Chudacek, *Pure Appl. Chem.*, 60, 607, (1988)

b Y. Kagami, T. Yamauchi, Y. Osada, *J. Appl. Phys.*, **68** (2), 610, (1990)

3 J. Laimer, H. Stori, P. Rodhammer, *Thin Solid Films*, **191**, 77, (1990)

4 Y. Osada, K. Yamada, *Thin Solid Films*, **151**, 71, (1987)

5 Y. Kagami, K. Yamada, T. Yamauchi, J. Gong, Y. Osada, *J. Appl. Polym. Sci., Appl. Polym. Symp.*, **46**, 289, (1990)

6 B. Chapman, "Glow Discharge Processes, Sputtering and Plasma Etching", New York, Wiley, (1980)

7 J. Kirschner, H.-W. Etzkorn in "Thin Film and Depth Profile Analysis", *Topics in Current Physics*, **37**, Berlin, Springer-Verlag, (1984)

8 "CRC Handbook of Chemistry and Physics", Ed. W. C. Weast, (1982)

9 "Comprehensive Inorganic Chemistry", Eds. J. C. Bailer, H. J. Emeleus, R. Nyholm, A. F. Trotman-Dickenson, Pergamon Press, (1973)

10 O. Takai, *Int. Symp. Plasma Chem. 9*, **3**, 1371, (1989)

11 Aldrich Chemical Company Ltd., Catalogue, (1990-91)

12 J. E. Mark, S. -B. Wang, *Polymer Bulletin*, **20**, 443, (1988)

13 a F. Hasegawa, T. Takehashi, K. Kubo, Y. Nannichi, *Jpn. J. Appl. Phys.*, **26**, 1555, (1987)

b H. Nomura, S. Meikle, Y. Nakanishi, Y. Hatanaka, *J. Appl. Phys.*, **69** (2), 990, (1991)

14 Y. Someno, M. Sasaki, T. Hirai, *Jpn. J. Appl. Phys.*, **29**, L358, (1990)

15 L. M. Sheppard, *Ceramic Bulletin*, **69**, 1801, (1990)

16 K. P. Pande, V. K. R. Nair, D. Gutierrez, *J. Appl. Phys.*, **54**, 5436, (1983)

17 N. Nakanoto, P. J. McCarthy, A. E. Martell, *J. Am. Chem. Soc.*, **83**, 1272, (1961)

18 D. Briggs, M. P. Seah, "Practical Surface Analysis", Wiley, (1983)

19 C. H. Steinbruchel, B. J. Curtis, H. W. Lehman, R. Widmer, *IEEE Transactions on Plasma Science*, **14**, 2, (1986)

20 R. M. Silverstein, G. C. Bassler, T. C. Morrill, "Spectrometric Identification of Organic Compounds", 4th Ed., Wiley, (1981)

21 S. H. Pine, "Organic Chemistry", 5th Ed., McGraw-Hill, (1987)

22 E. Nasser, "Fundamentals of Gaseous Ionisation and Plasma Electronics", Wiley Interscience, (1971)

23 K. S. Chen, Y. L. Juang, *Polym. Mater. Sci. Eng.*, ACS, Boston, **62**, 538, (1990)

24 Y. Uchimoto, Z. Ogumi, Z. Takehara, *Solid State Ionics*, **40/41**, 624, (1990)

Chapter 6

Co-Deposition Characteristics of Zinc acetylacetonate, Aluminium tri-*sec* - butoxide and Perfluorohexane

6.1 Introduction

The inclusion of metal and metal oxide species into polymer matrixes is of considerable interest because of the influence on the chemical and physical properties of the polymer[1]. There are many ways of producing such materials[2]. The hydrolysis of unstable organometallic compounds is used to incorporate metal oxides into conventional polymers[3]. When the organic part is a plasma polymer, the metal can be evaporated into the glow discharge and simultaneously condensed with the polymer. Alternatively, a metal electrode can be sputtered by reactive species in the plasma to achieve the same effect. Incorporation of metals into fluorocarbon plasma polymers has been investigated by this sputtering technique[4,5]. Sputtering of the electrode is enhanced by the formation of volatile fluorides (such as silicon and germanium), but in these cases no metallic inclusion was found. It is important therefore to choose a metal that has a non-volatile fluoride salt. Another method is to use a volatile organometallic material, such as copper acetylacetonate, as a co-monomer. This vapour has been deposited with an organic matrix to improve the conductivity of the resulting film[6].

In this chapter two organometallic compounds and a fluorocarbon material are used as co-monomers. The polymerisation of zinc acetylacetonate, aluminium tri-*sec* -butoxide and perfluorohexane with each other is investigated. Formation of films with each of these as the sole monomer has been reported in previous chapters. Material produced from combinations of pairs of the monomers were examined (i.e. $Zn(acac)_2/Al(OBut)_3$, $Zn(acac)_2/C_6F_{14}$ and $Al(OBut)_3/C_6F_{14}$). If volatile metal fluorides can form the latter two combinations will exhibit little or no metal content, however, both zinc fluoride and

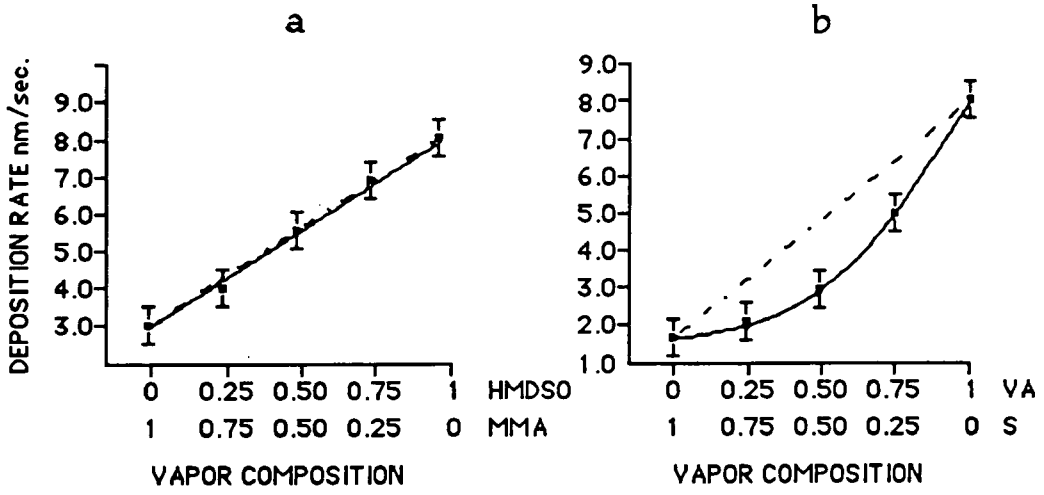

Figure 6.1 Deposition rate versus vapour composition showing (a) codeposition and (b) copolymerisation

aluminium fluoride have high melting points (872° C and 1290° C respectively[7]).

The processes involved in film formation from more than one monomer can be exceedingly complex. If there is no influence from one monomer on the other's deposition characteristics and *vice-versa* , then the product will be a linear combination of the plasma polymers of the individual monomers; this is known as "plasma codeposition". The term "plasma copolymerisation" implies some sort of interaction between the two co-monomers in the gas phase to produce a material that may vary greatly from that expected. The difference between plasma copolymerisation and plasma codeposition can be found in the deposition rates of some systems. For example[8], mixtures of hexamethyldisiloxane and methyl methacrylate show a linear relationship between deposition rate and vapour composition which indicates codeposition (see figure 6.1a). Whereas styrene and vinyl acetate mixtures show a significant negative deviation from that

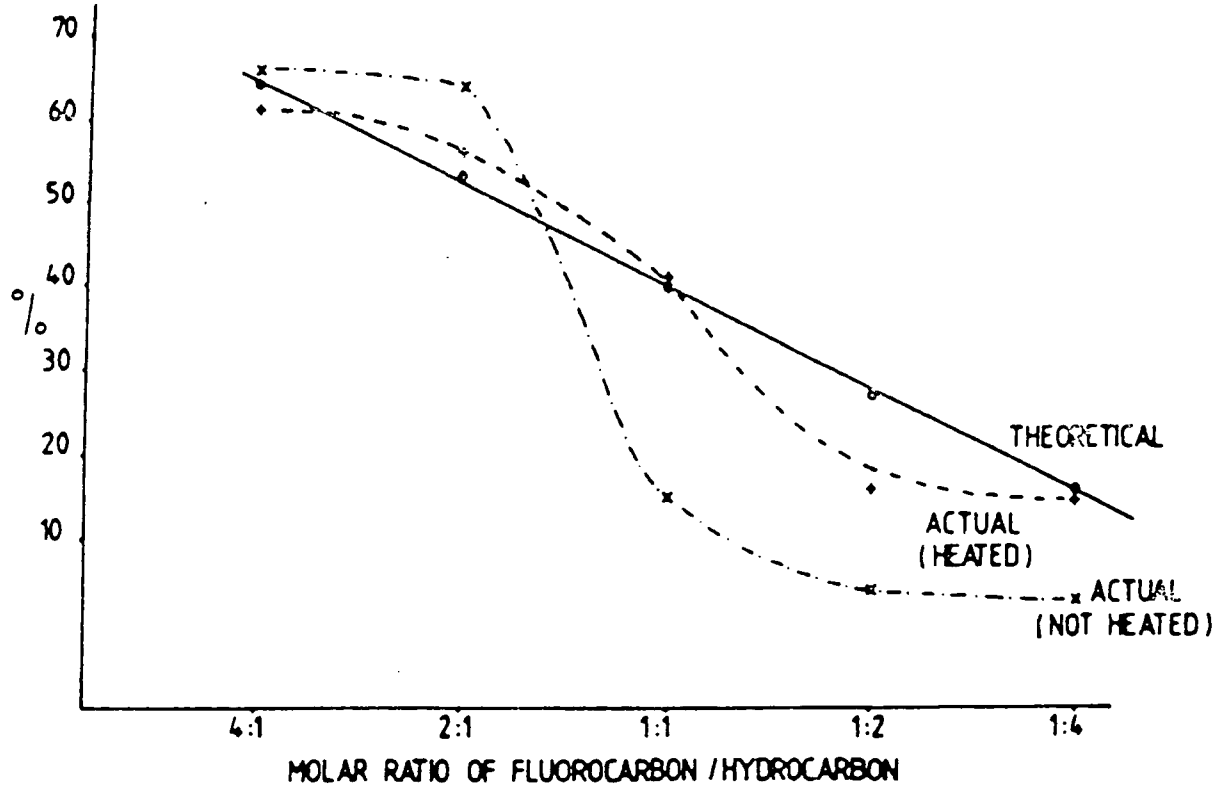

Figure 6.2 Percentage composition of fluorocarbon in plasma copolymers of naphthalene and perfluoronaphthalene against molar feed ratio into the plasma

expected (see figure 6.1b), which suggests that a copolymerisation reaction is occurring. An example of a copolymerisation reaction which affects the composition of the plasma polymer is found with naphthalene and perfluoronaphthalene[9], which demonstrates considerable deviation from theoretical compositions, see figure 6.2.

6.2 Experimental

The apparatus used in this chapter was very similar to that used in chapter 5, see figure 6.3. The reactor was evacuated to a pressure of better than 5×10^{-2} torr, and perfluorohexane or oxygen allowed to enter at the required flow rate. After the plasma was struck the metal

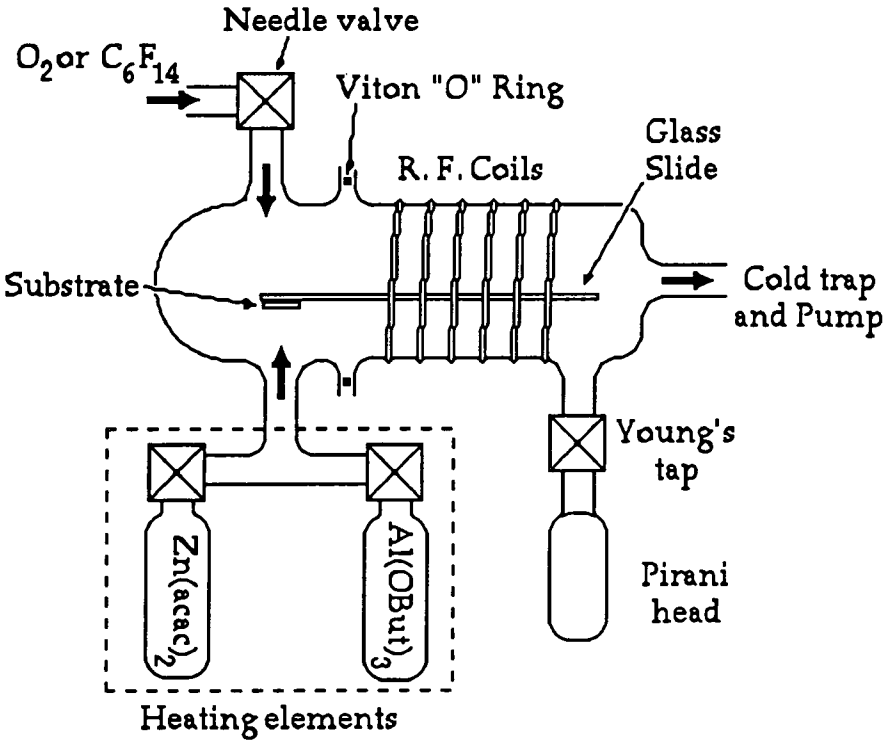

Figure 6.3 Reactor used for copolymerisation of metal containing monomers

containing monomer(s) were opened to the reactor and heated through the system described in chapter 5. Once again the power of the plasma had to be kept low (5W), otherwise there was minimal metal incorporation into the growing film. Depositions were allowed to occur for one hour before closing off and cooling the monomer(s), and extinguishing the plasma. The reactor was then flushed through with nitrogen, before letting up to atmospheric pressure under nitrogen. The samples were transported through air to be analysed. Glass substrates were used for XPS, and potassium bromide discs for infrared analysis.

XPS spectra were collected on a Kratos ES200 spectrometer, in the fixed retarding ratio (FRR) analyser mode and a Kratos ES300 in the fixed analyser transmission (FAT) mode. The regions analysed were

identical to those in chapter 5 with the exception that when the ES200 was used to examine zinc containing films, the Zn3P (binding energy ~90 eV) rather than the $Zn2P_{\frac{3}{2}}$ (binding energy ~1022 eV) region was collected due to the low sensitivity of the FRR mode to low kinetic energy electrons. Deconvolution of C1S spectra in films containing both fluorine and oxygen cannot be reliably carried out due to the numerous possible environments. A peak fit was only attempted when one of the electronegative elements was in a large enough excess to make contribution from the other element negligable. Infrared spectra were collected on a Mattson-Polaris FT-IR spectrometer.

6.3 Zinc acetylacetonate and Aluminium tri-*sec* -butoxide

6.3.1 Results and Discussion

Thin films formed via evaporation of both zinc acetylacetonate and aluminium tri-*sec* -butoxide separately into non-polymer forming plasmas were investigated in chapter 5. The actual flow rates and deposition rates of the two monomers were unknown, so predicting from a codeposition standpoint the theoretical composition of a film given individual monomer tube temperatures is difficult. It was found that the products from the zinc compound varied less with changes in the resevoir temperature than the aluminium compound. To try and find a reaction scheme whereby the deposition rate from each compound is similar it was decided, therefore, to keep the zinc acetylacetonate resevoir temperature constant at 110 °C and vary the aluminium tri-*sec* - butoxide monomer tube temperature.

The oxygen flow rate through the reactor was kept constant at 1.39 ml/min, double the flow used as a standard in chapter five. When

both monomers are entering the reactor there should be an increased consumption of oxygen. With this flow rate of oxygen the product formed when the aluminium tri-*sec* -butoxide resevoir is at ~165 °C will be a direct combination of the pure monomer deposits (with 0.70 ml/min. oxygen flow) if codeposition is occuring.

Figure 6.4 shows the results of elemental surface analyses for experiments conducted over a range of Al(OBut)3 temperatures. In some films, an Si2P peak was visible, these have been left out of the diagram for clarity. The Si:C ratio for films formed at an aluminium tri-*sec* -butoxide resevoir temperature of 20°C and 60°C were 0.10 and

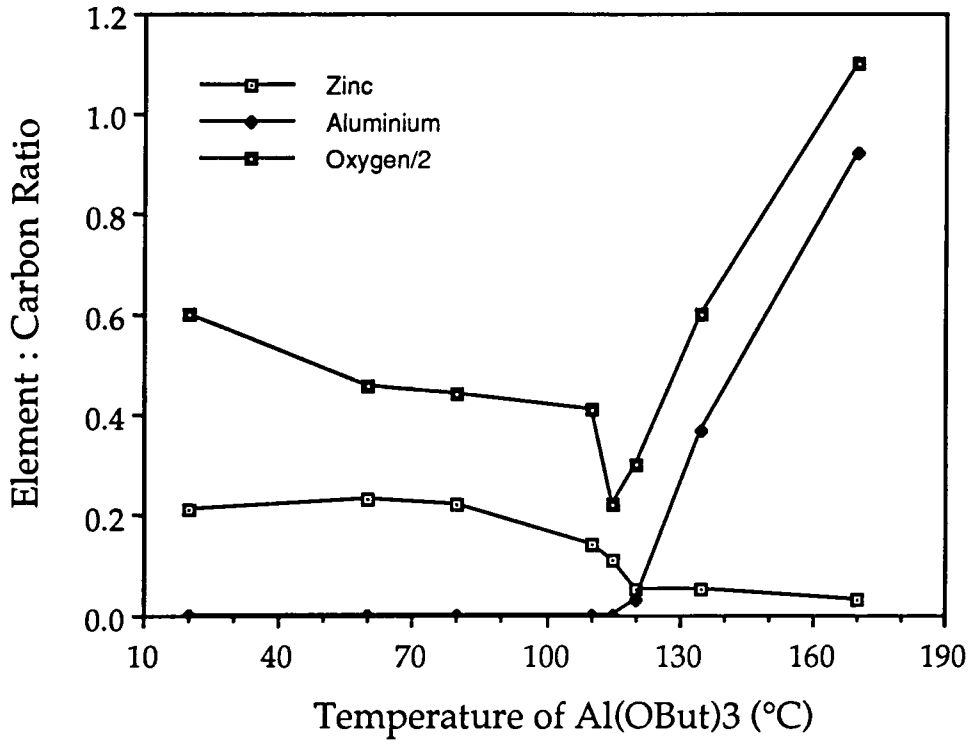

Figure 6.4 Elemental composition of films formed from the co-deposition of Zn(acac)2 and Al(OBut)3

0.02 respectively. At low temperatures the deposit is similar to films formed from just zinc acetylacetonate and oxygen (see chapter 5). There is an increase in the carbon content relative to all other elements (c.f. result for $Zn(acac)_2$ at 110°C and O_2 flow 1.39 ml/min). This effect can be ascribed to volatile material (possibly butanol or butanone) entering the chamber from the aluminium compound resevoir. The rate of film formation increased upon raising the temperature from 20°C to 80°C, without substantially altering zinc content. This is evident in the fall of the silicon to carbon ratio, the decrease in the oxygen to carbon ratio is also due to greater film thickness. The increase in temperature aids evaporation of organic material from the $Al(OBut)_3$ resevoir which competes with the zinc monomer for oxygen. The lower availability of oxygen allows a higher deposition rate of zinc acetylacetonate.

As the aluminium monomer is heated above 80°C to about 120°C there is a fall in the zinc to carbon ratio of the product. If organic material is coming from the aluminium resevoir, at this point it is entering the chamber with a high enough pressure to be incorporated within the product, hence the higher percentage of carbon in the film. Aluminium incorporation is not detectable until the monomer tube temperature is at 120°C or higher. Above this temperature aluminium content increases dramatically. At 170°C the film is very similar to the pure $Al(OBut)_3$ films formed in chapter 5. The deposition rate of the aluminium compound at this temperature must be substantially greater than that of the zinc compound.

If codeposition is taking place, the atomic percentages of the elements at 170°C should be consistent with results from chapter 5. Table 6.1 compares these values, $\%Zn(acac)_2$ character was calculated from equation 6.1. The

$$\%Zn(acac)_2 \text{ character (element)} = \frac{\text{at.\%(copol.)} - \text{at.\%(Al(OBut}_3\text{))}}{\text{at.\%(Zn(acac)}_2\text{)} - \text{at.\%(Al(OBut}_3\text{))}} \quad 6.1$$

	Atomic percent of element			
Film	C	Zn	Al	O
$Zn(acac)_2$ 110°C 0.70 ml/min	43	13	0	44
$Al(OBut)_3$ 165°C 0.70 ml/min	20	0	28	52
Copolymer of the above	25	1	23	51
% $Zn(acac)_2$ character	21%	8%	18%	12%

Table 6.1 Comparison of atomic compositions of polymers

contribution from zinc acetylacetonate to the intensity of each element was calculated, an average value of about 15% being obtained. This implies that the aluminium compound is being deposited 5 to 6 times faster than the zinc compound. There is quite a large degree of variance between the results, however, which indicates that there is some degree of interaction between the two monomers during film formation.

Peak fitting of the C_{1S} envelope gives some insight into the chemical state of carbonaceous material within the product, see table 6.2. There is quite a large degree of scatter across the range of materials studied. This is due to a small signal to noise ratio for the C_{1S} level using the FAT mode (typical spectra shown in figure 6.5). Deconvolution of these spectra was difficult and the results shown should be taken only as an indication of the functional groups present. Some trends do emerge, most noticeable is the fairly steady decrease in the carboxylate group concentration, coupled with a more erratic rise in

Al(OBut)3 Temperature	C-H	C-O	C=O	O-C=O	CO3
20	37	14	4	45	0
60	33	13	12	34	8
80	34	24	8	28	6
110	53	14	2	31	0
115	61	13	10	16	0
120	53	16	11	19	1
135	57	18	7	18	0
170	58	18	9	8	7

Table 6.2 Results of C1S peak fits shown as percent contributions to the total peak area

the number of unoxidised carbon atoms on increasing the aluminium tri-*sec* -butoxide temperature. The hydrocarbon intensity rises sharply at about 110 °C which is also the point at which the zinc ion level begins to fall. This again points to organic decomposition products from Al(OBut)3 reaching the growing surface and influencing the nature of the product. The intensities of the other groups present always fall in the order C-O > C=O > CO3, although the absence or presence of carbonate groups follows no apparent pattern. At the two extremes of temperature the organic film component is similar to the expected composition from the previous chapter.

6.3.2 Synopsis

Zinc acetylacetonate and Aluminium tri-*sec* -butoxide have been deposited together in the presence of oxygen. By adjusting the

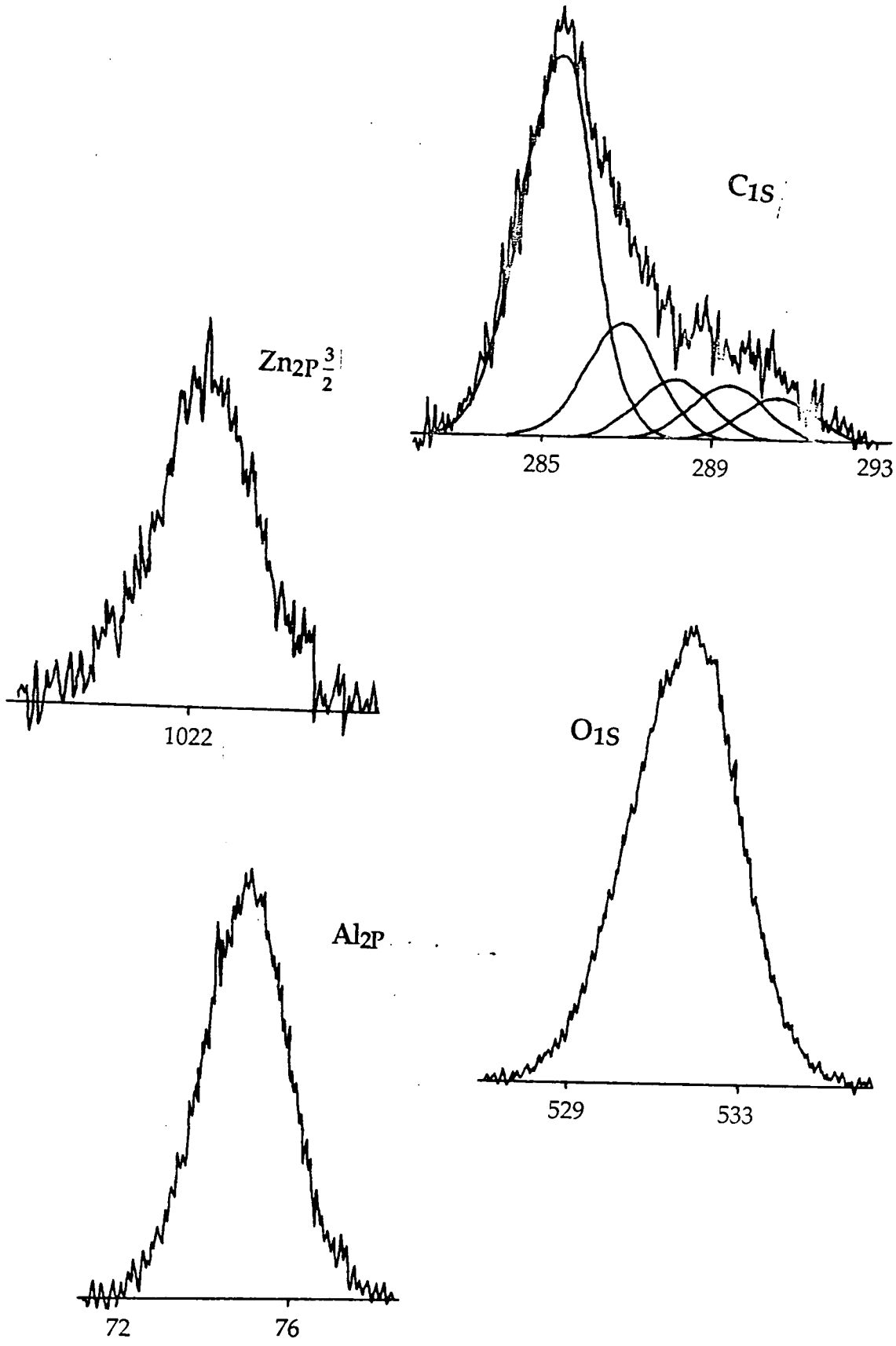

Figure 6.5 XPS spectra from a film formed at an $Al(OBut)_3$ temperature of 170°C

temperature of the aluminium compound resevoir the rapid breakdown of this compound within a plasma is evident. If there is insufficient heating no aluminium is found in the resulting film but the organic part of the monomer influences deposition. The metal part of the compound therefore must rapidly condense out of the gas phase, and a very high flow rate must be used to enable it to travel to the substrate. It has also been shown that under conditions typically used in chapter five the aluminium compound is deposited roughly 5 or 6 times faster than the zinc compound.

Interactions between the two monomers, specifically the organic ligands, mean that overall this is a copolymerisation rather than a codeposition. The two metal compounds follow different reaction pathways, one forming metal oxide clusters and the other remaining strongly associated with its ligand. These features of the deposition of these compounds appear to remain unaltered during copolymerisation implying that the metallic parts are actually codepositing within a copolymerising organic matrix.

6.4 Zinc acetylacetonate and Perfluorohexane

6.4.1 Results and Discussion

In chapter three the plasma polymerisation of perfluorohexane was examined specifically with regard to the site of collection. The substrate in this case is situated at the upstream edge of the plasma, where film formation is minimal for neat perfluorohexane. Without any heating of the $Zn(acac)_2$ resevoir (20°C) silicon is visible under XPS (Si:C = 0.12). Heating of the zinc acetylacetonate container causes a reduction in Si_{2P} intensity (80°C; Si:C = 0.04), until at 90 °C there is no

detectable signal from the glass, typical spectra are shown in figure 6.6. The addition of the metal containing monomer increases deposition in the upstream region of the reactor. There is a concomitant rise in both the fluorine peak area and the zinc intensity which indicates that both monomers are strongly influencing the film character (see figure 6.7).

The F_{1S} region often gave a complex signal, as can be seen in figure 6.6, which could be resolved into no fewer than three peaks with binding energies of approximately 689 eV, 687.6 eV and 685.5 eV. These peaks where assigned to ionic, covalent and partially charged fluorine, with reference to literature values. Binding energy ~685.5 eV, F^- ion (c.f. ZnF_2 684.3 eV, CsF 685.8 eV[6]), ~687.6 eV, $F^{\delta-}$ (c.f. C_4F graphite intercalate 687.2 eV, $Ni(O_2CCF_3)_2$ 688.2 eV[6]) and ~689 eV, F_{cov} (c.f. PTFE 689 eV). The low binding energy fluorine atoms are ionically bound to zinc and the high binding energy atoms covalently bound to carbon. The intermediate peak is due to covalent fluorine atoms closely associated with negative charges such as carboxyl ions. The results of peak fitting this region is shown in figure 6.8. The ratio of Zn : F^- is between 1 and 2 for all samples examined. This indicates that some zinc fluoride is being formed during reaction in the glow discharge. The remaining fluorine atoms are present in the organic matrix, C_{1S} peak fits cannot accurately confirm this because of the presence of oxygen in the film.

A sample was made at a higher flow rate of perfluorohexane (0.93 ml./min.) and a zinc acetylacetonate temperature of 100 °C. Under these conditions there was about ten times as many fluorine atoms in the product as oxygen atoms. A C_{1S} deconvolution was carried out with the assumption that there was negligable contribution from the

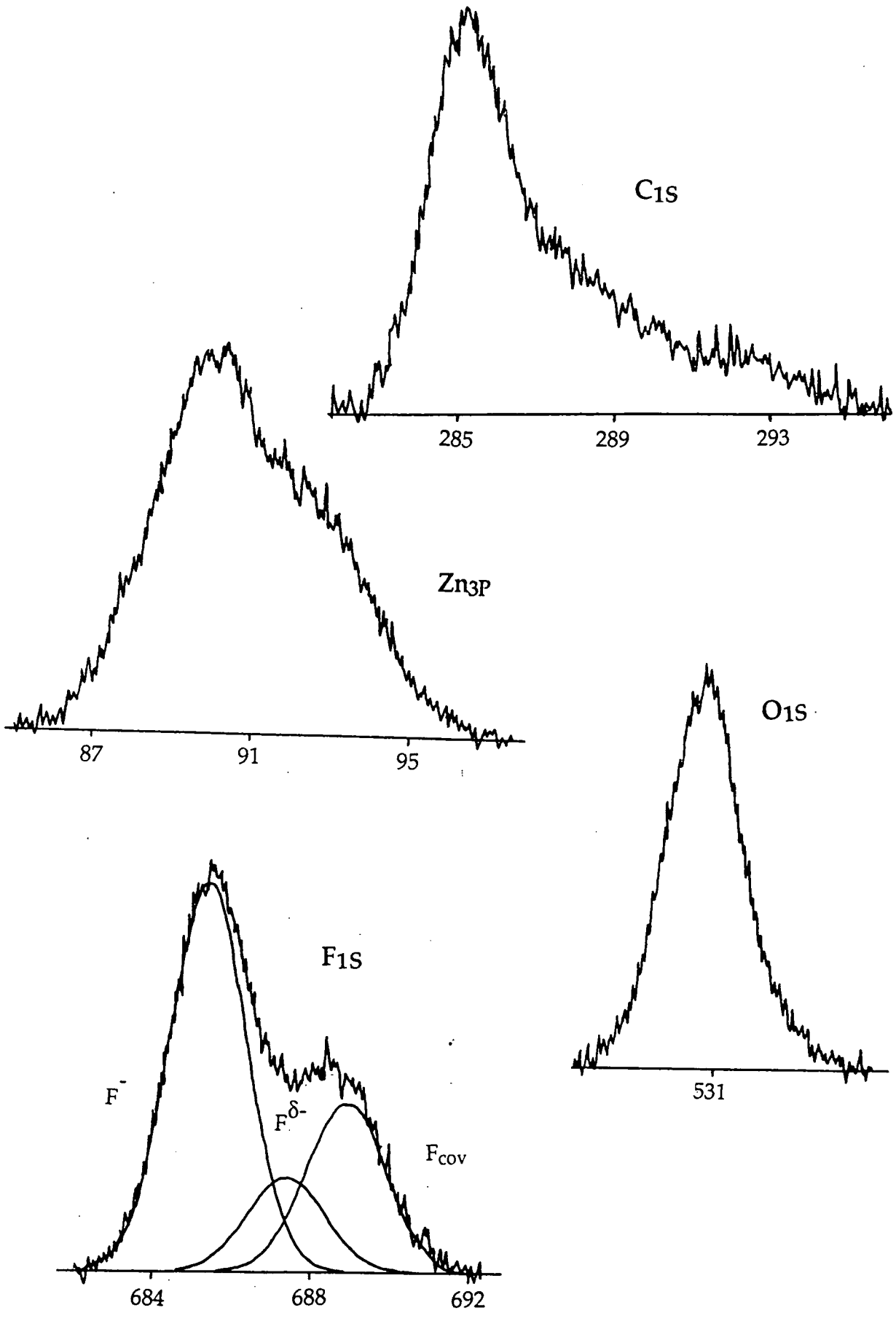

Figure 6.6 XPS spectra from a $Zn(acac)_2$ temperature of 110°C and a C_6F_{14} flow rate of 0.28 ml./min.

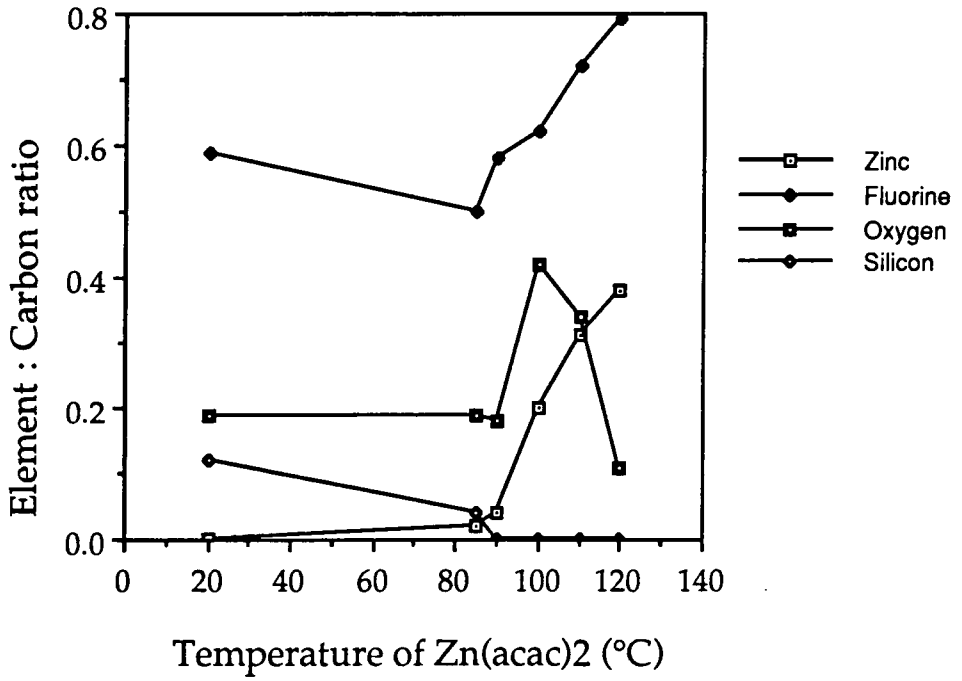

Figure 6.7 Elemental composition of films versus $Zn(acac)_2$ temperature

oxygen atoms. The results, C-H 21%, C-CF 9%, CF 7%, CF-CF 9%, CF_2 48%, CF_3 6% show that most of the fluorocarbon component exists as CF_2 links. In this region of the reactor (the inlet end) there will be only a small disruption of the monomer structure, especially with the very low powers employed. The expected polymeric matrix should thus consist of mainly CF_2 and CF_3 type carbon atoms. The low intensity of the CF_3 component is probably caused by such groups being associated with non-polymer forming species. The hydrocarbon and part of the lower binding energy peaks (which will have some contribution from carbon bound to oxygen) result from the organic component of the $Zn(acac)_2$ monomer. From the C_{1S} peak fit the expected fluorine to carbon ratio is $CF_{1.30}$ which is close to the value from the elemental peaks (C_{1S} to covalently bound F_{1S}) of $CF_{1.26}$. The zinc content of the

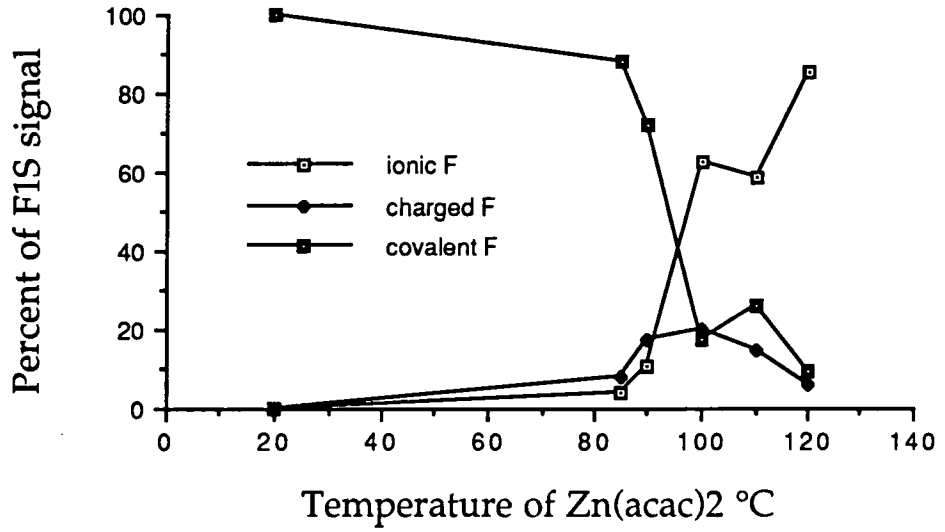

Figure 6.8 Distribution of ionised and covalent fluorine as a function of zinc acetylacetonate temperature

film is very small, a result of the increased partial pressure of perfluorohexane.

The oxygen signal follows a strange pattern, first increasing then decreasing with a rise in the rate of zinc acetylacetonate volatilisation (see figure 6.7). There is undeniably some form of copolymerisation occuring since a replacement of the acetyacetonate ligand with fluoride ions occurs during deposition. If it is assumed that this reaction (see scheme 6.1) occurs in the gas phase very rapidly, then the first products would be zinc fluorides and acetylacetonate moieties. This is not an unreasonable assumption since even at high rates of $Zn(acac)_2$ vapourisation the major metal product is zinc fluoride.

$$2F^- + Zn(C_5O_2)_2 \Longrightarrow ZnF_2 + 2(C_5O_2)^- \qquad 6.1$$

With this reaction occuring, the solid product will be composed of two parts, a condensate of zinc fluoride and a plasma polymer from the mixture of acetylacetonate and perfluorohexane. The rate of

deposition of the ionic salt will be dependent solely on the rate of evaporation of zinc acetylacetonate, given that reaction 6.1 is extremely fast. This is shown by the almost linear increase of Zn^{2+} and F^- upon raising the monomer tube temperature. The plasma polymerisation reaction, however, is more complex and the organic part of the film will probably form at a more constant rate regardless of the $Zn(acac)_2$ evaporation rate. The initial rise in oxygen signal will then be due to volatilisation of enough zinc acetylacetonate to influence the film character. The subsequent fall is explained by the higher relative deposition rate of the metal fluoride and peculiarities in the organic copolymerisation reaction.

Infrared spectra taken of these films (see figure 6.9) are dominated by the $-CF_2-$ absorbance at ~1150 cm^{-1} and the $-CF_3$

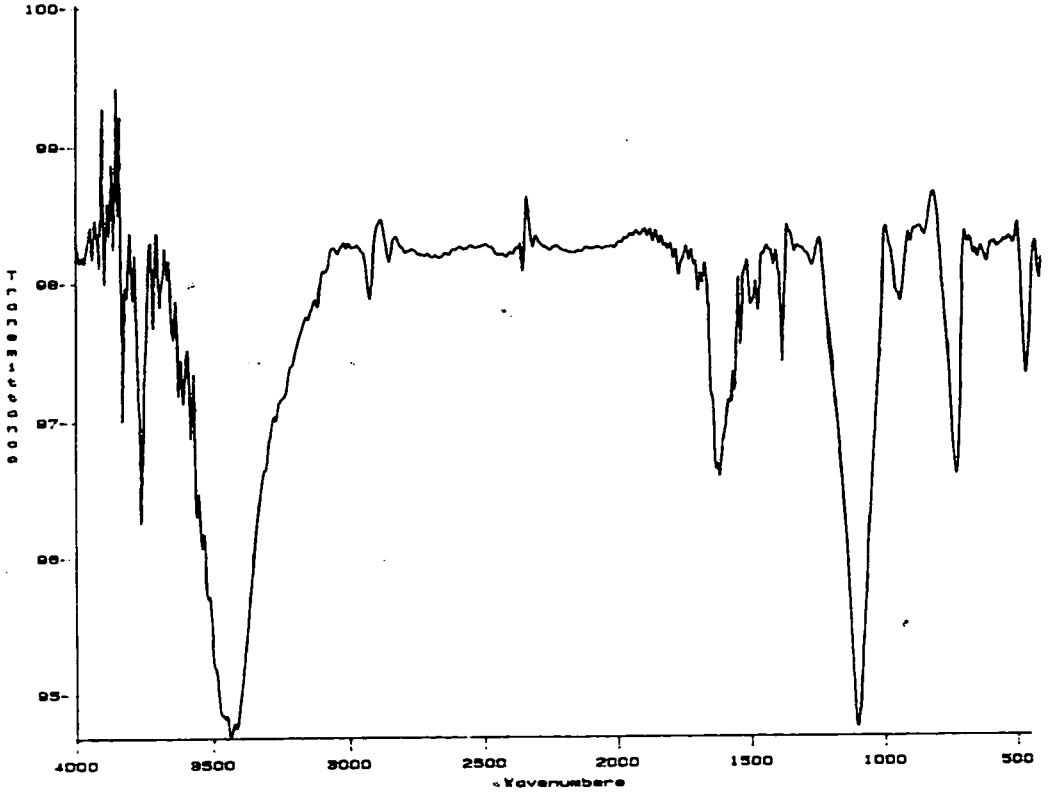

Figure 6.9 Infrared spectrum of film formed at C_6F_{14} flow rate of 0.28 ml./min., $Zn(acac)_2$ temperature of 100°C

absorbance at ~700 cm^{-1}. There is no indication of any vinyl or acetylinic bonds, but there is an absorbance at ~1600 cm^{-1} probably due to carbonyl groups. The presence of the $(F\text{-}H\text{-}F)^-$ ion should be detectable by infrared and has been reported in similar films[10], but no absorbance indicative of this species was found despite the ready supply of metal counterions and hydrogen.

6.4.2 Synopsis

Plasma copolymerisation of zinc acetylacetonate and perfluorohexane was examined. The major film components were zinc fluoride and an organic matrix. It was found that the zinc molecule rapidly broke down into a metal part and a ligand part, contrary to the results from the zinc acetylacetonate/oxygen plasma reaction. This can be ascribed to the more reactive nature of fluorine species. Copolymerisation, rather than codeposition, occured; this is easily seen from the presence of fluoride ions in the product which are not produced when $Zn(acac)_2$ or C_6F_{14} are the sole monomers.

6.5 Aluminium tri-*sec* -butoxide and Perfluorohexane

6.5.1 Results and Discussion

When aluminium tri-*sec* -butoxide is reacted in non-polymerisable gas plasmas it was found that a temperature of roughly 165 °C was needed to produce a film containing aluminium but without condensing liquid $Al(OBut)_3$ onto the substrate. Temperatures

of about this value were found, with a perfluorohexane plasma to give films with little fluorine incorporation (C6F14 flow rate, 0.23 ml/min; Al(OBut)3 temp, 170°C gave Al:C 0.21, O:C 0.39, F:C 0.00). This is perhaps because of the high deposition rate of the metal monomer at such elevated temperatures. Reducing the resevoir temperature enabled films to be formed that contained both aluminium and fluorine in reasonable quantities (see figures 6.10 and 6.11).

Typical XPS results are shown in figure 6.12, the Al_{2P} peak appeared at ~76.5 eV which indicates aluminium fluoride formation (AlF_3 76 eV, Al_2O_3 74.5 eV[11]). The absence of any signal in the silicon region suggests that the films are at least 70 Å thick. The F_{1S} envelope demonstrated little structure, the shift of the main peak being either typical of ionic fluoride or covalently bound fluorine atoms. Fluoride

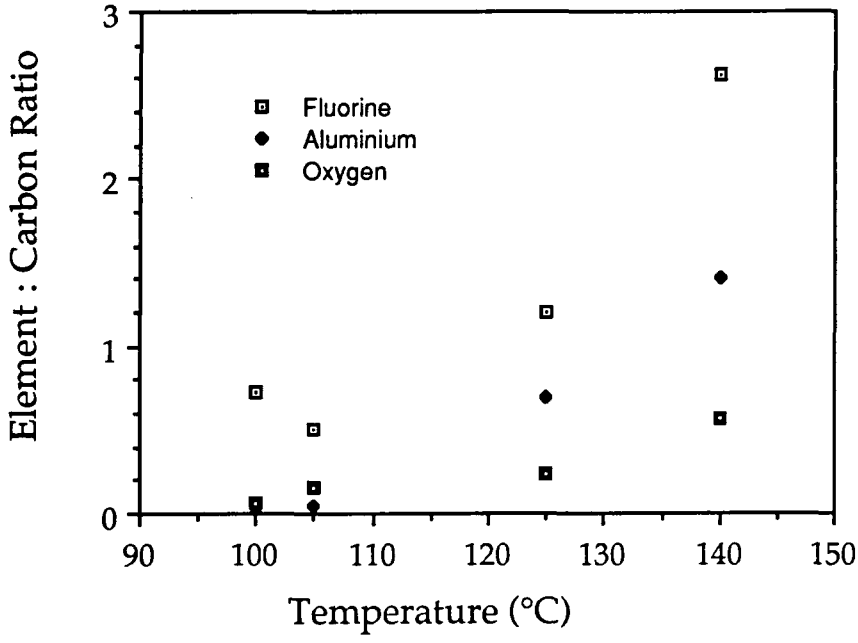

Figure 6.11 Elemental composition of films versus temperature of Al(OBut)3 resevoir

ions were present when the aluminium to carbon ratio was greater than 0.5, otherwise mainly organic fluorine could be detected. In the cases were ionic fluorine was formed, the F : Al ratio was 1.8 ± 0.1, suggesting that a large amount of aluminium fluoride condenses on the substrate, but also some oxide and/or organic ligands are associated with aluminium ions. Extensive structure typified the carbon spectra, however, with two electronegative elements within the product deconvolution of them would be extremely difficult and uninformative.

The metal content of material collected is larger when the $Al(OBut)_3$ resevoir temperature is higher (figure 6.10). When there is only moderate heating (about 100 °C) there is virtually no aluminium content at all in the product. There is however an appreciable rate of film formation since no silicon signal could be found. On its own

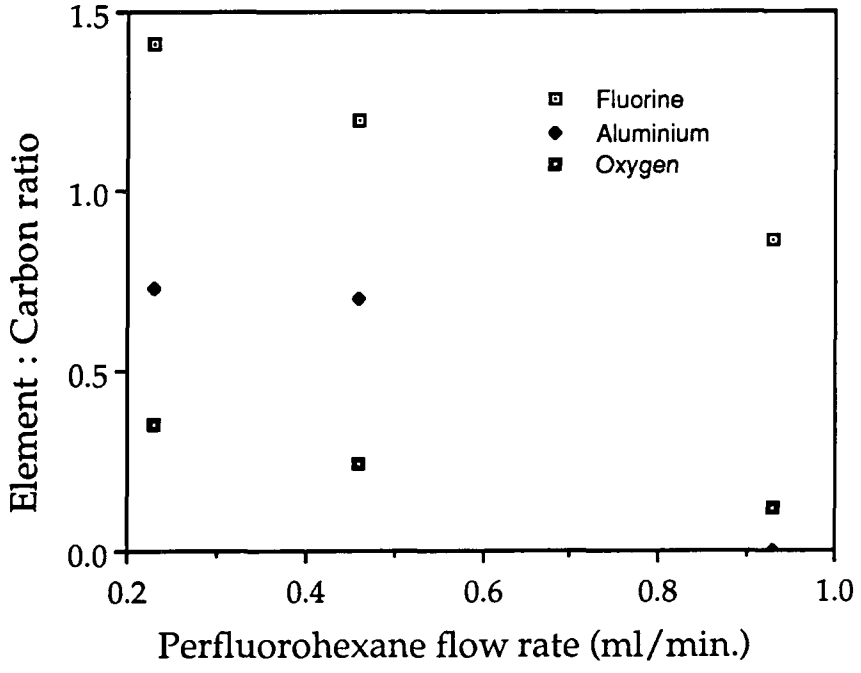

Figure 6.12 Elemental composition of films versus flow rate of perfluorohexane

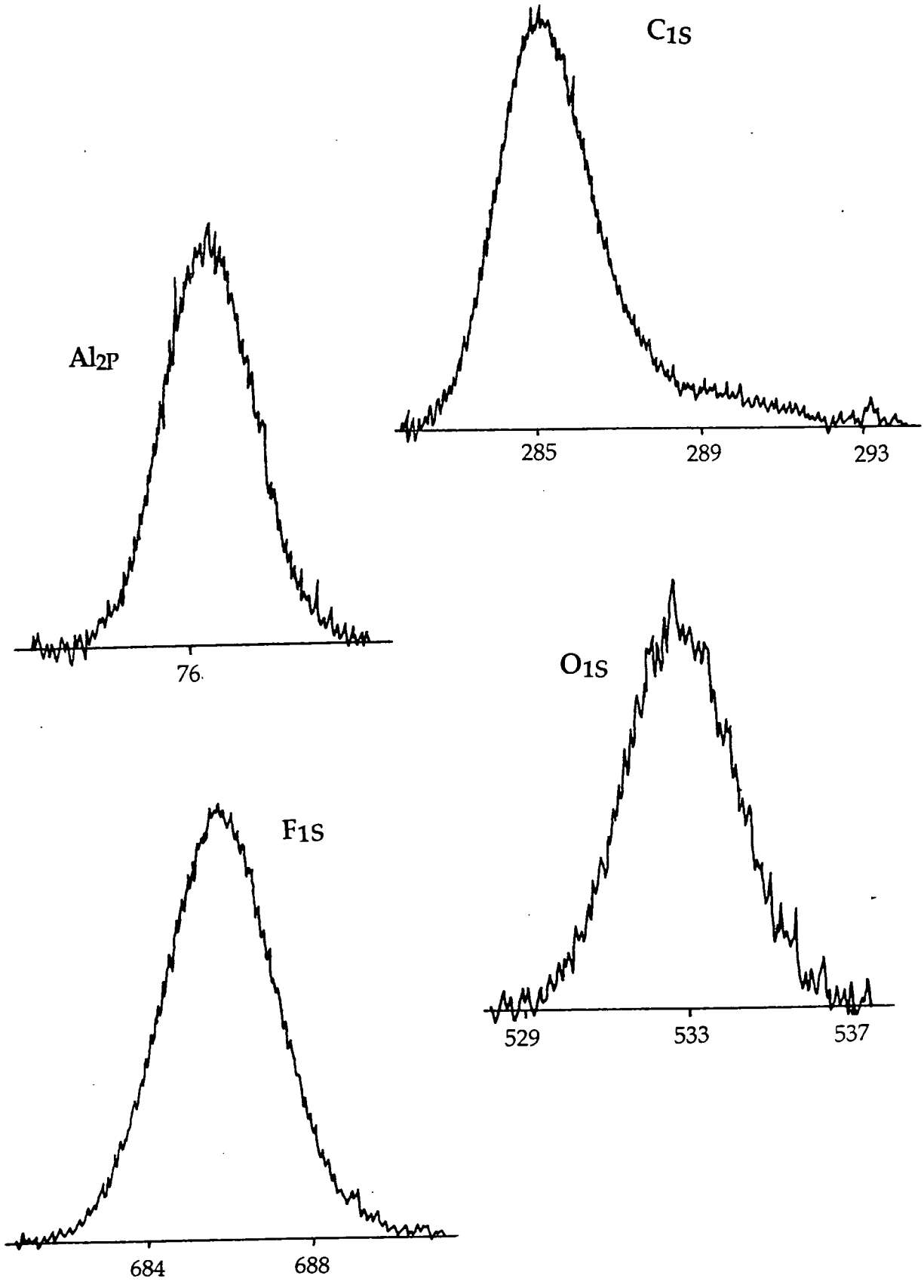

Figure 6.12 XPS spectra of deposit formed at C_6F_{14} flow rate of 0.23 ml/min. and $Al(OBut)_3$ temperature of 125°C

perfluorohexane does not have a high deposition rate in this region of the reactor (see section 6.4), the addition of another monomer is needed. Decomposition products of aluminium tri-*sec* -butoxide are enhancing film production on the substrate, as in section 6.3. This would explain the relatively high oxygen content of the products, since the most likely decomposition compounds are butanol and butanone.

As the rate of evaporation of the metal compound is raised, the amount of aluminium in the film increases. As this occurs there is also a rise in the ionic fluorine level in the product. The C_{1S} region in the cases of high temperature deposition confirm that fluorine is not a major part of the organic matrix; there is little structure on the high binding energy side of the hydrocarbon peak. In the case of the copolymerisation of zinc acetylacetonate and perfluorohexane there was always a substantial proportion of covalent fluorine remaining in the film. This suggests a reaction scheme whereby fluorine is actively removed from fluorocarbon species in the plasma, or free fluorine is more efficiently scavenged by the metal ions. The formation of aluminium-fluorine bonds is thermodynamically favoured; the bond strengths[12] for diatomic molecules being Al-F 664 kJ/mol and C-F 536 kJ/mol (c.f. Zn-F 368 kJ/mol). The rise in oxygen incorporation with increasing resevoir temperature is much less dramatic than when $Al(OBut)_3$ is deposited in an oxygen plasma. Some oxygen remains associated with the metal ions, although replacement of ligand moieties with fluoride ions severely reduces its presence in the product.

Figure 6.11 demonstrates the change in film composition with a constant resevoir temperature and an increasing perfluorohexane flow rate. The amount of fluorine found in the material collected actually decreases with a rise in flow rate. This is probably due to less metal

depositing, and hence, fewer fluoride ions. At the highest flow investigated there is no detectable aluminium and all the fluorine present is covalently bonded to carbon. Aluminium fluoride formed at high perfluorohexane fluxes probably condenses rapidly from the gas phase before reaching the substrate. Oxygen (from the butoxide ligand) is visible at all flow rates, showing a steady decline as the fluoropolymer character of the film increases.

6.5.2 Synopsis

As with zinc acetylacetonate, a copolymerisation reaction occurs between aluminium tri-*sec* -butoxide and perfluorohexane. The main product is an aluminium fluoride salt and an organic matrix. The metal still retains some oxide character, and a stoichiometry of roughly $AlF_2O_{0.5}$ can be found in films with a substantial metal content, regardless of reaction conditions. The main carbon peak in the C_{1S} envelope in such products is at 285 eV which is typical of carbon not bound to an electronegative element. This means that either the perfluoro compound is not well expressed in these materials or that there is a loss of fluorine from it before or during deposition.

6.6 Conclusion

Copolymerisation of zinc acetylacetonate and aluminium tri-*sec* -butoxide in an oxygen plasma results in organic films which may include one or both metal ions. The composition of the films is not vastly different from the oxygen plasma deposits of the neat monomers. It appears that little interaction occurs between the metal parts in the gas phase, and the reaction is likely to be a codeposition

rather than a copolymerisation. The stoichiometry of the carbonaceous component does suggest that some interaction between the two ligands occurs which means that the organic matrix is actually to some degree copolymerising.

In contrast, the reaction between the metal containing monomers and perfluorohexane is undeniably a copolymerisation reaction. The formation of fluorides from these reactions demonstrates interaction between the two monomers. The films formed by copolymerisation of zinc acetylacetonate and perfluorohexane show that zinc species react with fluoride ions during deposition. The condensation of metal halide material is divorced from polymerisation of carbon containing species and appears to be mostly dependent on the evaporation rate of zinc acetylacetonate.

A more severe interaction occurs during copolymerisation of aluminium tri-*sec* -butoxide and perfluorohexane, where it appears that aluminium ions actively remove fluorine from the fluorinated monomer to produce the metal fluoride. A mixed aluminium oxide/ aluminium fluoride compound is the main metallic product, the organic component consisting mostly of hydrocarbon material.

References

1 C. U. Pittman, J. E. Sheats, C. E. Carraher, M. Zeldin, B. Currel, *Polym. Mater. Sci. Eng.*, ACS, Florida, **61**, 91, (1989)

2 E. Kay, M. Hecq, *J. Appl. Phys.*, **55**, 370, (1984)

3 J. E. Mark, S. -B. Wang, *Polymer Bulletin*, **20**, 443, (1988)

4 A. Dilks, E. Kay, *ACS Symp. Ser.*, **108**, 195, (1979)

5 L. Martinu, H. Biederman, *Int. Symp. Plasma Chem. 7*, 1313, (1985)

6 Y. Osada, Q. S. Yu, H. Yasunaga, Y. Kagami, F. S. Wang, J. Chen, *J. Polym. Sci., Polym. Chem. Ed.*, **27**, 3799, (1989)

7 F. A. Cotton, G. Wilkinson, "Advanced Inorganic Chemistry", 4th Ed., J. Wiley and Sons, (1980)

8 M. Sanchez, H. P. Schreiber, M. R. Wertheimer, *ACS Polym. Mater. Sci. Eng.*, **56**, 792, (1987)

9 H. S. Munro, C. Till, *J. Polym. Sci., Polym. Chem. Ed.*, **25**, 1065, (1987)

10 Y. Haque, B. D. Ratner, *J. Polym. Sci., Polym. Phys. Ed.*, **26**, 1237, (1988)

11 C. D. Wagner, W. M. Riggs, L. E. Davis, J. F. Moulder, G. E. Muilenberg, "Handbook of X-Ray Photoelectron Spectroscopy", Perkin Elmer Corp., Minnesota, USA, (1979)

12 "CRC Handbook of Chemistry and Physics", 63rd Edition, Ed. R. C. Weast, CRC press, USA, (1982)

UNIVERSITY OF DURHAM

Board of Studies in Chemistry

COLLOQUIA, LECTURES AND SEMINARS GIVEN BY INVITED SPEAKERS
1ST AUGUST 1988 to 31st JULY 1989

AVEYARD, Dr. R. (University of Hull) — 15th March, 1989
Surfactants at your Surface

AYLETT, Prof. B.J. (Queen Mary College, London) — 16th February, 1989
Silicon-Based Chips:- The Chemist's Contribution

BALDWIN, Prof. J.E. (Oxford University) — 9th February, 1989
Recent Advances in the Bioorganic Chemistry of Penicillin Biosynthesis

BALDWIN & WALKER, Drs. R.R. & R.W. (Hull University) — 24th November, 1988
Combustion: Some Burning Problems

BUTLER, Dr. A.R. (St. Andrews University) — 15th February, 1989
Cancer in Linxiam: The Chemical Dimension

CADOGAN, Prof. J.I.G. (British Petroleum) — 10th November, 1988
From Pure Science to Profit

CASEY, Dr. M. (University of Salford) — 20th April, 1989
Sulphoxides in Stereoselective Synthesis

CRICH, Dr. D. (University College London) — 27th April, 1989
Some Novel Uses of Free Radicals in Organic Synthesis

DINGWALL, Dr. J. (Ciba Geigy) — 18th October, 1988
Phosphorus-containing Amino Acids: Biologically Active Natural and Unnatural Products

ERRINGTON, Dr. R.J. (University of Newcastle-upon-Tyne) — 1st March, 1989
Polymetalate Assembly in Organic Solvents

FREY, Dr. J. (Southampton University) — 11th May, 1989
Spectroscopy of the Reaction Path: Photodissociation Raman Spectra of NOCl

GRADUATE CHEMISTS, (Polytechs and Universities in North East England) — 12th April, 1989
R.S.C. Symposium for presentation of papers by postgraduate students

HALL, Prof. L.D. (Addenbrooke's Hospital, Cambridge) — 2nd February, 1989
NMR - A Window to the Human Body

HARDGROVE, Dr. G. (St. Olaf College, U.S.A.) — December, 1988
Polymers in the Physical Chemistry Laboratory

HARWOOD, Dr. L. (Oxford University) — 25th January, 1988
Synthetic Approaches to Phorbols Via Intramolecular Furan Diels-Alder Reactions: Chemistry under Pressure

JÄGER, Dr. C. (Friedrich-Schiller University GDR) 9th December, 1988
NMR Investigations of Fast Ion Conductors of the NASICON Type

JENNINGS, Prof. R.R. (Warwick University) 26th January, 1989
Chemistry of the Masses

JOHNSON, Dr. B.F.G. (Cambridge University) 23rd February, 1989
The Binary Carbonyls

LUDMAN, Dr. C.J. (Durham University) 18th October, 1988
The Energetics of Explosives

MACDOUGALL, Dr. G. (Edinburgh University) 22nd February, 1989
Vibrational Spectroscopy of Model Catalytic Systems

MARKO, Dr. I. (Sheffield University) 9th March, 1989
Catalytic Asymmetric Osmylation of Olefins

McLAUCHLAN, Dr. K.A. (University of Oxford) 16th November, 1988
The Effect of Magnetic Fields on Chemical Reactions

MOODY, Dr. C.J. (Imperial College) 17th May, 1989
Reactive Intermediates in Heterocyclic Synthesis

PAETZOLD, Prof. P. (Aachen) 23rd May, 1989
Iminoboranes XB≡NR: Inorganic Acetylenes?

PAGE, Dr. P.C.B. (University of Liverpool) 3rd May, 1989
Stereocontrol of Organic Reactions Using 1,3-dithiane-1-oxides

POLA, Prof. J. (Czechoslovak Academy of Sciences) 15th June, 1989
Carbon Dioxide Laser Induced Chemical Reactions - New Pathways in Gas-Phase Chemistry

REES, Prof. C.W. (Imperial College London) 27th October, 1988
Some Very Heterocyclic Compounds

SCHMUTZLER, Prof. R. (Technische Universitat Braunschweig) 6th October, 1988
Fluorophosphines Revisited - New Contributions to an Old Theme

SCHROCK, Prof. R.R. (M.I.T.) 13th February, 1989
Recent Advances in Living Metathesis

SINGH, Dr. G. (Teesside Polytechnic) 9th November, 1988
Towards Third Generation Anti-Leukaemics

SNAITH, Dr. R. (Cambridge University) 1st December, 1988
Egyptian Mummies: What, Where, Why and How?

STIBR, Dr. B. (Czechoslovak Academy of Sciences) 16th May, 1989
Recent Developments in the Chemistry of Intermediate-Sited Carboranes

VON RAGUE SCHLEYER, Prof. P. (Universitat Erlangen Nurnberg) 21st October, 1988
The Fruitful Interplay Between Calculational and Experimental Chemistry

WELLS, Prof. P.B. (Hull University) 10th May, 1989
Catalyst Characterisation and Activity

UNIVERSITY OF DURHAM

Board of Studies in Chemistry

COLLOQUIA, LECTURES AND SEMINARS GIVEN BY INVITED SPEAKERS 1ST AUGUST 1989 TO 31ST JULY 1990

BADYAL, Dr. J.P.S. (Durham University) Breakthoughs in Heterogeneous Catalysis	1st November, 1989
BECHER, Dr. J. (Odense University) Synthesis of New Macrocylic Systems using Heterocyclic Building Blocks	13th November, 1989
BERCAW, Prof. J.E. (California Institute of Technology) Synthetic and Mechanistic Approaches to Ziegler–natta Polymerization of Olefins	10th November, 1989
BLEASDALE, Dr. C. (Newcastle University) The Mode of Action of some Anti–tumour Agents	21st February, 1990
BOWMAN, Prof. J.M. (Emory University) Fitting Experiment with Theory in Ar–OH	23rd March, 1990
BUTLER, Dr. A. (St. Andrews University) The Discovery of Penicillin: Facts and Fancies	7th December, 1989
CHEETHAM, Dr. A.K. (Oxford University) Chemistry of Zeolite Cages	8th March, 1990
CLARK, Prof. D.T. (ICI Wilton) Spatially Resolved Chemistry (using Natures's Paradigm in the Advanced Materials Arena)	22nd February, 1990
COLE–HAMILTON, Prof. D.J. (St. Andrews University) New Polymers from Homogeneous Catalysis	29th November, 1989
CROMBIE, Prof. L. (Nottingham University) The Chemistry of Cannabis and Khat	15th February, 1990
DYER, Dr. U. (Glaxo) Synthesis and Conformation of C–Glycosides	31st January, 1990
FLORIANI, Prof. C. (University of Lausanne, Switzerland) Molecular Aggregates – A Bridge between homogeneous and Heterogeneous Systems	25th October, 1989
GERMAN, Prof. L.S. (USSR Academy of Sciences – Moscow) New Syntheses in Fluoroaliphatic Chemistry: Recent Advances in the Chemistry of Fluorinated Oxiranes	9th July, 1990
GRAHAM, Dr. D. (B.P. Reserch Centre) How Proteins Absorb to Interfaces	4th December, 1989
GREENWOOD, Prof. N.N. (University of Leeds) Novel Cluster Geometries in Metalloborane Chemistry	9th November, 1989

HOLLOWAY, Prof. J.H. (University of Leicester) — 1st February, 1990
Noble Gas Chemistry

HUGHES, Dr. M.N. (King's College, London) — 30th November, 1989
A Bug's Eye View of the Periodic Table

HUISGEN, Prof. R. (Universität München) — 15th December, 1989
Recent Mechanistic Studies of [2+2] Additions

KLINOWSKI, Dr. J. (Cambridge University) — 13th December 1989
Solid State NMR Studies of Zeolite Catalysts

LANCASTER, Rev. R. (Kimbolton Fireworks) — 8th February, 1990
Fireworks – Principles and Practice

LUNAZZI, Prof. L. (University of Bologna) — 12th February, 1990
Application of Dynamic NMR to the Study of Conformational Enantiomerism

PALMER, Dr. F. (Nottingham University) — 17th October, 1989
Thunder and Lightning

* PARKER, Dr. D. (Durham University) — 16th November, 1989
Macrocycles, Drugs and Rock 'n' roll

PERUTZ, Dr. R.N. (York University) — 24th January, 1990
Plotting the Course of C–H Activations with Organometallics

PLATONOV, Prof. V.E. (USSR Academy of Sciences – Novosibirsk) — 9th July, 1990
Polyfluoroindanes: Synthesis and Transformation

POWELL, Dr. R.L. (ICI) — 6th December, 1989
The Development of CFC Replacements

POWIS, Dr. I. (Nottingham University) — 21st March, 1990
Spinning off in a huff: Photodissociation of Methyl Iodide

ROZHKOV, Prof. I.N. (USSR Academy of Sciences – Moscow) — 9th July, 1990
Reactivity of Perfluoroalkyl Bromides

STODDART, Dr. J.F. (Sheffield University) — 1st March, 1990
Molecular Lego

SUTTON, Prof. D. (Simon Fraser University, Vancouver B.C.) — 14th February, 1990
Synthesis and Applications of Dinitrogen and Diazo Compounds of Rhenium and Iridium

THOMAS, Dr. R.K. (Oxford University) — 28th February, 1990
Neutron Reflectometry from Surfaces

THOMPSON, Dr. D.P. (Newcastle University) — 7th February, 1990
The role of Nitrogen in Extending Silicate Crystal Chemistry

REVISED VERSION

UNIVERSITY OF DURHAM

Board of Studies in Chemistry

COLLOQUIA, LECTURES AND SEMINARS GIVEN BY INVITED SPEAKERS 1ST AUGUST 1990 TO 31ST JULY 1991

ALDER, Dr. B.J. (Lawrence Livermore Labs., California) — 15th January, 1991
Hydrogen in all its Glory

BELL†, Prof. T. (SUNY, Stoney Brook, U.S.A.) — 14th November, 1990
Functional Molecular Architecture and Molecular Recognition

* BOCHMANN‡, Dr. M. (University of East Anglia) — 24th October, 1990
Synthesis, Reactions and Catalytic Activity of Cationic Titanium Alkyls

BRIMBLE, Dr. M.A. (Massey University, New Zealand) — 29th July, 1991
Synthetic Studies Towards the Antibiotic Griseusin-A

BROOKHART, Prof. M.S. (University of N. Carolina) — 20th June, 1991
Olefin Polymerizations, Oligomerizations and Dimerizations Using Electrophilic Late Transition Metal Catalysts

BROWN, Dr. J. (Oxford University) — 28th February, 1991
Can Chemistry Provide Catalysts Superior to Enzymes?

* BUSHBY‡, Dr. R. (Leeds University) — 6th February, 1991
Biradicals and Organic Magnets

COWLEY, Prof. A.H. (University of Texas) — 13th December, 1990
New Organometallic Routes to Electronic Materials

CROUT, Prof. D. (Warwick University) — 29th November, 1990
Enzymes in Organic Synthesis

DOBSON‡, Dr. C.M. (Oxford University) — 6th March, 1991
NMR Studies of Dynamics in Molecular Crystals

* GERRARD‡, Dr. D. (British Petroleum) — 7th November, 1990
Raman Spectroscopy for Industrial Analysis

HUDLICKY, Prof. T. (Virginia Polytechnic Institute) — 25th April, 1991
Biocatalysis and Symmetry Based Approaches to the Efficient Synthesis of Complex Natural Products

JACKSON‡, Dr. R. (Newcastle University) — 31st October, 1990
New Synthetic Methods: α-Amino Acids and Small Rings

KOCOVSKY‡, Dr. P. (Uppsala University) — 6th November, 1990
Stereo-Controlled Reactions Mediated by Transition and Non-Transition Metals

LACEY, Dr. D. (Hull University) — 31st January, 1991
Liquid Crystals

LOGAN, Dr. N. (Nottingham University) — 1st November, 1990
Rocket Propellants

MACDONALD, Dr. W.A. (ICI Wilton) — 11th October, 1990
Materials for the Space Age

MARKAM, Dr. J. (ICI Pharmaceuticals) — 7th March, 1991
DNA Fingerprinting

PETTY, Dr. M.C. (Durham University) — 14th February, 1991
Molecular Electronics

* PRINGLE[+], Dr. P.G. (Bristol University) — 5th December, 1990
Metal Complexes with Functionalised Phosphines

PRITCHARD, Prof. J. (Queen Mary & Westfield College, London University) — 21st November, 1990
Copper Surfaces and Catalysts

SADLER, Dr. P.J. (Birkbeck College London) — 24th January, 1991
Design of Inorganic Drugs: Precious Metals, Hypertension + HIV

SARRE, Dr. P. (Nottingham University) — 17th January, 1991
Comet Chemistry

SCHROCK, Prof. R.R. (Massachusetts Institute of Technology) — 24th April, 1991
Metal-ligand Multiple Bonds and Metathesis Initiators

SCOTT, Dr. S.K. (Leeds University) — 8th November, 1990
Clocks, Oscillations and Chaos

* SHAW[+], Prof. B.L. (Leeds University) — 20th February, 1991
Syntheses with Coordinated, Unsaturated Phosphine Ligands

* SINN[+], Prof. E. (Hull University) — 30th January, 1991
Coupling of Little Electrons in Big Molecules. Implications for the Active Sites of (Metalloproteins and other) Macromolecules

* SOULEN[+], Prof. R. (South Western University, Texas) — 26th October, 1990
Preparation and Reactions of Bicycloalkenes

* WHITAKER[+], Dr. B.J. (Leeds University) — 28th November, 1990
Two-Dimensional Velocity Imaging of State-Selected Reaction Products

[+] Invited specifically for the postgraduate training programme.